공학석사 학위논문

Experimental Study on Shear Strength of Prestressed PC-CIP Composite Beams

프리스트레스트 PC-CIP 복합보의 전단강도에 대한 실험적 연구

2015년 2 월

서울대학교 대학원

건축학과

서 정 일

Experimental Study on Shear Strength of Prestressed PC-CIP Composite Beams

지도 교수 박 홍 근

이 논문을 공학석사 학위논문으로 제출함
2015 년 2 월

서울대학교 대학원
건축학과
서 정 일

서정일의 공학석사 학위논문을 인준함
2015 년 2 월

위 원 장 _____ (인)

부위원장 _____ (인)

위 원 _____ (인)

Abstract

Experimental Study on Shear Strength of Prestressed PC-CIP Composite Beams

Suh, Jung-Il
Department of Architecture and Architectural Engineering
College of Engineering
Seoul National University

Recently, demands of precast (PC) composite method combined prestressed PC concrete and cast-in place(CIP) concrete increase in modular architectures. Because there is not obvious design code for shear strength of composite beam, in spite of increasing demands, engineers lead to being in difficulty to estimate shear strength of composite beams. Current design code (KCI 2012, ACI 318-11) suggests that properties of the individual elements or the most critical values shall be used in design if the specified strength, unit weight, or other properties of the various elements are different. Based on current code, 34 of prestressed composite specimens were tested and investigated consideration for shear design of composite beam. Test variables were section type, prestressing force (f_{se}/f_{pu}), shear span-to-depth ratio (a/d), and shear reinforcement ratio ($\rho_v f_y$).

In the result of tests, there were three failure modes: shear compression failure, horizontal shear failure, and web shear failure. Shear strength occurred shear compression failure was 2.4 times higher than that occurred horizontal shear failure and web shear failure. Also, shear strength increased as prestressed area and prestressing force increased and shear span-to-depth ratio decreased.

Especially, in the case of specimens having a/d=3.0 and 62 percent~65 percent of effective prestressing force, shear strength did not increase though shear reinforcement ratio increased.

Comparison between experimental values in this study and predicted values with current design code (KCI 2012, ACI 318-11), Eurocode2, empirical equation of Sozen et al., and theoretical equation of Bažant et al. was investigated. Consequently, shear strength with simplified method and detailed method of ACI 318 were in safety side and detailed method was rather conservative than simplified method. Thus it is reasonable to estimate shear strength of composite beams using current design code (ACI 318-11) which reflects properties of the individual elements.

In addition, shear database (UTPCSDB) analysis which the number of specimens is 159 was performed included data in this study. As a results according to experimental variables, there was 2.3 percent of non-safety side in the case of upper 40 percent effective prestressing force in the case of simplified method (ACI 318-11) but all specimens were in safety side in case of detailed method.

Keywords : composite beam, precast concrete, prestressed beam, shear strength

Student Number : 2013-20561

Contents

List of Tables

List of Figures

List of Symbols

A_s area of nonprestressed longitudinal tension reinforcement, mm^2

A_{ps} area of prestressing steel in flexural tension zone, mm^2

A_v area of shear reinforcement within spacing s, mm^2

b_w web width, wall thickness, or diameter of circular section, mm

d distance from extreme compression fiber to centroid of longitudinal tension reinforcement, mm

d_p distance from extreme compression fiber to centroid of prestressing steel, mm

f_{ck} specified compressive strength of concrete, MPa

f_d stress due to unfactored dead load, at extreme fiber of section where tensile stress caused by externally applied loads, MPa

f_{pc} compressive stress in concrete (after allowance for all prestress losses) at centroid of cross section resisting externally applied loads or at junction of web and flange when the centroid lies within the flange, MPa (In a composite member, f_{pc} is the resultant compressive stress at centroid of composite section, or at junction of web and flange when the centroid lies within the flange, due to both prestress and moment resisted by precast member acting alone)

f_{pcc} compressive stress in concrete due to effective prestress forces only (after allowance for all prestress losses) at extreme fiber of section where tensile stress is caused by externally applied loads, MPa

f_{pj} temporary jacking stress exerted by device that introduces tension into prestressing tendon

f_{ps} stress in prestressing steel at nominal flexural strength, MPa

f_{pu} specified tensile strength of prestressing, MPa

f_{yt} specified yield strength f_y of transverse reinforcement, MPa

h overall thickness or height of member, mm

I moment of inertia of section about centroidal axis, mm4

M_{cre} moment causing flexural cracking at section due to externally applied loads, kN·m

M_{max} maximum factored moment at section due to externally applied loads, kN·m

M_u factored moment at section, kN·m

s center-to-center spacing of items, such as longitudinal reinforcement, transverse reinforcement, prestressing tendons, wires or anchors, mm

V_c nominal shear strength provided by concrete, N

V_{ci} nominal shear strength provided by concrete when diagonal cracking results from combined shear and moment, N

V_{cw} nominal shear strength provided by concrete when diagonal cracking results from high principal tensile strength in web, N

V_d shear force at section due to unfactored dead load, N

V_i factored shear force at section due to externally applied loads occurring simultaneously with M_{max} , N

V_n nominal shear strength, N

V_{nh} nominal horizontal shear strength, N

V_p vertical component of effective prestress force at section, N

V_s nominal shear strength provided by shear reinforcement, N

V_u factored shear force at section, N

y_t distance from centroidal axis of gross section, neglecting reinforcement, to tension face, mm

λ modification factor reflecting the reduced mechanical properties of lightweight concrete, all relative to normalweight concrete of the same compressive strength

ρ_v ratio of tie reinforcement area to area of contact surface

ρ_w ratio of A_s to $b_w d$

Chapter 1. Introduction

1.1 General

Precast concrete (PC) means a concrete member that is cast and cured at a location other than its final designated location. There are advantages of using PC members that are rapid speed of erection, good quality control and rapid construction in site. Because of these advantages, precast concrete method has been generalized in Europe, America and Japan. Also, precast concrete method was applied to domestic construction site (e.g., wall type apartment) in 1990. But because of frequent occurrence of structural defect, low cost efficiency and difficulty of maintenance control, requirement of precast concrete method decreased.

Recently precast concrete composite construction method using precast concrete (PC) and cast-in-place (CIP) concrete is gradually applied to modular architectures (e.g., underground parking lot, major supermarket). As shown in **Fig 1.1**, PC members that are beams, slabs, and columns are generally manufactured in advance and are assembled in construction site. After assembling PC members, CIP concrete is placed on upper side of PC members which can integrate with PC members. Thus, there are various advantages of PC composite method that light lifted load of PC members, good economic feasibility because of not requirement of separate formwork and structural integrity.

When PC members are manufactured, especially, prestressing force (pre-tension) to PC members is universally applicable to improve structural performance. This application of prestressing can reduce the size and number of the structural members and produce long span girders and slabs. Thus,

prestressed PC members can be more efficiently applied to modular architectures rather than general PC members and predicted to become more common.

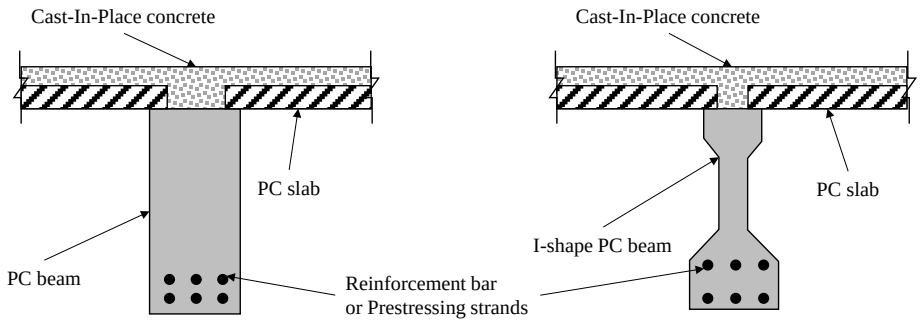

Fig 1.1 Precast composite construction method using PC and CIP concrete

In precast composite construction method, PC members is high strength (more than 40 MPa) concrete and CIP member is low strength (24 MPa) concrete. Because of difference of concrete strength as well as prestressing force, shear strength is difficult to calculate.

According to concrete structure design code (KCI 2012 [1], ACI 318-11 [2]), when estimate vertical shear capacity of beam member, these suggest only shear strength estimation formula of the total cross section not composite section. Also, according to the code (KCI 2012 17.2, ACI 318-11 17.2.3), if the specified strength, unit weight, or other properties of the various elements are different, properties of the individual elements or the most critical values shall be used in design. However using the most critical values lead to uneconomical design and using properties of the individual element does not present quantitative analysis result. Currently, a large number of structural engineer's offices are using mixed estimating methods to calculate shear strength of composite member. As a result, there are not sufficient experimental verification and theoretic analysis supporting these methods. Furthermore, because strength of PC members and CIP members is significantly different caused by high strengthening trend of concrete than before, deviation of shear

strength derived from various estimating methods increases considerably. Thus, clear criteria is needed to estimate vertical shear strength of PC-CIP composite members.

Also, horizontal shear strength of interface which are formed between PC concrete and CIP concrete should be considered. According to current design code (KCI 2012 17.2, ACI 318-11 17.2.3), contact surfaces state of interconnected elements and horizontal shear reinforcement influence to horizontal shear strength. These values estimated from current design code are rather conservative to apply to practice. The many methods of estimation were developed and many researchers have studied in the last few years.

1.2 Scope and Objectives

In the recent researches of Kim et al. [3-5], the shear strength of nonprestressed PC-CIP composite beams was developed. In actual construction site, prestressed members are also used as well as nonprestressed beam. Thus, to develop the previously experimental study on shear strength of nonprestressed PC-CIP composite beams, studies for prestressed beams are necessary.

The primary objective of this dissertation is to study the shear strength of prestressed PC-CIP composite beams according to variable experiments. To achieve this objective, a push-over test for simple supported beams were performed and analysis were developed.

From investigating shear strength and failure mechanisms of prestressed PC-CIP composite beams without or with web reinforcement, contribution of web reinforcement and other variables were defined. Also, according to comparison with RC composite beams, contribution of prestressing force could be found.

To propose design recommendations for the shear strength of prestressed PC-CIP composite beams, experimental results were compared with current design codes, compression zone failure models, empirical model and fracture mechanics model.

1.3 Outline of Master's Thesis

In Chapter 2, review of current design codes and previous experimental studies were performed. Estimation methods of vertical shear strength provided by concrete, prestressed concrete and shear reinforcement and also that of horizontal shear strength were investigated. Also previous experimental studies done by Revesz [6] (1953), Saemann and Washa [7](1964), Bryson, Skoda, and Watstein [8] (1965), and Loov and Patnaik [9] (1994) were surveyed.

In Chapter 3, experimental study was performed to investigate the shear strength of prestressed PC-CIP composite beams without shear reinforcement. Total 16 specimens which 4 specimens were added to investigate contribution of shear reinforcement were tested. Test parameters are the area ratio of PC and CIP, prestressing force, shear span-to-depth ratio and shear reinforcement ratio (ρ_v). Based on test results, contribution of parameters was investigated and experimental values were compare with predicted values calculated by current design code.

In Chapter 4, also experimental study was performed to investigate the shear strength of prestressed PC-CIP composite beams with shear reinforcement. Total 22 specimens were tested. Test parameters are same as above. On the basis of experimental values, contribution of shear reinforcement ratio was mainly investigated and vertical shear strength and horizontal shear strength calculated by current design code were compared with test results.

In Chapter 5, to investigate effect of experimental variables, experimental values of this study were compared with predicted values according to ACI 318-11 , Eurocode2 [10] , Sozen et al. [11], Bažant et al. [12] included shear database called 'The University of Texas Prestressed Concrete Shear Database (UTPCSDB) [13]'.

Finally, summary and conclusions were presented in Chapter 6.

Chapter 2. Review

2.1 Design Codes

According to structural design codes (KCI 2012 [1], ACI 318-11 [2]) toward vertical shear strength, there are shear strength provided by concrete for nonprestressed members, shear strength provided by concrete for prestressed members, shear strength provided by shear reinforcement, and horizontal shear strength in a composite member.

2.1.1 ACI 318-11

2.1.1.1 Shear Strength Provided by Concrete for Nonprestressed Members

In nonprestressed members, shear strength provided by concrete is able to be divided by general equation and detailed equation. General equation is function of compressive strength of concrete and size of section. In addition to compressive strength of concrete and size of section, detailed equation considers longitudinal reinforcement ratio and shear span-to depth ratio.

$$V_c = \frac{1}{6}\lambda\sqrt{f_{ck}}b_w d \tag{2-1}$$

$$V_c = (0.16\lambda\sqrt{f_{ck}} + 17.6\rho_w \frac{V_u d}{M_u})b_w d \tag{2-2}$$

where $V_c \le 0.29\lambda\sqrt{f_{ck}}b_w d$, $V_u d / M_u \le 1.0$.

2.1.1.2 Shear Strength Provided by Concrete for Prestressed Members

In prestressed members, shear strength provided by concrete is able to be also divided by general equation and detailed equation.

For members with effective prestress force not less than 40 percent of the tensile strength of flexural reinforcement,

$$V_c = (0.05\lambda\sqrt{f_{ck}} + 4.9\frac{V_u d_p}{M_u})b_w d \qquad (2\text{-}3)$$

where $(\lambda\sqrt{f_{ck}}/6)b_w d \le V_c \le (5\lambda\sqrt{f_{ck}}/12)b_w d$, $V_u d / M_u \le 1.0$ and $d_p \ge 0.8h$.

In the case of detailed equation, shear strength shall be the lesser of flexural-shear cracking strength (V_{cw}) and web-shear cracking strength (V_{ci}) as shown in **Fig 2.1**.

$$V_{ci} = 0.05\lambda\sqrt{f_{ck}}b_w d + V_d + \frac{V_i M_{cre}}{M_{\max}} \qquad (2\text{-}4)$$

$$M_{cre} = (\frac{I}{y_t})(0.5\lambda\sqrt{f_{ck}} + f_{pcc} - f_d) \qquad (2\text{-}5)$$

where $d_p \ge 0.8h$ and $V_{ci} \ge 0.17\lambda\sqrt{f_{ck}}b_w d$.

$$V_{cw} = (0.29\lambda\sqrt{f_{ck}} + 0.3 f_{pc})b_w d_p + V_p \qquad (2\text{-}6)$$

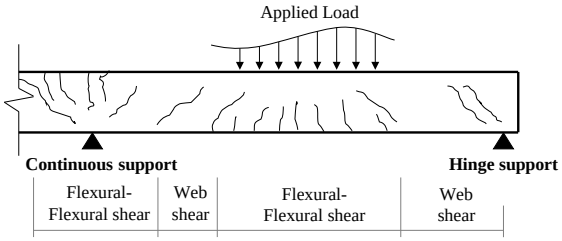

Fig 2.1 Type of cracking in prestressed concrete beams

2.1.1.3 Shear Strength Provided by Shear Reinforcement

Spacing of shear reinforcement placed perpendicular to axis of member shall not exceed *d*/2 and in nonprestressed member or 0.75*h* in prestressed member, nor 600 mm.

$$V_s = \frac{A_v f_{yt} d}{s} \tag{2-7}$$

2.1.1.4 Horizontal Shear Strength in a Composite Member

Where contact surfaces are clean, free of laitance, and intentionally roughened, or where minimum ties are provided and contact surfaces are clean and free of laitance, but not intentionally roughened,

$$V_{nh} \le 0.56 b_v d \tag{2-8}$$

Where ties are provided, and contact surfaces are clean, free of laitance, and intentionally roughened to a full amplitude of approximately 6 mm,

$$V_{nh} \le (1.8 + 0.6\rho_v f_y) b_v d \tag{2-9}$$

where, $V_{nh} \le 3.5 b_v d$.

Where ties are provided to transfer horizontal shear, tie area shall not be less than requirement, and ties spacing shall not exceed four times the least dimension of supported element, nor exceed 600 mm.

$$A_{v,\min} = 0.0625\sqrt{f_{ck}}\frac{b_w s}{f_{yt}} \tag{2-10}$$

For prestressed members with an effective prestress force not less than 40 percent of the tensile strength of flexural reinforcement,

$$A_{v,\min} = \frac{A_{ps}}{80}\frac{f_{pu}}{f_{yt}}\frac{s}{d}\sqrt{\frac{d}{b_w}} \qquad (2\text{-}11)$$

where, $A_{v,\min} \geq 0.35 b_w s / f_{yt}$.

2.1.2 Other Design Codes for Prestressed Member

Eurocode 2 [10] proposes estimation of shear strength which is able to be applied to the beam-column elements subjected to bending moment, axial force or prestressing force. And this provides different equation according to cracked region and uncracked region. The shear strength equation for the cracked region contains the size effect coefficient *k*, and it does not consider shear span-to-depth ratio.

Sozen et al. [11] developed empirical shear estimation method based on the test result of 43 rectangular beams. This equation targets the inclined cracking load. It considers effect of shear span-to-depth ratio, tensile strength of concrete, and the width of flange. The tensile strength of concrete is calculated by the principal stress analysis to the test results of I-beams which failed in web-shear failure.

Based on fracture mechanics model, Bažant and Cao [12] suggested shear estimation method. In their research, size effect was observed in the shear failure pattern of prestressed members because it is a brittle failure caused by tensile cracking of concrete rather than yielding of steel. And nominal shear strength and size effect coefficient are applied to shear strength equation which were developed by moment equilibrium condition and empirical parameters respectively.

Table 2.1 Estimation methods of shear strength for prestressed concrete beams

Researcher	Shear strength model (SI Units)
Eurocode 2 [10]	In the cracked regions, $V_{Rd,c} = \left[0.12k(100\rho_p f'_c)^{1/3} + \sigma_{cp} \right] b_w d$ $\geq \left[0.035k^{3/2} \sqrt{f'_c} + 0.15\sigma_{cp} \right] b_w d$ In the uncracked regions, $V_{Rd,c} = (Ib_w / S)\sqrt{(f_{ctd})2 + \sigma_{cp} f_{ctd}}$ $k = 1 + \sqrt{200/d} \leq 2.0$, d in mm, $\rho_p \leq 0.02$ $\sigma_{cp} = P_e / A_c < 0.2 f_{cd}$ in MPa f_{cd}, f_{ctd} = design value of concrete compressive and tensile strength
Sozen, Zwoyer, and Siess [11]	$V_c = \left(\frac{f'_t + P_e / A_c}{a/d} \sqrt{\frac{b}{b_w}} \right) b_w d$ $f'_t = 6.9 / (1 + 41.4 / f'_c)$ in MPa
Bažant and Cao [12]	$V_c = \left(\frac{0.33\sqrt{f'c} + 0.4P_e / A_c}{a/d} \right) \left(1 + \frac{d}{25d_a} \right)^{-1/2} b_w d$

2.2 Preceding Research

2.2.1 Revesz (1953)

Revesz [6] tested five composite T-beams to destruction to observe the behavior under loading. Four of those were prestressed with high tensile strength wire (L, J, G, and F) and one was reinforced with mild steel (N). **Fig 2.2** shows cross-section of beam tested by Revesz. The roughness of the contact surface was smooth. And there were no shear reinforcement. The load was applied at the third-points of the 14 ft beam. The predicted ultimate loads were exceeded in every case. Out of the five beams, four failed in flexure and one in horizontal shear (J). At the time of the test, the concrete cylinder strength of specimen J was approximately 2,480 psi for the cast-in-place flange and 5,225 psi for the precast web. The age of the concrete at the time of the test was 4 days for the cast-in-place flange and 85 days for the precast web. There have been some differences on the value of horizontal shear stress at which specimens J failed. Revesz reported that at failure the calculated shear intensity was 134 psi.

Conclusively, Revesz suggested that if concrete in the precast beam had been poor, the bonding may not have been sufficient to prevent failure due to excessive rise of the neutral axis caused by wider crack widths. And he suggested that it is desirable to roughen contact surfaces of the precast web and cast-in-place concrete of composite beams, or even introduce shallow serrations, to prevent failure by horizontal shear. However, he did not suggest specific state of surface of the precast web.

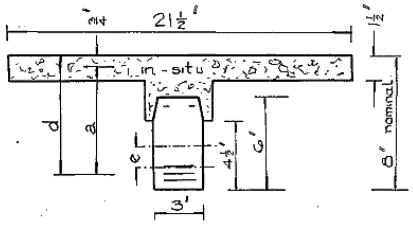

Fig 2.2 Cross-section of beam tested by Revesz

2.2.2 Saemann and Washa (1964)

To evaluate of the strength of the joint between precast concrete beams and cast-in-place concrete slabs, Saemann and Washa [7] tested 42 composite T-beams of which two specimens were zero shear reinforcement ratio crossing the interface (specimen 15C and 16C). The beams were designed so that high horizontal shear values at the contact surface were reached at loads well below those required for flexural failure. **Fig 2.3** shows cross-section of beam tested by Saemann and Washa. The test variables were degree of roughness of contact surface, length of shear span-to-depth ratio, percentage of steel across the joint, effect of shear keys, position of the joint with respect to the neutral axis, and concrete compressive strength. The horizontal shear stress was calculated by the equation $v = VQ / Ib_v$ and based on cracked section properties.

After the webs poured, the surface finish was applied. Rough contact surface was made by removing particles of coarse aggregate with boards having nails protruding 1 in. Surface depressions were 1/8 and 3/8 in. deep, respectively, in the intermediate and rough finishes.

Specimens regardless of roughness of contact surface having 20 ft span length, and 1.12 percent of shear reinforcement ratio (ρ_v) failed in flexure with fine horizontal shear crack. And Specimens having 11 ft or 8 ft span length, and more than 1 percent of shear reinforcement ratio (ρ_v) failed in flexural-shear failure and specimens having less than 0.58 percent of shear reinforcement ratio (ρ_v) failed in horizontal shear failure. Point of occurrence of flexural or shear failure was decided by yield stress of longitudinal steel and slip length of interface. And contribution of strain presented that flange and web behaved separately not uniformly.

With regard to position of the joint with respect to the neutral axis, horizontal shear strength of series B which joint was 50 mm lower than neutral axis was 14 percent higher than that of series A and C which joint was 50 mm higher

than neutral axis. And roughness of contact surface affected that horizontal shear strength did not be influenced by roughness but rough contact surface rather than smooth surface affected horizontal shear strength in the case of small shear span-to-depth ratio. And horizontal shear strength increased 14 percent as concrete strength increased from 21 MPa to 39 MPa.

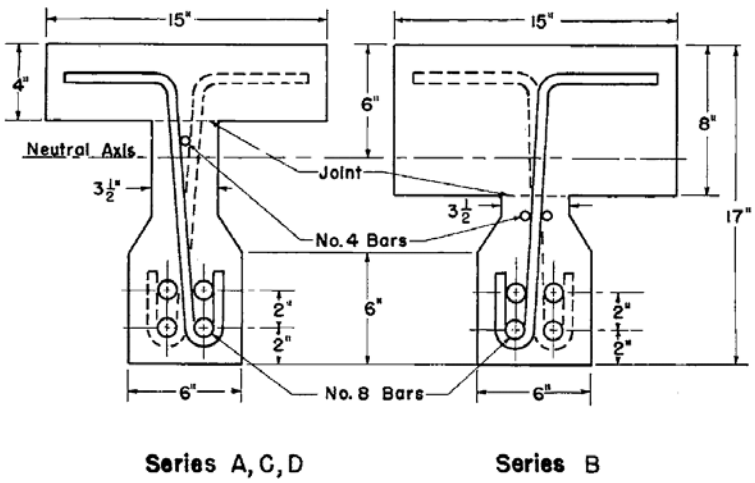

Fig 2.3 Cross-section of beam tested by Saemann and Washa

2.2.3 Bryson, Skoda, and Watstein (1965)

To investigate the general flexural characteristics of prestressed composite concrete beams, Bryson, Skoda, and Watstein [8] made composite beams separately formed the tensile and compressive sections. The tensile section was cast first and prestressed, and the compressive section was formed with plain concrete bonded to the prestressed element. There were three sets of split beams with interfaces at different levels which were tested in duplicate as shown in **Fig 2.4** and these were compared with two set of reference beams. Shear connects were not provided across the interface of the two concrete elements. The surface roughness was applied with a stiff wire hand brush to the extent that the largest size aggregate was exposed. The beams were tested simply supported in hydraulic testing machine and loads were applied at the third point.

It was noted that the relationship of the load-deflection curves for both split beams and reference beams prior to cracking were very similar. To determine approximately the cracking load, the relationships between the applied load and the distance to the neutral axis, *kd*, was examined and these were developed from the distributions of strain over the cross-section of the beams. The split beams responded to loading in accordance with the elastic theories of strain distribution, indicating that the abrupt changes of the strain gradients at the interface in the B and C beams prior to loading had no apparent effect on the linear strain distribution of the beams under the applied load.

All specimens failed in flexural compression which was “crushing of the concrete in the region of constant moment above a flexural crack which has reduced the area available for resisting compressive stresses”.

The first conclusion was that “the procedure that was used for combining the two elements of the split beams proved to be adequate for the development of sufficient bond for monolithic beam action throughout the test”

And second is that the presetressing force required for split beams is

considerably less than that required for a conventionally prestressed beam and consequently a significant reduction in the amount of reinforcing steel can be achived by this method of construction for the same working load capacity.

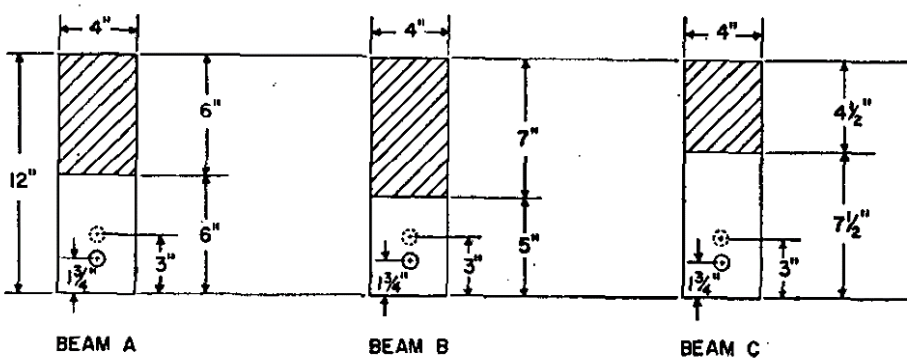

Fig 2.4 Cross-section tested by Bryson, Skoda, and Watstein

2.2.4 Loov and Patnaik (1994)

16 specimens were tested by Loov and Patnaik [9] to investigate the behavior of “rough” joint in composite concrete beams and their capacity to develop interface shear for a wide range of steel ratios. **Fig 2.5** shows cross-section tested by Loov and Patnaik and **Fig 2.6** shows elevation view of loading setup for the beam tests. As shown in **Fig 2.6**, the interface was left as-cast with some of the coarse aggregate protruding, instead of mad as a rough surface with an amplitude of 5 mm required by the ACI Code. Test variables were the clamping stress which are shear reinforcement ratio and concrete strength. They suggested equation which considered these variables as shown in Eq. (2-11). Current design code takes account of only shear reinforcement ratio.

$$v_n = k\lambda\sqrt{(0.1+\rho_v f_y) f'_c} \le 0.25 f'_c \qquad (2\text{-}11)$$

To investigate contribution of the interface beyond the location where the horizontal crack meets the diagonal crack, two kind of specimens which were beams with full length flanges and beams with short flanges were tested as shown in **Fig 2.6**. And to control shear reinforcement ratio, interface area was changed as shown in **Fig 2.5**.

Crack pattern was that early flexural cracks developed to neutral axis and horizontal crack formed. This horizontal crack propagated all the way to full length of interface and finally beams failed in horizontal shear failure. In the case of beams with full length flanges, horizontal shear cracks reached to encounter point of inclined crack and interface. In the case of beams with short flanges, whereas, only horizontal crack occurred without inclined cracks.

Test results indicated that the shear reinforcements were not stressed until a horizontal shear stress of about 1.5 to 2 MPa was reached. In other words, the strength of an interface without shear reinforcement. The shear reinforcement become relatively effective when the shear stress reaches about 3 MPa.

Loov and Patnaik concluded that because an as-cast concrete surface with coarse aggregate left protruding from the surface can develop sufficient horizontal shear resistance, more elaborate finishing is no required. And the effectiveness of shear reinforcements is improved when they are placed further from the center of the span, but shear reinforcements in the region near the supports are not effective.

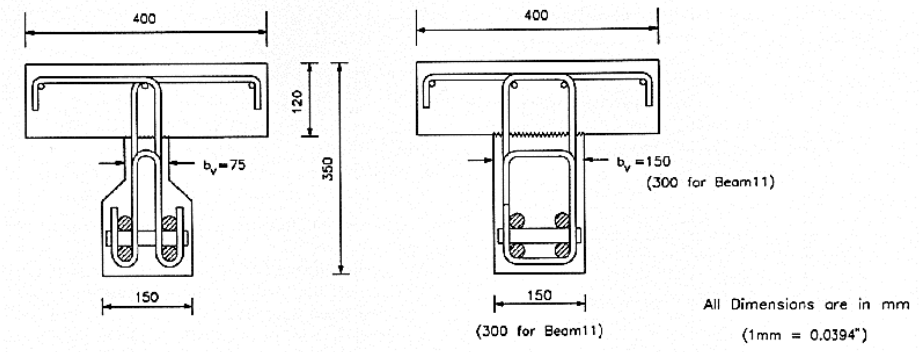

Fig 2.5 Cross-section tested by Loov and Patnaik

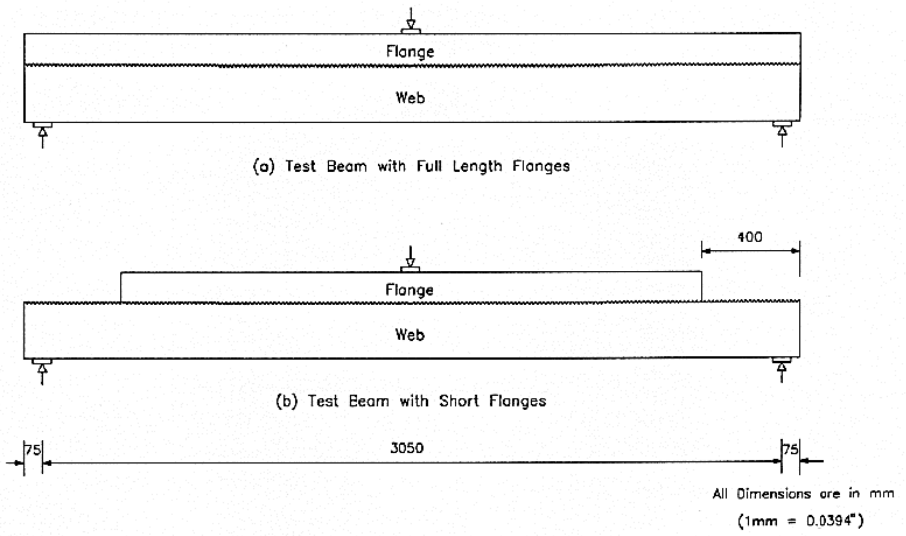

Fig 2.6 Elevation view of loading setup for the beam tests by Loov and Patnaik

According to these researches, there are very much part of the investigations of horizontal shear strength between PC member and CIP member. Although composite beam have different properties of PC and CIP members it should behave like monolithic beam in practice. According to current design codes, if the specified strength, unit weight, or other properties of the various elements are different, properties of the individual elements or the most crictical values shall be used in design. If the most crictical values are used, vertical shear strength is excessively conservative. And if respective properties are used, there is not appropriate estimation method of vertical shear strength of composite beam without verification. Hence engineers could not use proper method. Therefore, investigation of estimation method of vertical shear strength is needed.

Chapter 3. Shear Strength of Prestressed PC-CIP Composite Beams without Web Reinforcement

3.1 Test Program

3.1.1 Test Parameters

To investigate shear strength of PC-CIP composite members, 16 simply supported beams were tested. There are four kinds of main parameters: the area ratio of PC and CIP, prestressing force, shear span-to-depth ratio and shear reinforcement ratio (ρ_v).

As the first main parameter, there are four types of area ratio of PC (60 MPa) and CIP (24 MPa) as shown in **Fig 3.1**. Section A and B are gross section of 24 MPa and 60 MPa respectively. These are control specimens to compare with composite section C and D. In composite section C and D, high-strength concrete of 60 MPa are 5/8 and 3/8 of PC members respectively and the rest of section was filled with low-strength concrete of 24 MPa. To obtain definite results for increasing difference between high-strength concrete and low-strength concrete and reflect tendency of high strengthening of materials, 60 MPa strength concrete for high-strength concrete were used instead of 40 MPa.

The second parameter is prestressing force. To investigate the effect of prestressing force on shear strength, there are two jacking forces were applied at six strands. One is 55 percent of tensile strength of prestressing steel and the other is 70 percent of that. These prestressing (generally pre-tension) forces applied to PC members (60 MPa) only, thus CIP members (24 MPa) were not applied. In the case of section A which are gross section of 24 MPa strength concrete, six strands were placed in members but did not be applied tensile force.

The third main parameter is shear span-to-depth ratio (*a/d*). The member can be defined as deep beam and slender beam when *a/d* is less or more than 2.5 respectively. To investigate the effect of shear span-to-depth ratio on failure mechanisms and shear strength, 3.0 and 4.0 of shear span-to-depth ratios are applied.

The last parameter is shear reinforcement ratio (ρ_v). Minimum shear reinforcement for resisting horizontal shear was applied.

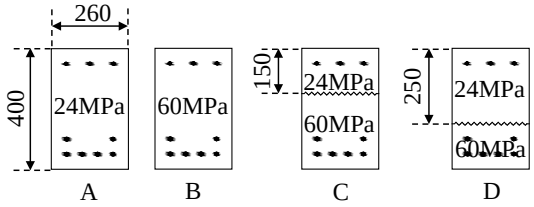

Fig 3.1 Cross section types A~D

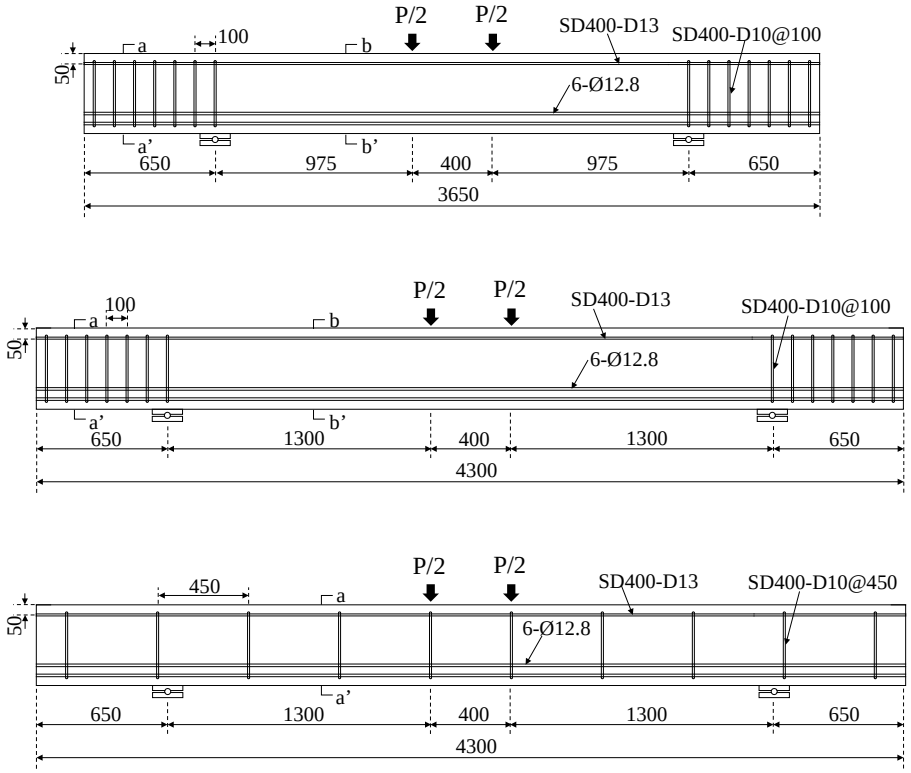

Fig 3.2 Reinforcement Arrangement

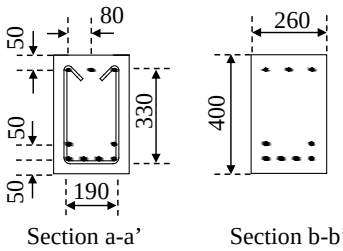

Fig 3.3 Cross section of specimens (a-a' and b-b')

Table 3.1 Test variables and predictions of moment and shear capacities of specimens

Specimens	Section type	Re-bar (ρ)	Stirrup (ρ_v)	s (mm)	Prestressing force (f_{pj})	a/d	M_n (kN·m)	V_m (kN)	V_n (kN)	$\frac{V_m}{V_n}$	V_{nh} (kN)	V_{hv} (kN)	$\frac{V_{hv}}{V_{nh}}$
1-A	A	6-ϕ12.7 (0.57%)	-		0.55f_{pu}	3.0	218	224	69	3.24			
1-B	B	6-ϕ12.7 (0.57%)	-		0.55f_{pu}	3.0	287	294	263	1.12			
1-C	C	6-ϕ12.7 (0.57%)	-		0.55f_{pu}	3.0	226	232	173	1.34	142	590	4.19
1-D	D	6-ϕ12.7 (0.57%)	-		0.55f_{pu}	3.0	221	227	114	1.99	142	385	2.75
2-A	A	6-ϕ12.7 (0.57%)	-		0.70f_{pu}	3.0	218	224	69	3.24			
2-B	B	6-ϕ12.7 (0.57%)	-		0.70f_{pu}	3.0	287	294	263	1.12			
2-C	C	6-ϕ12.7 (0.57%)	-		0.70f_{pu}	3.0	226	232	173	1.34	142	590	4.19
2-D	D	6-ϕ12.7 (0.57%)	-		0.70f_{pu}	3.0	221	227	114	1.99	142	385	2.75
3-A	A	6-ϕ12.7 (0.57%)	-		0.70f_{pu}	4.0	218	168	69	2.43			
3-B	B	6-ϕ12.7 (0.57%)	-		0.70f_{pu}	4.0	287	220	205	1.07			
3-C	C	6-ϕ12.7 (0.57%)	-		0.70f_{pu}	4.0	226	174	142	1.22	189	646	3.44
3-D	D	6-ϕ12.7 (0.57%)	-		0.70f_{pu}	4.0	221	170	100	1.69	189	453	2.43
4-A	A	6-ϕ12.7 (0.57%)	2-D10 (0.12%)	450	0.70f_{pu}	4.0	218	168	100	1.68			
4-B	B	6-ϕ12.7 (0.57%)	2-D10 (0.12%)	450	0.70f_{pu}	4.0	287	220	236	0.93			
4-C	C	6-ϕ12.7 (0.57%)	2-D10 (0.12%)	450	0.70f_{pu}	4.0	226	174	173	1.00	683	654	1.16
4-D	D	6-ϕ12.7 (0.57%)	2-D10 (0.12%)	450	0.70f_{pu}	4.0	221	170	131	1.29	683	471	0.88

3.1.2 Test Specimens and Set-up

Fig 3.2 shows reinforcement arrangement and characteristics of specimens. And **Fig 3.3** shows size and arrangement of re-bar of cross section. In all the specimens, size of cross section is 260 mm by 400 mm. The span length between supporting point are 2,350 mm and 3,000 mm for a/d=3.0 and 4.0, respectively. Considering transfer length of prestressing, span length was extended to 650 mm from supporting points of both side. As shown in **Fig 3.3**, the six strands are arranged with two layers in the precast members and covering depth which is distance from center of strands to extreme tension fiber is 50 mm. Also, to resist tensile force acting upper apart of beams due to prestressing, three SD 400-D13 were arranged with a layer in the compression zone. To resist horizontal shear, shear reinforcements SD 300-D10 were arranged from outward of supporting point.

Table 3.1 shows predicted values of flexural moment, vertical shear and horizontal shear strength in 16 specimens. The required shear strength (V_m) to lead to flexural capacity (M_n) is more than vertical shear capacity, thereby, all the specimens were designed to lead to shear failure before flexural failure. Flexural capacity of prestressed members was calculated according to ACI 318-11 10.2 and vertical shear strength of composite members which consist of PC member and CIP member was calculated by Eq. (2-1) and Eq.(2-3) respectively.

Also, **Table 3.1** shows the comparison between nominal horizontal shear strength (V_{nh}) and horizontal shear force based on nominal vertical shear strength (V_{hv}). The former is calculated by Eq. (2-8) and the latter is multiplied shear stress of interface by contact area. As shown in **Table 3.1**, V_{hv}/V_{nh} of composite member without shear reinforcement was ranged from 2.43 to 4.19, thus horizontal shear failure was predicted before vertical shear failure. Whereas that of composite member with minimum shear reinforcement were 0.88 and 1.16 causing vertical shear failure.

Fig 3.4 shows procedure for manufacture of composite beams. The main

process of manufacture was twice placing of concrete. First, six strands and shear reinforcement were arranged in forms and strands were prestressed using hydraulic pumps. After attaching strain gauges to strands and stirrups, 60 MPa strength concrete was placed and cured with steam during about 6 hours. After 24 hours, prestressed strands were cut when concrete strength was 35 MPa. And laitance of surface was eliminated and surface was roughened to a full amplitude of approximately 6 mm. And 24 MPa strength concrete was placed on 60 MPa concrete and cured with steam also. Standard specimens were made whenever concrete was placed.

(a) Arrangement re-bar (b) Prestressing strands (c) Placing precast concrete (d) Spreading retarder

(e) Dissolution forms (f) Placing cast-in-place concrete (g) Making standard specimens (h) Steam curing

Fig 3.4 Procedure for manufacture of composite beams

Test method is two point loading shear test by 1,000 kN hydraulic oil jack as shown in **Fig 3.5**. The beams were supported by hinges at both ends. To investigate the crack pattern, crack was drawn by the 50 kN until specimens reached predicted shear capacity. In order to analyze failure mechanism, photographs and videos were taken.

Measurement methods is that loading forces were measured by load cell and

deflections of center of the specimens were measured by 5 LVDTs which are located in center, two loading point and 800 mm from center of the specimen at both side. To investigate yielding of strands occurred before flexural failure, strain gauges were attached to center of strands. In specimens with minimum shear reinforcement, to investigate contribute of stirrups, also strain gauges were attached to stirrups from loading point to hinge end. These loading data and strain data were collected by data logger.

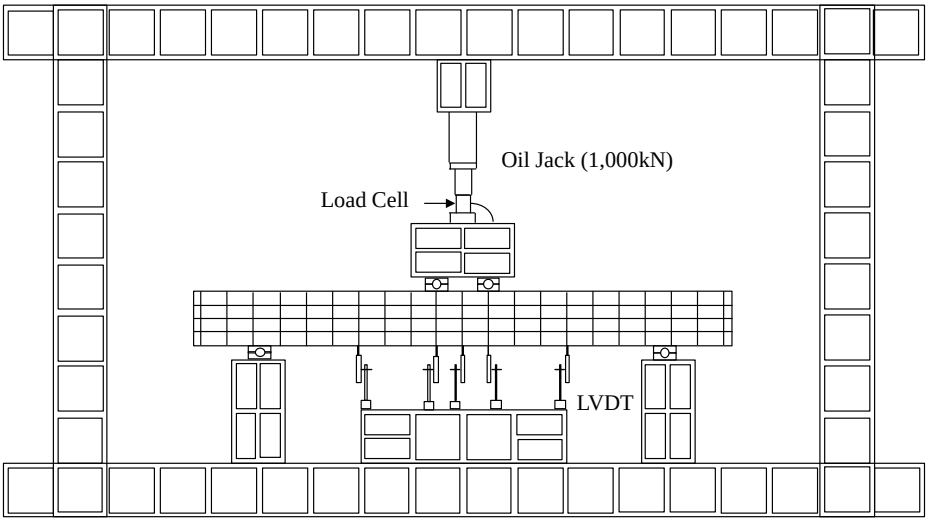

Fig 3.5 Test set-up

3.1.3 Materials

Table 3.2 shows mixture proportions of high-strength concrete and low-strength concrete of which nominal strengths are 60 MPa and 24 MPa respectively. Concrete standard specimens of 100 mm by 200 mm were made according to KS F 2403 and 3 standard specimens at a beam test were tested according to KS F 2405 called cylinder test. **Fig 3.6** shows actual concrete strength for 24 MPa and 60 MPa at test days. Actual compressive strength of 24 MPa and 60 MPa strength concrete were 22~23 MPa and 52~58 MPa. When estimating shear strength, concrete strengths on the day of beam test were used.

Table 3.2 Mixture proportions of concrete

Nominal strength	W/C (%)	Unit weight(kg/m^3)				
		W	C	S	G	SP
24	49.4	162	328	869	979	3.5
60	29	180	620	625	935	8.06

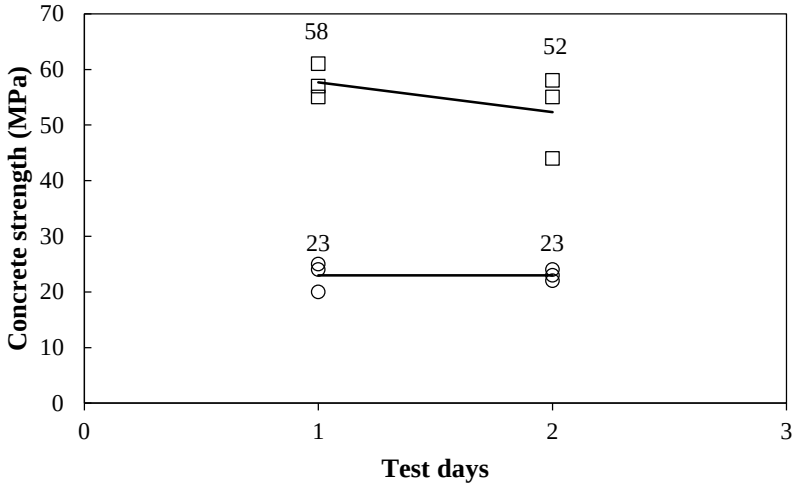

Fig 3.6 Concrete strength for 24 MPa and 60 MPa at test days

As shown in **Fig 3.2**, main reinforcement of beams were 12.7 mm SWPC 7BL which is called strands, SD300 D10, and SD400 D13. To evaluate mechanical properties of reinforcement, steel specimens were made according to KS B 0801 and these specimens were tested according to KS B 0802. **Table 3.3** shows these mechanical properties of reinforcement through the test. The yield strengths were f_y=1,854 MPa for 12.7 mm strand, and f_y=360 MPa for D10 bar, and f_y=480 MPa for D13 bars. As shown in **Fig 3.7**, the yield strength of the strands was estimated by the 1% extension method because there is no obvious yield point.

Table 3.3 Mechanical properties of reinforcement

Type	f_y (MPa)	ε_y (μ)	E_s (GPa)
12.7 mm SWPC 7BL	1,854	8,829	210
SD300 D10	360	1,847	184
SD400 D13	480	2,400	200

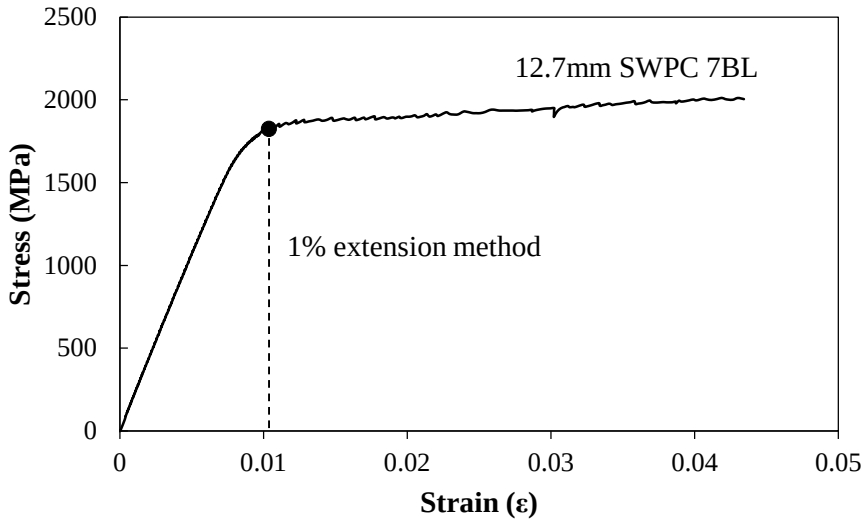

Fig 3.7 Yield stress of main reinforcement using offset method

3.2 Result

The test results are shown in **Table 3.4**, **Table 3.5**, **Table 3.6**, and **Table 3.7**. General and detailed equation for prestressed members ((Eq. (2-3), (2-4), and (2-6)) are used predict PC members (60 MPa) and general equation and detailed equation for nonprestressed members (Eq. (2-1), (2-2)) are used to predict CIP members (24 MPa).

3.2.1 Specimens 1-A ~ 1-D (a/d=3.0, f_{pj}=0.55f_{pu})

The specimens 1-A ~ 1-D are a/d=3.0 and f_{pj}=0.55f_{pu} and test result are shown in **Fig 3.8**, **Table 3.4** And **Fig 3.9** shows the crack pattern of specimens at the end of test. The shear strength is proportional to the area ratio of prestressed sections: 1-B (544 kN) > 1-C (392 kN) > 1-D (358 kN) > 1-A (200 kN). Flexural cracking strength of 1-B~1-D which are prestressed specimens was five times higher than that of nonprestressed specimen 1-A.

Diagonal tension failure occurred in all the specimens after incline cracking. In specimens 1-A~1-C, early flexural cracks propagated toward loading point and transformed inclined crack and finally diagonal tension failure occurred. In specimen 1-D, horizontal shear crack appeared to interface and also diagonal tension failure occurred. According to load-displacement relationship of 1-A, two peak load points appeared because load decreased at first peak point after inclined cracks and horizontal shear crack occurred and also load decreased at second peak point after the horizontal shear crack propagated to loading point and cause failure.

Crack patterns were different from that of RC composite beams. Crack patterns of RC specimens were that diagonal tension cracks with bond slip of flexural reinforcement occurred at the middle of shear span. Whereas that of prestressed PC composite beams appeared only inclined cracks near loading points without bond slip of flexural reinforcement.

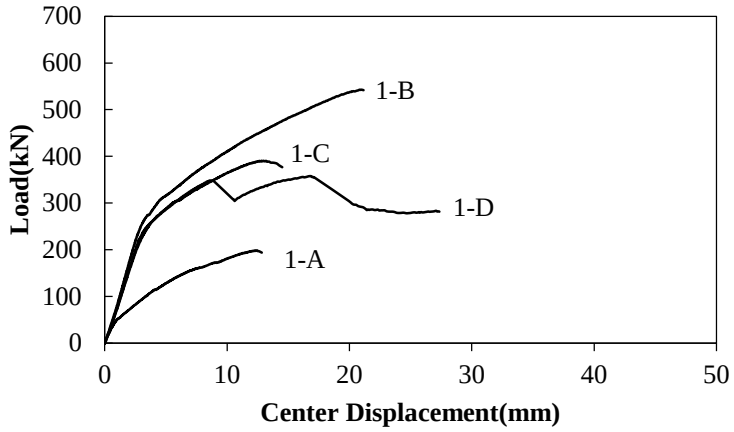

Fig 3.8 Load-center displacement relationship 1-A ~ 1-D (a/d=3.0, f_{pj}=0.55f_{pu})

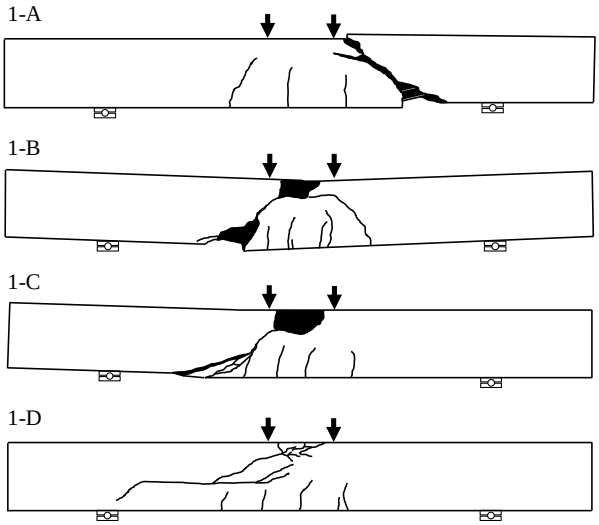

Fig 3.9 Crack pattern of specimen 1-A ~ 1-D at the end of test (a/d=3.0, f_{pj}=0.55f_{pu})

Table 3.4 Test result of specimen 1-A ~ 1-D (a/d=3.0, f_{pj}=0.55f_{pu})

Specimens	f_{ck} (MPa)		V_{test} (kN)	$V_{predicted}$ (kN)		$\frac{V_{test}}{V_{general}}$	$\frac{V_{test}}{V_{detailed}}$
	24MPa	60MPa		$V_{general}$	$V_{detailed}$		
1-A	23		100	68	71	1.48	1.42
1-B		57	272	262	233	1.04	1.17
1-C	23	57	196	172	208	1.14	0.94
1-D	23	57	179	112	149	1.59	1.20

3.2.2 Specimens 2-A ~ 2-D (a/d=3.0, f_{pj}=0.70f_{pu})

The specimens 2-A ~ 2-D are a/d=3.0 and f_{pj}=0.70f_{pu} and test result are shown in **Fig 3.10**, **Fig 3.11**, and **Table 3.5**. The shear strength is proportional to the area ratio of prestressed sections: 1-B (632 kN) > 1-C (456 kN) > 1-D (358 kN) > 1-A (154 kN). There is difference between shear strength of prestressed member and that of nonprestressed member. Flexural cracks occurred at 45 kN (2-A), 266 kN (2-C, 2-D), and 334kN (2-B). Thus, the strength of flexural cracking and diagonal shear cracking increases as jacking force increases from 0.55f_{pu} to 0.70f_{pu}.

As shown in **Fig 3.11**, crack patterns of specimens at the end of test were similar to specimens 1-A ~ 1-D. Failure of all the specimens were diagonal tension failure and horizontal cracking with inclined cracking occurred in 2-D.

In 2-A, shear strength provided by dowel action decreased caused by bond slip of strands thus shear strength of 2-A was 23 percent lower than that of 1-A. In 2-B and 2-C, early flexural cracking propagated to inclined cracking and finally concrete crushing of compressive zone occurred. Because strain of strands was respectively ε_{ps}=2,562 $\mu\varepsilon$ and ε_{ps}=4,987 $\mu\varepsilon$ which were less than ε_{pu}=8,829 $\mu\varepsilon$ thus flexural failure did not occur. In 2-D, there are three peak loading points according to load-displacement relationship. The first step is occurring horizontal shear cracking at right side of the beam and the second step is occurring horizontal shear cracking and inclined cracking at left side of beam. Finally inclined cracking and increasing of crack width occurred.

Failure mechanism of specimens having a/d=3.0 is different according to concrete strength of compressive zone. In the section B and C having 60 MPa in the web, a flexural crack propagated toward the loading point and was transformed to a diagonal shear crack. Then, shear failure occurred. On the other hand, in section A and D having 24 MPa in the web, a diagonal shear crack developed in the web was propagated to the loading and support points and then specimens failed.

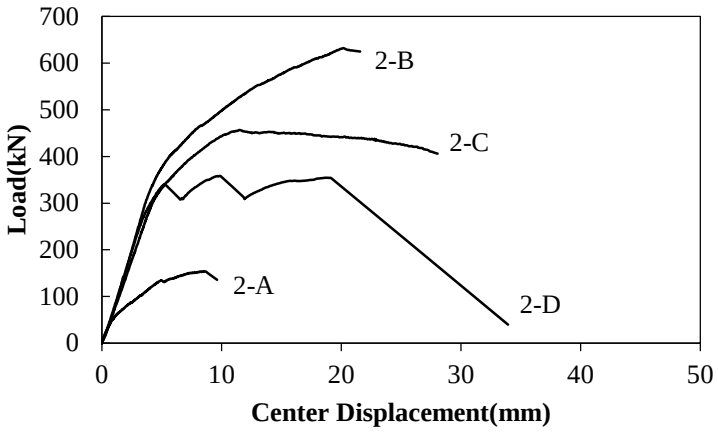

Fig 3.10 Load-center displacement relationship 2-A ~ 2-D (a/d=3.0, f_{pj}=0.70f_{pu})

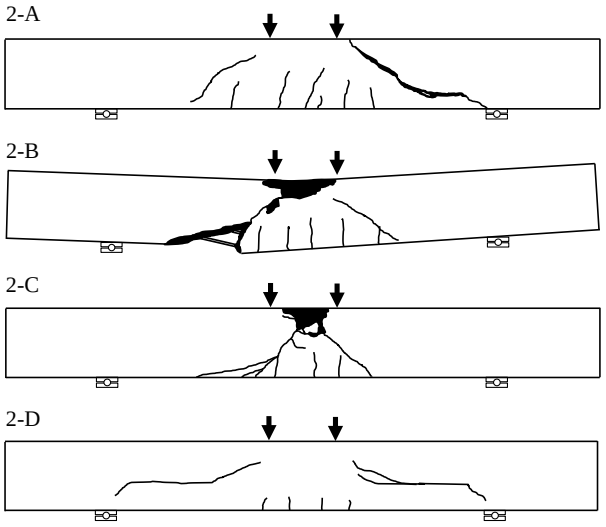

Fig 3.11 Crack pattern of specimen 2-A ~ 2-D at the end of test (a/d=3.0, f_{pj}=0.70f_{pu})

Table 3.5 Test result of specimen 2-A ~ 2-D (a/d=3.0, f_{pj}=0.70f_{pu})

Specimens	f_{ck} (MPa)		V_{test} (kN)	$V_{predicted}$ (kN)		$\frac{V_{test}}{V_{general}}$	$\frac{V_{test}}{V_{detailed}}$
	24MPa	60MPa		$V_{general}$	$V_{detailed}$		
2-A	23		77	68	71	1.14	1.09
2-B		57	316	262	277	1.21	1.14
2-C	23	57	228	172	225	1.32	1.01
2-D	23	57	179	112	157	1.59	1.14

3.2.3 Specimens 3-A ~ 3-D (a/d=4.0, f_{pj}=0.70f_{pu})

The test results of specimens 3-A ~ 3-D having a/d=4.0 and 0.70f_{pu} are shown in **Fig 3.12**, **Fig 3.13**, and **Table 3.6**. Also, shear strength of specimen increases as the prestressed area increases: 3-B (428 kN) > 3-C (284 kN) > 3-D (278 kN) > 3-A (144 kN). Early flexural cracks occurred at 42 kN (3-A), 156 kN (3-C, 3-D), and 223 kN (3-B). The strengths of flexural cracking and diagonal shear cracking decreased due to higher shear span to depth ratio. Thus shear strength of 3-B is 32 percent lower than that of 2-B. And maximum strain of strands is ε_{ps}=4,563 $\mu\varepsilon$ which is less than ε_{pu}=8,829 $\mu\varepsilon$ thus also flexural failure did not occur.

Flexural-shear failure occurred to specimens 3-A and 3-B. And In specimen 3-C and 3-C, horizontal shear crack occurred and propagated to loading point after early flexural cracking. By comparison between cracking pattern of 3-A and that of 3-B, compressive force caused by prestressing changed shear failure behavior. Shear failure of 3-B which is prestressed member was delayed by prestressing force even severe diagonal shear cracking occurred. However, nonprestressed member 3-A failed rapidly after diagonal shear crack occurred in the web. Prestressing force applied between diagonal shear cracking was contributed to increase shear strength. According to increase shear span to depth ratio, specimens are subjected to flexural action so failure modes of composite sections C and D were changed. Diagonal shear cracks initiated in CIP member (24 MPa) were propagated to the interface having lower friction resistance, and then diagonal and horizontal shear failure occurred.

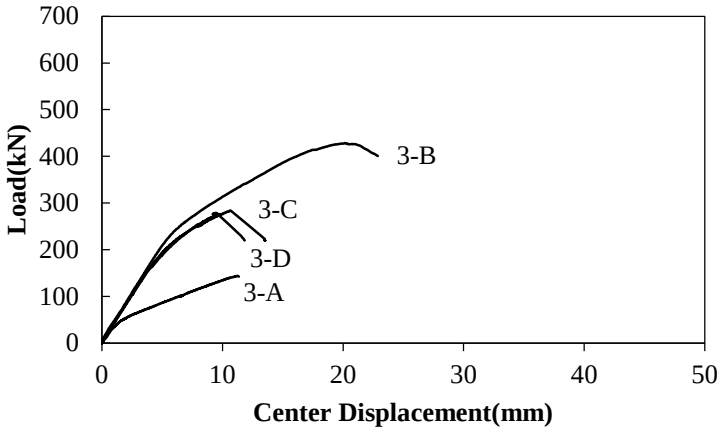

Fig 3.12 Load-center displacement relationship 3-A ~ 3-D (a/d=4.0, f_{pj}=0.70f_{pu})

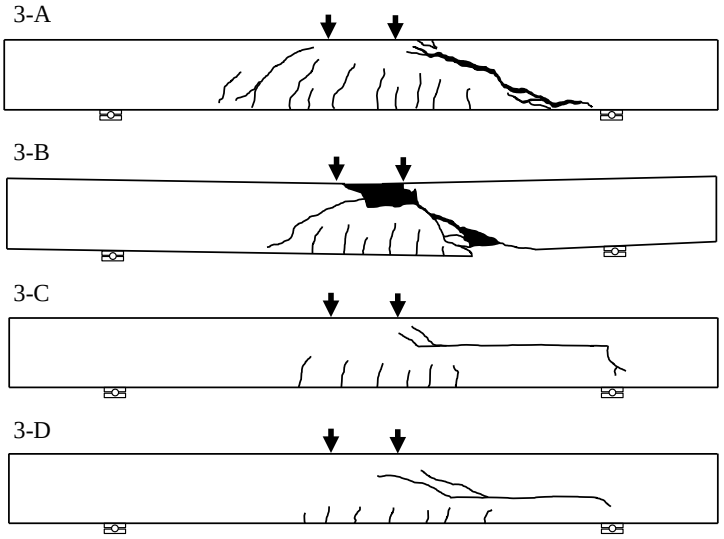

Fig 3.13 Crack pattern of specimen 3-A ~ 3-D at the end of test (a/d=4.0, f_{pj}=0.70f_{pu})

Table 3.6 Test result of specimen 3-A ~ 3-D (a/d=4.0, f_{pj}=0.70f_{pu})

Specimens	f_{ck} (MPa)		V_{test} (kN)	$V_{predicted}$ (kN)		$\frac{V_{test}}{V_{general}}$	$\frac{V_{test}}{V_{detailed}}$
	24MPa	60MPa		$V_{general}$	$V_{detailed}$		
3-A	23		72	68	69	1.07	1.04
3-B		57	214	204	215	1.05	0.99
3-C	23	57	142	141	200	1.01	0.71
3-D	23	57	139	99	140	1.40	0.99

3.2.4 Specimens 4-A ~ 4-D (a/d=4.0, f_{pj}=0.70f_{pu}, s=450 mm)

Specimens 4-A ~ 4-D are a/d=4.0, 0.70f_{pu}, and s=450 mm which is minimum shear reinforcements for horizontal shear strength. Test result are shown in **Fig 3.14**, **Fig 3.15**, and **Table 3.7**. In **Fig 3.15**, the location of shear reinforcement is indicated with gray line. Shear strength of specimens was presented: 4-B (514 kN) > 4-C (382 kN) > 4-D (366 kN) > 4-A (200 kN). These values also present that shear strength of specimen increases as the prestressed area increases. The shear strength of 4-A ~ 4-D which are specimens with shear reinforcement increased 20~39 percent rather than specimens 3-A ~ 3-D which are specimens without shear reinforcement. Early flexural crack occurred at 75 kN (4-A), 240 kN (4-B), 230 kN (4-C), and 250 kN (4-D). And maximum strain of strands was ε_{ps}=9,286 με which was less than ε_{pu}=12,803 με thus also flexural failure did not occur.

According to load-center displacement relationship, flexural stiffness and flexural cracking strength are same as 3-A ~ 3-D but shear strength increases because minimum shear reinforcements simultaneously resist vertical and horizontal shear after diagonal shear cracking. Also center displacement of beam with shear reinforcement at peak load is higher than that of beam without shear reinforcement.

And shear compression failure with diagonal shear cracks occurred in all the specimens. Also, as horizontal shear crack was controlled by shear reinforcement, composite section 4-C and 4-D showed different crack patterns from 3-C and 3-D. Diagonal shear crack were penetrated to shear reinforcement, shear strength of all the specimens increased in spite of same test conditions of 3-A ~ 3-D.

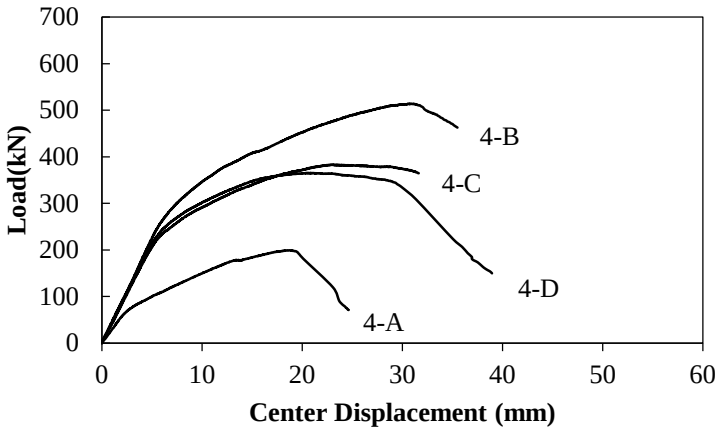

Fig 3.14 Load-center displacement relationship 4-A ~ 4-D (a/d=4.0, f_{pj}=0.70f_{pu}, s=450 mm)

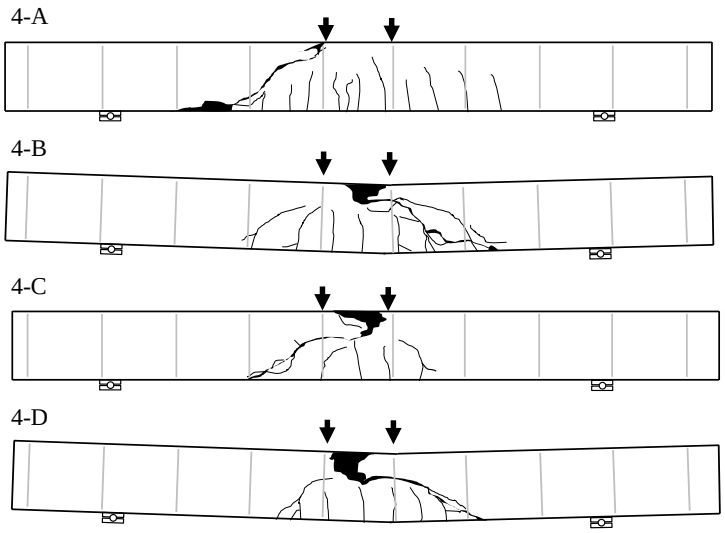

Fig 3.15 Crack pattern of specimen 4-A ~ 4-D at the end of test (a/d=4.0, f_{pj}=0.70f_{pu}, s=450 mm)

Table 3.7 Test result of specimen 4-A ~ 4-D (a/d=4.0, f_{pj}=0.70f_{pu}, s=450 mm)

Specimens	f_{ck} (MPa)		V_{test} (kN)	$V_{predicted}$ (kN)		$\frac{V_{test}}{V_{general}}$	$\frac{V_{test}}{V_{detailed}}$
	24MPa	60MPa		$V_{general}$	$V_{detailed}$		
4-A	22		100	97	99	1.03	1.01
4-B		53	257	234	244	1.10	1.05
4-C	22	53	191	188	245	1.02	0.78
4-D	22	53	183	157	196	1.17	0.93

3.3 Analysis

3.3.1 Effect of Test Parameters

Fig 3.16 shows shear strength according to test parameters which are prestress force, shear span-to-depth ratio (*a/d*), and shear reinforcement ratio (ρ_v). Because flexural stiffness and strength of section C and Section D which are prestressed composite sections are different from that of section A which is nonprestressed section, these sections are compared with section B which is prestressed total cross section.

Fig 3.16(a) shows shear strength according to prestress force. With respect to prestressed specimens having *a/d*=3.0, shear strength of section B and section C increases as prestress force increases. Shear strength of section B and section C with $0.70f_{pu}$ increased 16 percent higher than that of specimens with $0.55f_{pu}$. In section D, shear strength did not change in spite of increasing prestress force because horizontal crack and diagonal tensile failure occurred in CIP concrete which has no direct influence of prestress force. Thus location of crack pattern is important factor that prestress force can influence shear strength.

Fig 3.16(b) shows effect of shear span-to-depth ratio (*a/d*) on shear strength. With regard to specimens having $0.70f_{pu}$, shear strength of section B, section C and section D with *a/d*=4.0 is 22~37 percent less than that of specimens with *a/d*=3.0. Section A which is non prestressed section shows that shear strength decreases 6 percent.

Fig 3.16(c) shows effect of shear reinforcement ratio (ρ_v) on shear strength. For specimens having a/d=3.0, $0.70f_{pu}$, shear strength of all the specimens with minimum shear reinforcement increased. In composite section C and section D, horizontal crack did not occurred because shear reinforcement constrained horizontal crack and shear strength increased 35 percent and 32 percent respectively. The shear strength of total cross section B increased 20 percent

due to shear reinforcement penetrated to diagonal shear crack. Maximum strain of shear reinforcement at the maximum load is 1,143 $\mu\varepsilon$ which dos not reach yield strain (1,847 $\mu\varepsilon$) of shear reinforcement.

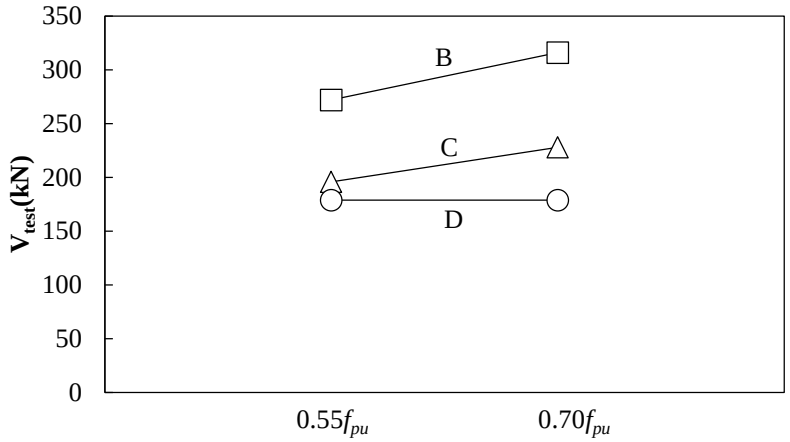

(a) Prestress force (f_{pj})

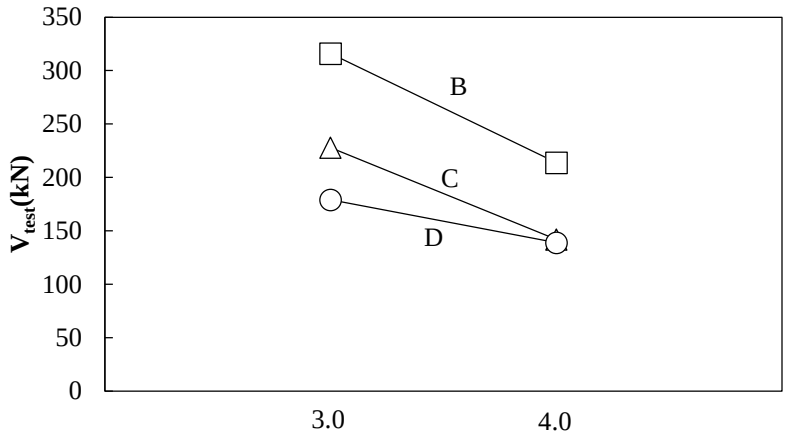

(b) Shear span-to-depth ratio (a/d)

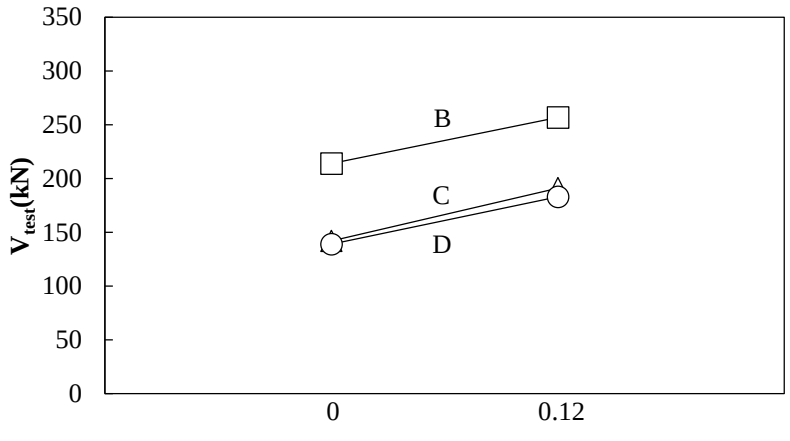

(c) Shear reinforcement ratio (%)

Fig 3.16 Effect of test parameters

3.3.2 Contribution of prestress force

To investigate effect of prestress force on shear strength, comparison between prestressed section (PSC) and nonprestressed section (RC) was conducted and classified by section type as shown in **Fig 3.17**. Flexural reinforcement ratio of RC specimens are similar to that of PSC specimens. And because section A is nonprestressed section of total cross section, it is excluded from comparison.

Fig 3.17(a) shows load-center displacement relationship of RC and PSC having a/d=3.0. Solid line presents results of PSC and dotted line presents result of RC. In RC specimens, flexural stiffness decreased with occurring early flexural crack. In PSC specimens, early flexural strengths with $0.55f_{pu}$ and $0.70f_{pu}$ were 2.3~2.5 times and 2.7~3.3 times higher than that of RC specimens. And shear strength increases as prestress force increases.

In $0.55f_{pu}$, shear strengths of total cross section B (60 MPa) increased 2.0 times and that of composite section C and D increased 1.6 and 1.7 times higher than shear strength of RC specimens. And In $0.70f_{pu}$, shear strength of section B increased 2.3 times and that of section C and D increased 1.8 and 1.7 times higher than shear strength of RC specimens. Center displacements at shear failure of all the specimens increased because of prestress force.

Also, **Fig 3.17(b)** shows load-center displacement relationship of RC and PSC having a/d=4.0. In RC specimens, flexural stiffness decreased with occurring early flexural crack. However, in PSC specimens, early flexural strength was 3.3~3.8 times higher than that of RC specimens because of prestress force. Shear strength of total cross section B (60 MPa) increased 2.2 times higher than that of RC specimen and shear strength of composite section C and D increased 1.3 and 1.5 times respectively.

And at occurring shear failure of composite section C and D, there is no difference between center displacement of PSC and RC regardless of prestress

force. In PSC specimens, shear strength is higher than that of RC specimens because early flexural stiffness maintained due to prestress force. Whereas after horizontal cracking, diagonal tension crack occurred in nonprestressed CIP concrete (24 MPa) even though flexural cracking strength was increased due to prestress force as shown in **Fig 3.13**.

Thus, contribution of prestress force on shear strength of flexural members without shear reinforcement is as fallows. In section B which is total cross section with prestress force, early flexural strength and inclined cracking strength significantly increased. In case of composite section C and D which prestress force applied to only PC member, flexural strength increased but inclined cracking occurred in nonprestressed CIP concrete did not be influenced by prestress force.

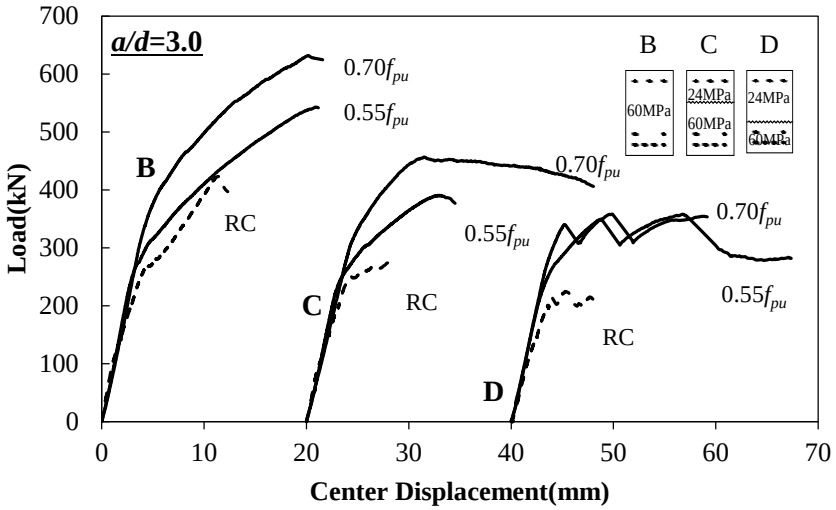

(a) Load-center displacement relationship (*a/d*=3.0)

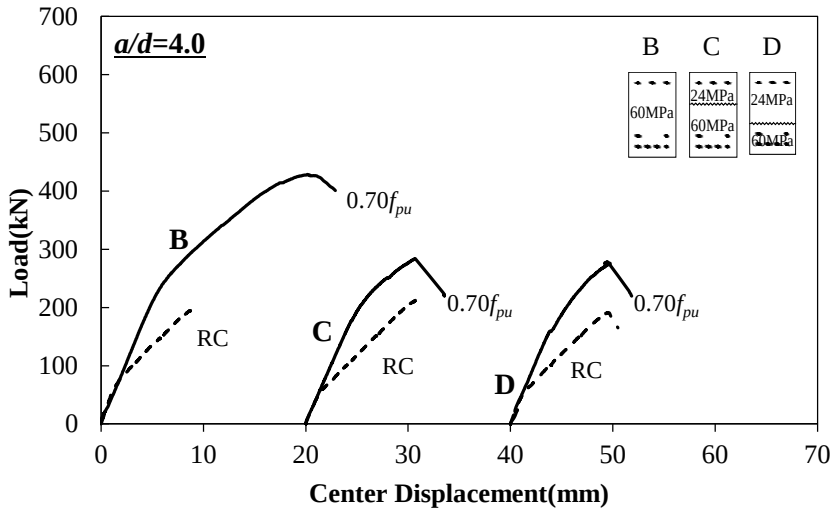

(b) Load-center displacement relationship (*a/d*=4.0)

Fig 3.17 Comparison between PSC and RC specimens

3.3.3 Comparison with Criteria of Vertical Shear Strength

To estimate vertical shear strength of prestressed PC-CIP composite beams, test results and predicted values with current code are compared. Because composite beams consist of two different elements, shear strength of prestressed PC member is calculated by general equation Eq. (2-3) and detailed equation Eq. (2-4), and Eq. (2-6) and that of CIP members is calculated by general equation Eq. (2-1) and detailed equation Eq. (2-2) individually.

Shear strength of prestressed PC members increases due to pre-compression. However shear strength of CIP members does not increase because of nonprestress. Thus, combined method to predict shear strength of composite members which shear strength of prestressed PC member and CIP member are calculated respectively and combined each other were used.

Fig 3.18 shows shear strength prediction of all the specimens. Circle shows values used general equations and square shows values detailed equations. In case of values used general equations, shear strength is calculated by combining Eq. (2-1) and Eq. (2-3). And in case of values used detailed equations, shear strength calculated by combining Eq. (2-2) and minimum value between Eq. (2-4) and Eq. (2-6).

When using combined method with general equation, all the specimens are predicted in safety side. Test value versa predicted value of section D (1-D, 2-D, 3-D, 4-D) which proportion of prestressed area is 3/8 of gross section ranges from 1.40 to 1.59 and this range shows rather conservative. Despite prestressed area is relatively less than gross section, prestress force contribute to increase shear strength.

When using combined methods with detailed equation, shear strength of composite section (1-C, 3-C, 4-C) are in non-safety side and rest of specimens are in safety side. Thus, if shear strength of composite beams are predicted with detailed equation, safety probability shall be considerate. And more theoretical

approaches about detailed equations are needed.

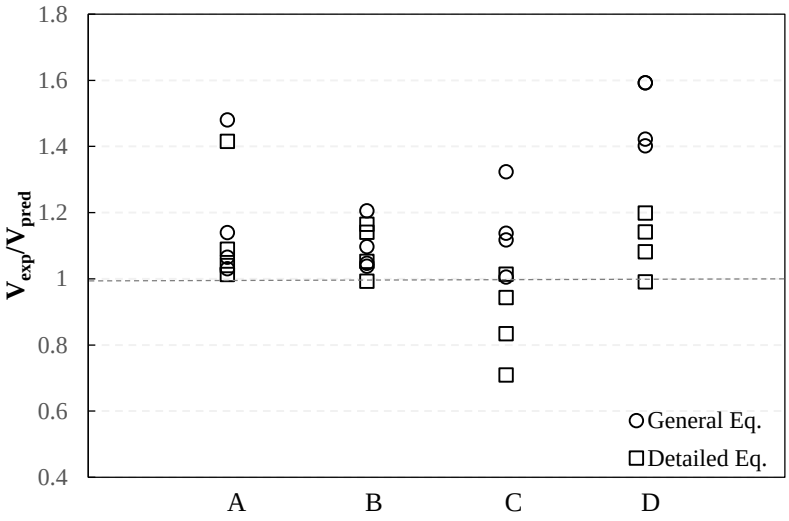

Fig 3.18 Shear strength prediction of specimens

3.3.4 Comparison with Criteria of Horizontal Shear Strength

In this study, horizontal shear cracks and diagonal tensile crack occurred in composite specimens without shear reinforcement except 1-C and 2-C. Before early flexural cracks develop inclined crack, inclined crack occurring in compressive zone propagated to support following interface. Finally horizontal shear failure and diagonal tensile failure occurred. Because shear reinforcement did not be arranged, there is the potential for horizontal shear crack to happen thus calculation of horizontal shear strength is important. As shown in **Fig 3.19**, horizontal shear stress in interface of PC composite beams is due to shear flow according to difference between inflection point of moment and maximum moment point (l_{vh}). Horizontal shear stress is able to be calculated from vertical shear stress or actual variation (F_h) of compressive force or tensile force as shown in **Fig 3.20** and Eq.(3-1).

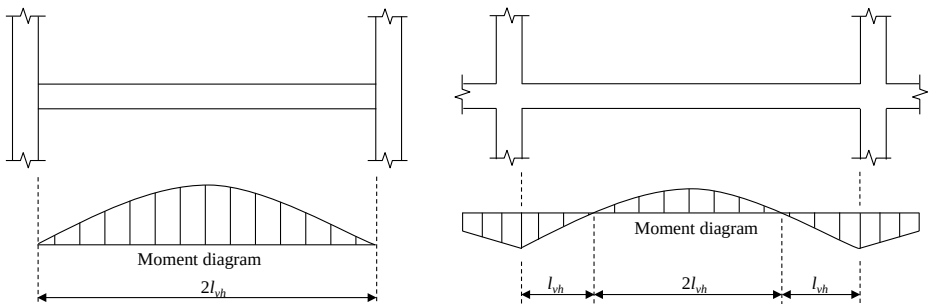

Fig 3.19 Length (l_{hv}) for horizontal shear

$$v_u = f_h = \frac{F_h}{A_{cr}} = \frac{F_h}{b_v l_{vh}} \tag{3.1}$$

where, $F_h = \min\left[0.85 f_{cc}' A_{top}, A_s f_y + A_{ps} f_{ps}\right]$

l_{vh} = length from inflection point to maximum moment point,

b_v = width of the interface

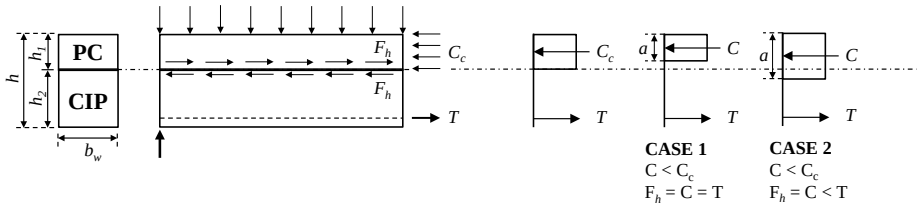

Fig 3.20 Horizontal shear in composite section

ACI 318-11 [2] suggests that where contact surfaces are clean, free of laitance, and intentionally roughened, (Eq. 2-8) shall be used and Eq.(2-8) is based on horizontal shear transfer mechanism.

Horizontal shear strengths of composite section without shear reinforcement (1-C,D, 2-C,D, 3-C,D) are shown in **Table 3.8**. These values are 3.3~5.4 times higher than current design code Eq. (2-8). Thus current design code evaluates horizontal shear strength conservatively. Whereas, not horizontal shear crack but diagonal tensile crack occurred in 4-C, 4-D which are composite beams with shear reinforcement. Ratios of experimental values to predicted values are 1.19 and 1.24. Thus experimental values are 20 percent higher than current code (Eq. 2-9) with horizontal shear transfer mechanism.

In early studies about horizontal shear strength of composite section without shear reinforcement, CTA 11 [14] suggested horizontal shear strength that 0.63 MPa in case of smooth interface, 1.12 MPa in case of 1.5 mm roughen surface, 2.1 MPa in case of 6 mm roughen surface. And in experimental study of Jonathan and Clay [15], horizontal shear strength showed 6~10 times higher than current design code and 4 MPa in case of 6 mm roughen contact surface could be applied to shear design according to state of contact surface.

In simple supported beams, diagonal strut action and arch action occurred near the loading points and hinges at both ends. In interface between PC and CIP, therefore, horizontal shear force which is parallel with interface and compressive force which is perpendicular to interface are applied to composite beams. And capacity of horizontal shear increases compared with current

design codes.

Table 3.8 Observed horizontal shear strength of specimens without shear reinforcement

Specimens	Section type	Calculated strength		P_{max} (kN)	M_{max} (kN·m)	Horizontal shear at the interface (MPa)		$\frac{v_u}{v_{nh}}$
		V_n (kN)	M_n/a (kN)			v_u	Shear transfer v_{nh}	
1-C	C	172	223	196	191	2.58	0.56	4.60
1-D	D	112	351	179	175	2.35	0.56	4.20
2-C	C	172	229	228	223	3.00	0.56	5.35
2-D	D	112	351	179	175	2.35	0.56	4.20
3-C	C	141	229	142	185	1.87	0.56	3.33
3-D	D	99	351	139	181	1.83	0.56	3.26
4-C	C	140	173	191	248	2.51	2.06	1.22
4-D	D	98	267	183	238	2.41	2.06	1.17

3.4 Discussion

To investigate shear strength of prestressed PC-CIP composite beams without shear reinforcement, tests were performed according to area ratio of prestressed PC and CIP, prestress force, shear span-to-depth ratio, and minimum shear reinforcement. And thereby analysis of test results, shear behaviors and design consideration of composite beams were investigated. Conclusion of this study is as follows:

1) Shear behaviors of composite section C and D was similar to that of total cross section B. Early flexural strength and early flexural stiffness of prestressed composite beams shows higher than that of nonprestressed specimens. Shear strength increased as prestressed area and prestress force increased and shear span-to-depth ratio decreased.

2) Failure mechanism of prestressed composite beams shows difference according to concrete strength of web. In section B and C which concrete strength of web is 60 MPa, early flexural crack developed inclined cracks occurred. In section A and C which concrete strength of web is 24 Mpa, brittle failure occurred due to diagonal tensile cracks. In case of 4.0 shear span-to-depth ratio, beam action was dominant thus horizontal shear crack preceded but horizontal shear crack did not occur when applying minimum shear reinforcement.

3) In case of using combined estimation with general equation, the test results of all the specimens are in safety side. In case of using detailed equation, experimental values of specimens with total cross section were in safety side. But in case of composite section, most test values were in non-safety side. Thus, estimation with detailed equation might cause stability problems.

4) In regard with horizontal shear of interface between prestressed PC and

CIP, comparison with test results and current design code was conducted. Horizontal shear strength of composite beams without shear reinforcement shows 3.4~4.3 times higher than current code and thus current code has predicted horizontal shear strength as conservative assessment. In case of specimens with minimum shear reinforcement, horizontal shear crack did not occur and test results showed 20 percent higher than current code.

Chapter 4. Shear Strength of Prestressed PC-CIP Composite Beams with Web Reinforcement

4.1 Test Program

4.1.1 Test Parameters

To investigate contribution of shear reinforcement ratio, 22 simply supported beams were tested. There are also four kinds of main parameters: the area ratio of PC and CIP, prestressing force, shear span-to-depth ratio and shear reinforcement ratio.

The first parameter is section type. As shown in **Fig 4.1**, there are four types of area ratio of PC (60 MPa) and CIP (24 MPa) as before. Section A and B are gross section of 24 MPa and 60 MPa respectively. In composite section C and D, high-strength concrete of 60 MPa are 5/8 and 3/8 of PC members respectively and the rest of section was filled with low-strength concrete of 24 MPa. To obtain definite results for increasing difference between high-strength concrete and low-strength concrete and reflect tendency of high strengthening of materials, 60 MPa strength concrete for high-strength concrete were used instead of 40 MPa.

The second parameter is prestressing force. To investigate the effect of prestressing force on shear strength, two jacking forces were applied at six strands. One is 55 percent of tensile strength of prestressing steel and the other is 70 percent of that. These prestressing (generally pre-tension) forces applied to PC members (60 MPa) only, thus CIP members (24 MPa) were not applied. In the case of section A which are gross section of 24 MPa strength concrete, six strands were placed in members but did not be applied tensile force.

The third main parameter is shear span-to-depth ratio (*a/d*). The member can be defined as deep beam and slender beam when *a/d* is less or more than 2.5 respectively. To investigate the effect of shear span-to-depth ratio on failure mechanisms and shear strength, 3.0 and 4.0 of shear span-to-depth ratios are applied.

The last parameter is shear reinforcement ratio. There are three kinds of shear reinforcement ratio. 0.27 percent and 0.18 percent of shear reinforcement ratio which are 200 mm and 300 mm spacing of shear reinforcement respectively are able to resist both vertical shear force and horizontal shear force. On the other hand, 0.12 percent of minimum shear reinforcement ratio which is 450 mm spacing of that is able to resist only horizontal shear force.

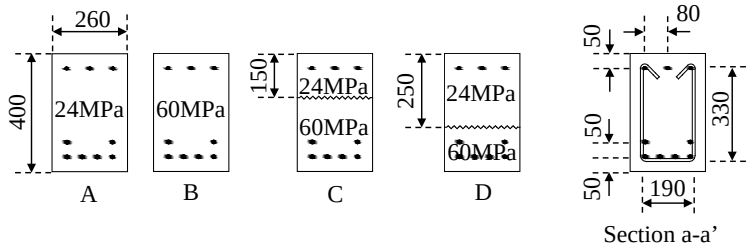

Fig 4.1 Cross section types A~D and cross section of specimen (a-a')

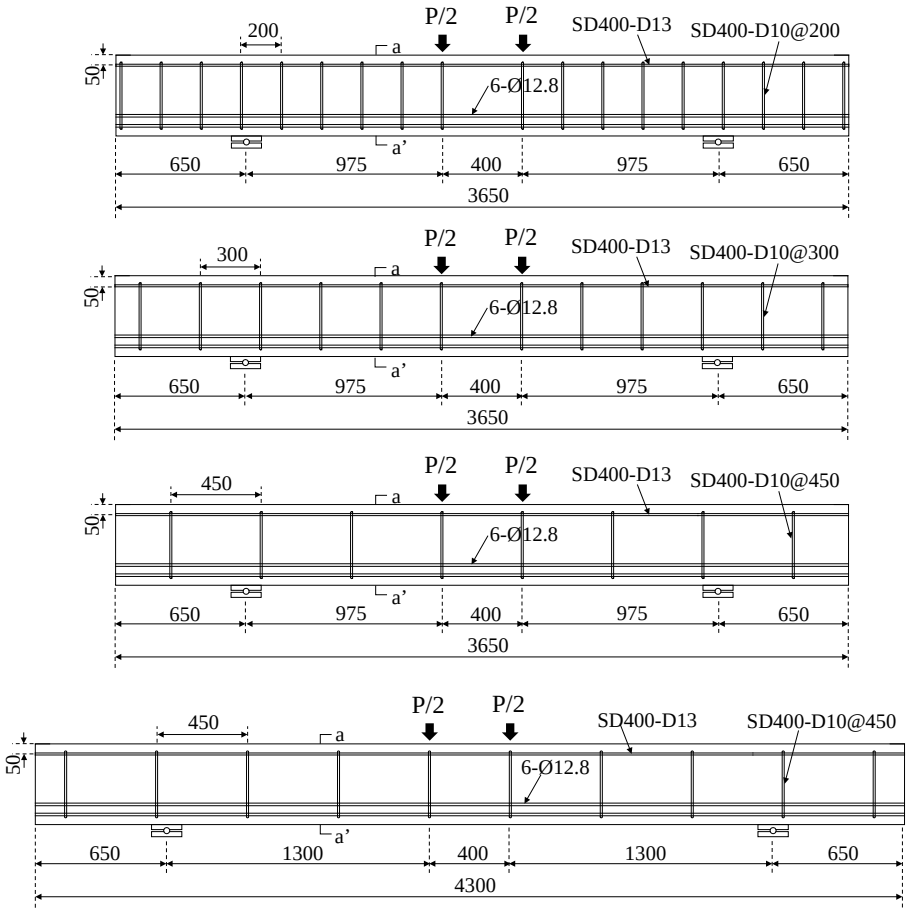

Fig 4.2 Reinforcement Arrangement

Table 4.1 Test variables and predictions of moment and shear capacities of specimens (Continued)

Specimens	Section type	Re-bar (ρ)	Stirrup (ρ_v)	s (mm)	Prestressing force (f_{pj})	a/d	M_n (kN·m)	V_m (kN)	V_n (kN)	$\frac{V_m}{V_n}$	V_{nh} (kN)	V_{hv} (kN)	$\frac{V_{hv}}{V_{nh}}$
1-AS	A	6-ϕ12.7 (0.57%)	2-D10 (0.27%)	200	$0.55f_{pu}$	3.0	219	224	139	1.61			
1-BS	B	6-ϕ12.7 (0.57%)	2-D10 (0.27%)	200	$0.55f_{pu}$	3.0	288	295	332	0.88			
1-CS	C	6-ϕ12.7 (0.57%)	2-D10 (0.27%)	200	$0.55f_{pu}$	3.0	227	232	243	0.95	581	833	1.43
1-DS	D	6-ϕ12.7 (0.57%)	2-D10 (0.27%)	200	$0.55f_{pu}$	3.0	222	227	183	1.24	581	628	1.08
2-AS	A	6-ϕ12.7 (0.57%)	2-D10 (0.12%)	450	$0.55f_{pu}$	3.0	219	224	100	2.24			
2-BS	B	6-ϕ12.7 (0.57%)	2-D10 (0.12%)	450	$0.55f_{pu}$	3.0	288	295	294	1.00			
2-CS	C	6-ϕ12.7 (0.57%)	2-D10 (0.12%)	450	$0.55f_{pu}$	3.0	227	232	204	1.13	512	700	1.37
2-DS	D	6-ϕ12.7 (0.57%)	2-D10 (0.12%)	450	$0.55f_{pu}$	3.0	222	227	145	1.57	512	496	0.97
3-BS	B	6-ϕ12.7 (0.57%)	2-D10 (0.27%)	200	$0.70f_{pu}$	3.0	288	295	332	0.88			
3-CS	C	6-ϕ12.7 (0.57%)	2-D10 (0.27%)	200	$0.70f_{pu}$	3.0	227	232	243	0.95	581	833	1.40
3-DS	D	6-ϕ12.7 (0.57%)	2-D10 (0.27%)	200	$0.70f_{pu}$	3.0	222	227	183	1.24	581	628	1.02
4-AS	A	6-ϕ12.7 (0.57%)	2-D10 (0.18%)	300	$0.70f_{pu}$	3.0	219	224	115	1.94			
4-BS	B	6-ϕ12.7 (0.57%)	2-D10 (0.18%)	300	$0.70f_{pu}$	3.0	288	295	309	0.95			
4-CS	C	6-ϕ12.7 (0.57%)	2-D10 (0.18%)	300	$0.70f_{pu}$	3.0	227	232	220	1.05	540	753	1.37
4-DS	D	6-ϕ12.7 (0.57%)	2-D10 (0.18%)	300	$0.70f_{pu}$	3.0	222	227	160	1.42	540	549	0.97
5-BS	B	6-ϕ12.7 (0.57%)	2-D10 (0.12%)	450	$0.70f_{pu}$	3.0	288	295	294	1.00			
5-CS	C	6-ϕ12.7 (0.57%)	2-D10 (0.12%)	450	$0.70f_{pu}$	3.0	227	232	204	1.13	512	700	1.16
5-DS	D	6-ϕ12.7 (0.57%)	2-D10 (0.12%)	450	$0.70f_{pu}$	3.0	222	227	145	1.57	512	496	0.76

■ **Table 4.1** Test variables and predictions of moment and shear capacities of specimens

Specimens	Section type	Re-bar (ρ)	Stirrup (ρ_v)	s (mm)	Prestressing force (f_{pj})	a/d	M_n (kN·m)	V_m (kN)	V_n (kN)	$\frac{V_m}{V_n}$	V_{nh} (kN)	V_{hv} (kN)	$\frac{V_{hv}}{V_{nh}}$
6-AS	A	6-ϕ12.7 (0.57%)	2-D10 (0.12%)	450	$0.70f_{pu}$	4.0	230	177	100	1.68			
6-BS	B	6-ϕ12.7 (0.57%)	2-D10 (0.12%)	450	$0.70f_{pu}$	4.0	280	216	236	0.93			
6-CS	C	6-ϕ12.7 (0.57%)	2-D10 (0.12%)	450	$0.70f_{pu}$	4.0	236	182	173	1.00	683	792	1.16
6-DS	D	6-ϕ12.7 (0.57%)	2-D10 (0.12%)	450	$0.70f_{pu}$	4.0	232	179	131	1.29	683	600	0.88

4.1.2 Test Specimens and Setup

Fig 4.1 shows size and arrangement of re-bar of cross section and **Fig 4.2** shows reinforcement arrangement and characteristics of specimens. Size of cross section is 260 mm by 400 mm. The span length between supporting point are 2,350 mm and 3,000 mm for a/d=3.0 and 4.0, respectively. Considering transfer length of prestressing, span length was extended to 650 mm from supporting points of both side also. As shown in **Fig 4.1**, the six strands are arranged with two layers in the precast members and covering depth which is distance from center of strands to extreme tension fiber is 50 mm. Also, to resist tensile force acting upper apart of beams due to prestressing, three SD400-D13 were arranged with a layer in the compression zone. And according to shear reinforcement parameter, shear reinforcement were placed in specimens.

Table 4.1 shows predicted values of flexural moment, vertical shear and horizontal shear strength in 22 specimens. The required shear strength (V_m) to lead to flexural capacity (M_n) is more than vertical shear capacity, thereby, comparison between required shear strength and nominal shear strength (V_m/V_n) is ranged from 0.88 to 2.24. Flexural capacity of prestressed members was calculated according to ACI 318-11 10.2 and vertical shear strength of composite members which consist of PC member and CIP member was calculated by Eq. (2-1) and Eq.(2-3) respectively. Except some specimens (1-BS, 1-CS, 3-BS, 3-CS, 4-BS, 6-BS) which V_m/V_n is less than 1.0, all the specimens were predicted to be occurred shear failure before flexural failure.

Also, **Table 4.1** shows the comparison between nominal horizontal shear strength (V_{nh}) and horizontal shear force based on nominal vertical shear strength (V_{hv}). The former is calculated by Eq. (2-8) and the latter is multiplied shear stress of interface by contact area. As a result of comparison between V_{hv} and V_{nh}, V_{hv}/V_{nh} is ranged from 0.76 to 1.43. In case of section C which V_{hv}/V_{nh} is more than 1.0, horizontal shear failure was predicted before vertical shear failure. Whereas, in case of section C which V_{hv}/V_{nh} is less than 1.0, vertical

shear failure is predicted before horizontal failure.

Fig 4.3 Procedure for manufacture of composite beams shows procedure for manufacture of composite beams. Six strands and shear reinforcement were arranged in forms and strands were prestressed using hydraulic pumps. After attaching strain gauges to strands and stirrups, 60 MPa strength concrete was placed and cured with steam during about 6 hours. After 24 hours, prestressed strands were cut when concrete strength was 35 MPa. And laitance of surface was eliminated and surface was roughened to a full amplitude of approximately 6 mm. This process was repeated in twice as above. Then, 24 MPa strength concrete was placed on all the precast members of 60 MPa and cured with steam also. Standard specimens were made whenever concrete was placed.

(a) Arrangement re-bar (b) Prestressing strands (c) Placing precast concrete (d) Spreading retarder

(e) Dissolution forms (f) Placing cast-in-place concrete (g) Making standard specimens (h) Steam curing

Fig 4.3 Procedure for manufacture of composite beams

Test method is two point loading shear test by 1,000 kN hydraulic oil jack as shown in **Fig 4.4**. The beams were supported by hinges at both ends. To investigate the crack pattern, crack was drawn by the 50 kN until specimens

reached predicted shear capacity. In order to analyze failure mechanism, photographs and videos were taken.

Measurement methods is that loading forces were measured by load cell and deflections of center of the specimens were measured by 5 LVDTs which are located in center, two loading point and 800 mm from center of the specimen at both side. **Fig 4.5** shows measurement for contribution of shear reinforcement and flexural yielding of strands. To investigate yielding of strands occurred before flexural failure, four strain gauges (C1, C2, C3, C4) were attached to center of strands. In specimens with various shear reinforcement ratio, to investigate contribute of shear reinforcement, also strain gauges were attached to shear reinforcement between loading point and hinge end. In addition, to measure the crack width of inclined shear crack, Pi-type gauges located 200 mm from loading points. These loading data, strain data and crack width were collected by data logger.

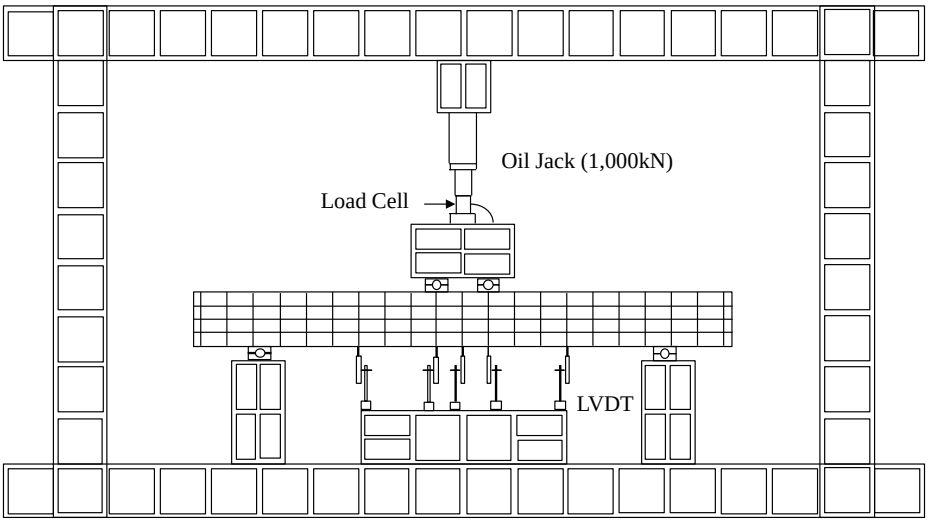

Fig 4.4 Test set-up

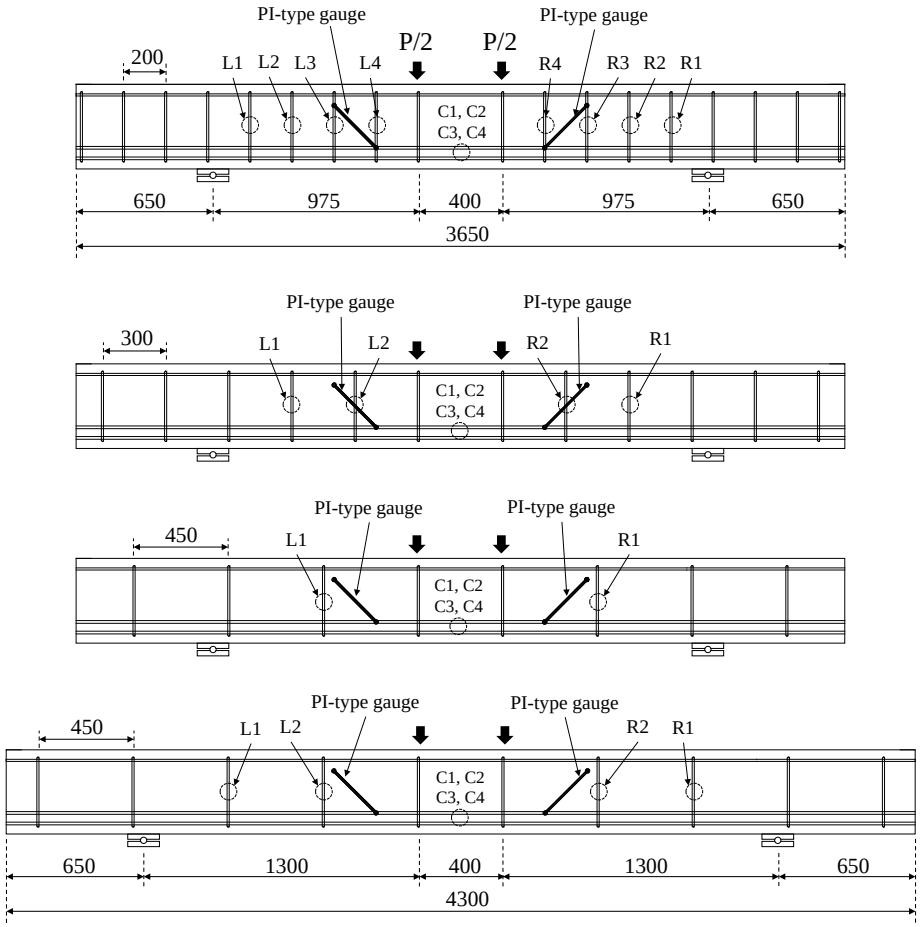

Fig 4.5 Measurement for contribution of shear reinforcement and flexural yielding

4.1.3 Materials

As before, **Table 4.2** shows mixture proportions of high-strength concrete and low-strength concrete of which nominal strengths are 60 MPa and 24 MPa respectively. Concrete standard specimens of 100 mm by 200 mm were made according to KS F 2403 and 3 standard specimens at a beam test were tested according to KS F 2405 called cylinder test. **Fig 4.6** shows actual concrete strength for 24 MPa and 60 MPa at test days. Actual compressive strength of 24 MPa and 60 MPa strength concrete were 22~23 MPa and 53~55 MPa. When estimating shear strength, concrete strengths on the day of beam test were used.

Table 4.2 Mixture proportions of concrete

Nominal strength	W/C (%)	Unit weight(kg/m^3)				
		W	C	S	G	SP
24	49.4	162	328	869	979	3.5
60	29	180	620	625	935	8.06

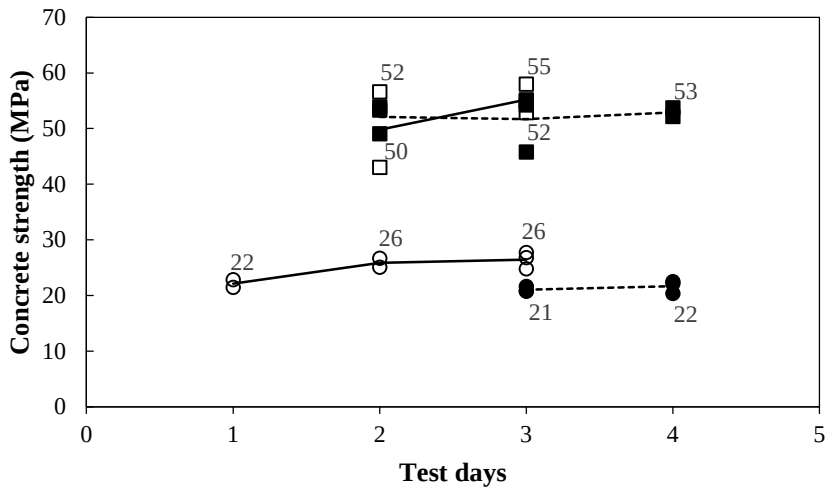

Fig 4.6 Concrete strength for 24 MPa and 60 MPa at test day

As shown in **Fig 4.7**, main reinforcement of beams were 12.7 mm SWPC 7BL which is called strands, SD300 D10, and SD400 D13. To evaluate mechanical properties of reinforcement, steel specimens were made according to KS B 0801 and these specimens were tested according to KS B 0802. **Table 4.3** shows these mechanical properties of reinforcement through the test. The yield strengths were f_y=1,869 MPa for 12.7 mm strand, and f_y=360 MPa for D10 bar, and f_y=480 MPa for D13 bars. As shown in **Fig 4.7**, the yield strength of the strands was estimated by the 1% extension method because there is no obvious yield point.

Table 4.3 Mechanical properties of reinforcement

Type	f_y (MPa)	ε_y (μ)	E_s (GPa)
12.7 mm SWPC 7BL	1,869	12,803	205
SD300 D10	360	1,847	184
SD400 D13	470	2,400	200

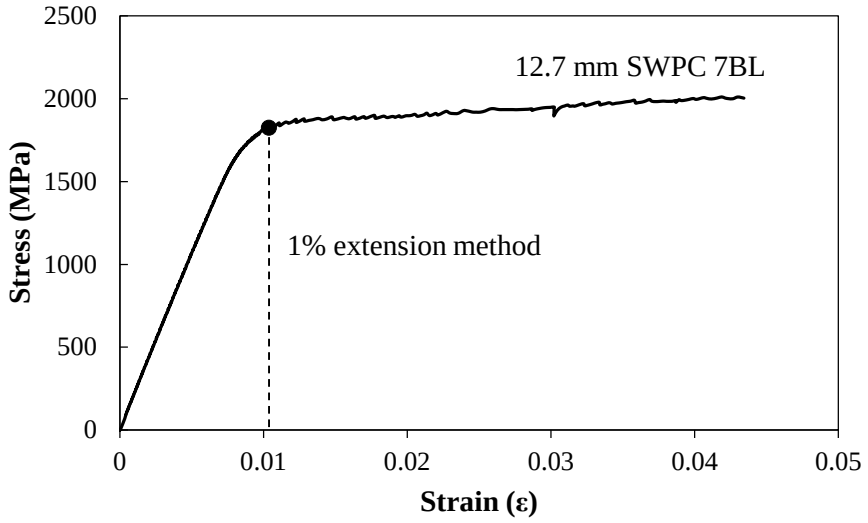

Fig 4.7 Yield stress of main reinforcement using offset method

4.2 Result

The test results are shown in **Table 4.4**, **Table 4.5**, **Table 4.6**, **Table 4.7**, **Table 4.8**, and **Table 4.9**. General and detailed equation for prestressed members ((Eq. (2-3), (2-4), and (2-6)) are used predict PC members (60 MPa) and general equation and detailed equation for nonprestressed members (Eq. (2-1), (2-2)) are used to predict CIP members (24 MPa) as former test.

4.2.1 Specimens 1-AS ~ 1-DS (a/d=3.0, f_{pj}=0.55f_{pu}, s=200 mm)

Specimens 1-AS ~ 1-DS are a/d=3.0, 0.55f_{pu} and s=200 mm which is able to resist horizontal shear and vertical shear. **Fig 4.8** shows load-center displacement relationship of specimens and **Fig 4.9** shows crack pattern at the end of the test and the location of shear reinforcement which is indicated with gray line. Comparison between experimental values and predicted values is shown in **Table 4.4**.

As a result of test, shear strength of specimens was presented that: 1-BS (686 kN) > 1-CS (490 kN) > 1-DS (424 kN) > 1-AS (372 kN). These values present that shear strength of specimen increases as the prestressed area increases. Early flexural strengths of 1-BS, 1-CS and 1-DS (310 kN, 260 kN, and 257 kN) are 2.65~3.20 times higher than that of 1-AS (97 kN). Thus shear strength and flexural strength of 1-A which is nonprestressed member are less than that of rest of specimens which are prestressed members

As shown in **Fig 4.9**, shear compressive failure occurred in all the specimens. In 1-AS, 1-BS, and 1-DS, early flexural crack propagated to inclined cracking and finally concrete crushing of compressive zone occurred. Because maximum strain of strands among 1-AS, 1-BS, 1-DS was ε_{ps}=9,152 $\mu\varepsilon$ which is less than ε_{pu}=12,803 $\mu\varepsilon$ thus flexural failure did not occur. In case of 1-CS, load decreased the moment horizontal shear crack occurred in left side of beam after early flexural cracking.

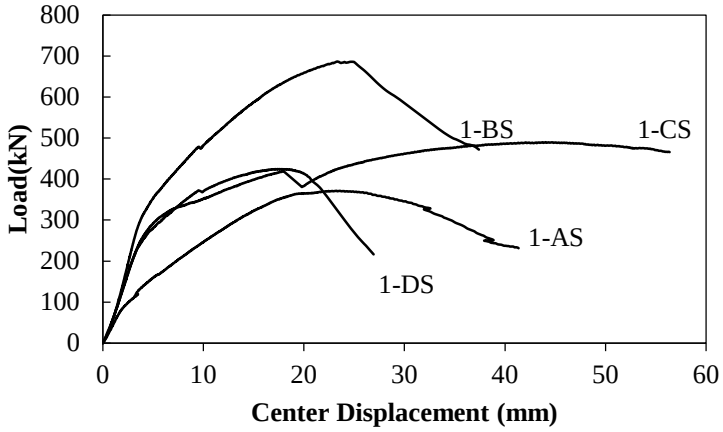

Fig 4.8 Load-center displacement relationship 1-AS ~ 1-DS (a/d=3.0, f_{pj}=0.55f_{pu}, s=200 mm)

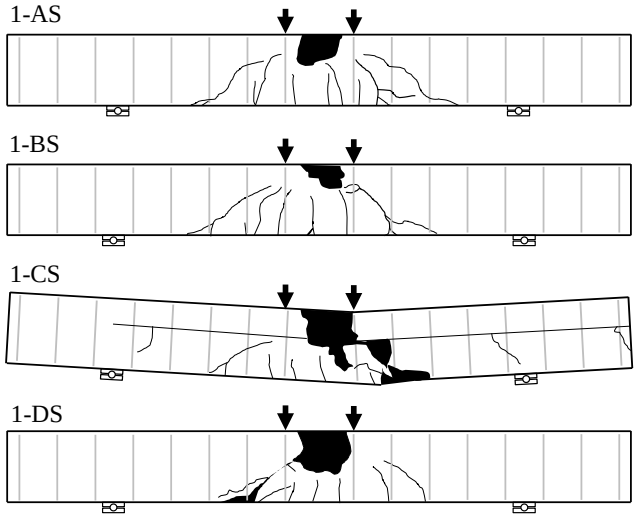

Fig 4.9 Crack pattern of specimen 1-AS ~ 1-DS at the end of test (a/d=3.0, f_{pj}=0.55f_{pu}, s=200 mm)

Table 4.4 Test result of specimen 1-AS ~ 1-DS (a/d=3.0, f_{pj}=0.55f_{pu}, s=200 mm)

Specimens	f_{ck} (MPa)		V_{test} (kN)	$V_{predicted}$ (kN)		$\frac{V_{test}}{V_{general}}$		$\frac{V_{test}}{V_{detailed}}$
	24 MPa	60 MPa		$V_{general}$	$V_{detailed}$			
1-AS	26		186	141	144	1.32		1.29
1-BS		55	343	331	302	1.03		1.13
1-CS	26	55	245	243	278	1.00		0.88
1-DS	26	55	212	185	221	1.15		0.96

4.2.2 Specimens 2-AS ~ 2-DS (a/d=3.0, f_{pj}=0.55f_{pu}, s=450 mm)

Test results of 2-AS ~ 2-DS having a/d=3.0, 0.55f_{pu}, s=450 mm is shown in **Fig 4.10**, **Fig 4.11**, and **Table 4.5**. Shear strengths of 2-AS ~ 2-DS were presented that: 2-BS (582 kN) > 2-CS (408 kN) > 2-DS (390 kN) > 2-AS (264 kN). Similar with 1-AS ~ 1-DS, shear strength of specimen increases as the prestressed area increases. In 2-BS, 2-CS and 2-DS, early flexural strengths were 300 kN, 260 kN, and 284 kN respectively and were 3.79~4.00 times higher than early flexural strength of 2-AS (75 kN). Maximum strain of strands is ε_{ps}=5,094 $\mu\varepsilon$ in 2-BS which is less than ε_{pu}=12,803 $\mu\varepsilon$ thus thus flexural failure did not occur.

As shown in **Fig 4.11**, crack patterns of all specimens at the end of test showed diagonal tensile failure. Location of shear reinforcement is indicated with gray line. In 2-A, bond slip occurred at early stage and diagonal tensile failure occurred. In 2-BS, compressive shear failure occurred at the end of the test. In 2-CS and 2-DS, according to **Fig 4.10**, load decreased with diagonal cracking after early flexural crack and load decreased again after horizontal shear cracking.

The specimens 1-AS~1-DS and 2-AS ~2-DS having a/d=3.0 and 0.55f_{pu}, crack pattern shows difference between specimens having 200 mm spacing of shear reinforcement and 450 mm spacing of that. In specimens having 200 mm spacing, concrete crushing called ‘shear compression failure’ occurred at compressive zone near the loading point. But in case of specimens having 450 mm spacing, a flexural crack propagated toward the loading point and was transformed to a diagonal shear crack.

In spite of applying 450 mm shear reinforcement which is able to resist horizontal shear, horizontal shear cracks occurred in composite specimens. Thus except shear reinforcement, state interface between CIP concrete and PC concrete can remarkably influence to resist horizontal shear.

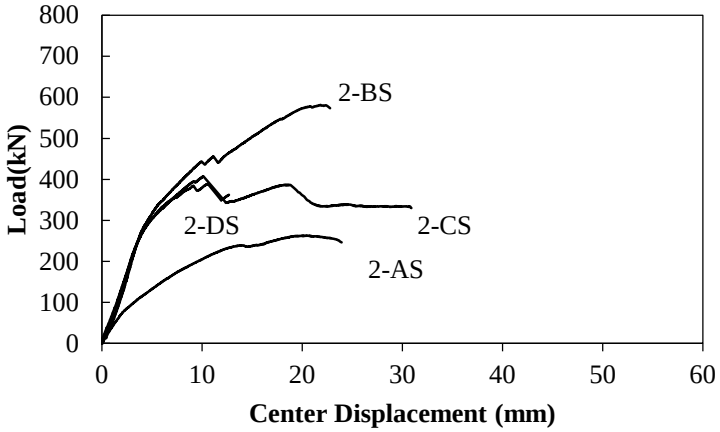

Fig 4.10 Load-center displacement relationship 2-AS ~ 2-DS (a/d=3.0, f_{pj}=0.55f_{pu}, s=450 mm)

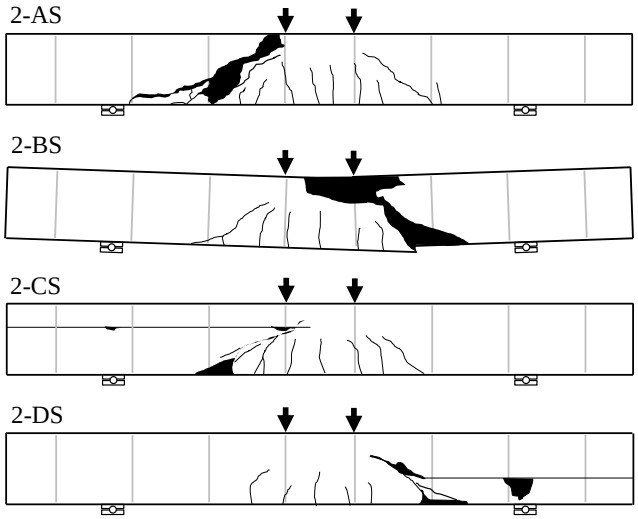

Fig 4.11 Crack pattern of specimen 2-AS ~ 2-DS at the end of test (a/d=3.0, f_{pj}=0.55f_{pu}, s=450 mm)

Table 4.5 Test result of specimen 2-AS ~ 2-DS (a/d=3.0, f_{pj}=0.55f_{pu}, s=450 mm)

Specimens	f_{ck} (MPa)		V_{test} (kN)	$V_{predicted}$ (kN)		$\frac{V_{test}}{V_{general}}$	$\frac{V_{test}}{V_{detailed}}$
	24 MPa	60 MPa		$V_{general}$	$V_{detailed}$		
2-AS	26		132	103	106	1.29	1.24
2-BS		55	291	292	264	1.00	1.10
2-CS	26	55	204	205	239	1.00	0.85
2-DS	26	55	195	146	183	1.33	1.07

4.2.3 Specimens 3-BS ~ 3-DS (a/d=3.0, f_{pj}=0.70f_{pu}, s=200 mm)

Test results of specimens 3-BS ~ 3-DS having a/d=3.0, 0.7f_{pu}, and 200 mm spacing of shear reinforcement were shown in **Fig 4.12**, **Fig 4.13**, and **Table 4.6**.

As shown in **Fig 4.12**, test result of 1-AS which is same variables with these specimens and nonprestressed member was used to compare with that of 3-BS ~ 3-DS. Thus shear strengths of specimens were presented that: 3-BS (682 kN) > 3-CS (486 kN) > 1-AS (372 kN) > 3-DS (356 kN). Also, shear strength of specimen increases as prestressed area increases. In the test, shear strength of 3-DS was 4 percent lower than that of 1-AS.

In 3-BS, 3-CS, early flexural strengths were 350 kN, 313 kN which were 3.23~3.61 times higher than that of 1-AS. Remarkably in the case of 3-DS, web-shear crack occurred at 150 kN. After web shear cracking, slope of load-center displacement decreased. Maximum strain is ε_{ps}=16,168 $\mu\varepsilon$ in 3-BS which is higher than ε_{pu}=12,803 $\mu\varepsilon$ thus flexural failure did occur before shear failure.

As shown in **Fig 4.13**, crack pattern of 3-DS was different with other typical crack patterns. In 3-BS and 3-CS, after early flexural cracking, inclined crack propagated toward loading point and finally compressive shear failure occurred at loading point. On the other hand, in 3-DS, web-shear crack in CIP concrete preceded at early stage and then flexural crack occurred at the bottom of beam. Crack width of web-shear crack increased as load increased. To verify cause of web-shear cracking in composite members, theoretical approaches are needed.

Comparison with specimens 1-AS ~ 1-DS, depending on prestressing force from 0.55f_{pu} to 0.70f_{pu}, location of incline crack converged near the loading points. However, shear strength was not proportional to prestressing force.

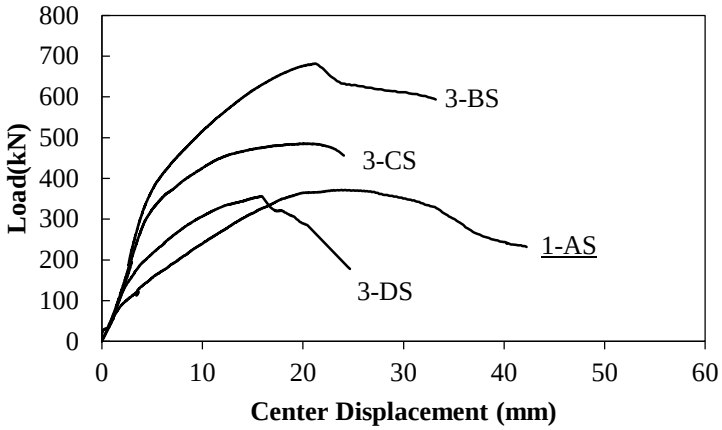

Fig 4.12 Load-center displacement relationship 3-BS ~ 3-DS (a/d=3.0, f_{pj}=0.70f_{pu}, s=200 mm)

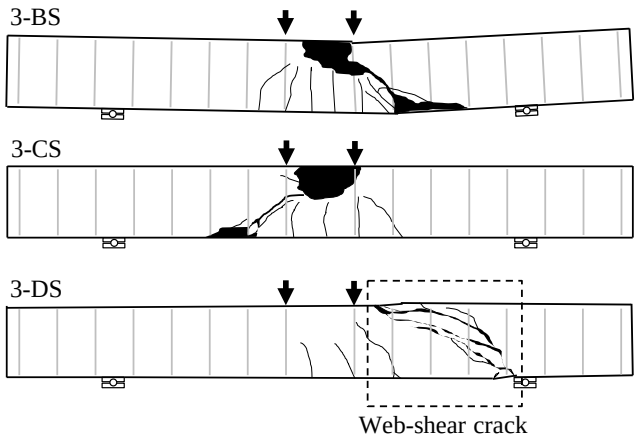

Fig 4.13 Crack pattern of specimen 3-BS ~ 3-DS at the end of test (a/d=3.0, f_{pj}=0.70f_{pu}, s=200 mm)

Table 4.6 Test result of specimen 3-BS ~ 3-DS (a/d=3.0, f_{pj}=0.70f_{pu}, s=200 mm)

Specimens	f_{ck} (MPa)		V_{test} (kN)	$V_{predicted}$ (kN)		$\frac{V_{test}}{V_{general}}$	$\frac{V_{test}}{V_{detailed}}$
	24 MPa	60 MPa		$V_{general}$	$V_{detailed}$		
1-AS	26		186	141	144	1.32	1.29
3-BS		53	341	330	345	1.03	0.99
3-CS	22	53	243	240	290	1.01	0.84
3-DS	22	53	178	181	224	0.99	0.80

4.2.4 Specimens 4-AS ~ 4-DS (a/d=3.0, f_{pj}=0.70f_{pu}, s=300 mm)

Specimens 4-AS ~ 4-DS are a/d=3.0, 0.70f_{pu} and s=300 mm which satisfies spacing limit for shear reinforcement and is able to resist horizontal shear and vertical shear. **Fig 4.14** shows load-center displacement relationship of specimens and **Fig 4.15** shows crack pattern at the end of the test. Comparison between experimental values and predicted values is shown in **Table 4.7**.

Results of the test is that: 4-BS (682 kN) > 4-CS (462 kN) > 4-DS (422 kN) > 4-AS (276 kN) which increased as prestressed area increased. Early flexural cracking occurred at 50kN (4-AS), 330kN (4-BS), 317kN (4-CS), and 328 kN (4-DS) that early flexural strength of 4-BS, 4-CS, 4-DS are 6.30~6.60 times higher than that of 4-DS. According to **Fig 4.14**, slope of load-center displacement of 4-BS, 4-CS, and 4-DS were similar to each other. After early flexural cracking, these slopes decreased and load decreased due to horizontal shear crack in the case of 4-CS and 4-DS. Maximum strain is ε_{ps}=5,381 $\mu\varepsilon$ in 4-B which is less than ε_{pu}=12,803 $\mu\varepsilon$ thus flexural failure did not occur before shear failure.

Crack patterns of 1-AS and 1-BS which are total cross section were that flexural cracks occurred at the early stage and developed inclined cracks. Finally diagonal tensile cracks occurred in both specimens and compressive shear failure occurred in 4-BS. In 4-CS and 4-DS, early flexural crack propagated toward only PC members and then horizontal shear cracks occurred at interface between PC-CIP concrete. After horizontal shear cracks, inclined cracks occurred in web of CIP members.

In spite of applying 300 mm shear reinforcement which is narrower than 450 mm and able to resist vertical and horizontal shear, horizontal shear cracks occurred in composite specimens. Alike 3-CS and 3-DS, state interface between CIP concrete and PC concrete can remarkably influence to restrain horizontal shear crack except shear reinforcement.

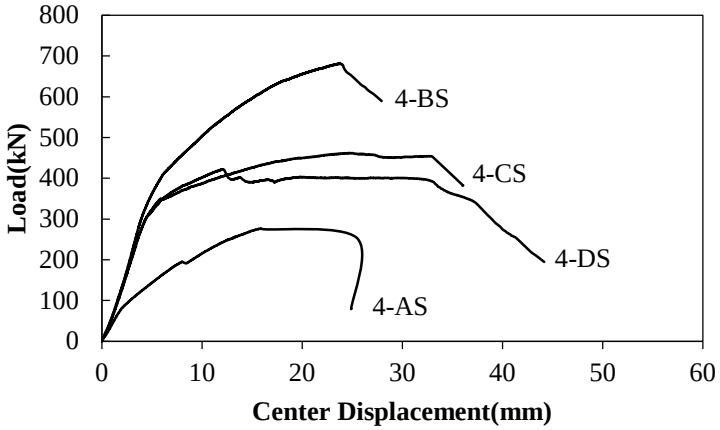

Fig 4.14 Load-center displacement relationship 4-AS ~ 4-DS (a/d=3.0, f_{pj}=0.70f_{pu}, s=300 mm)

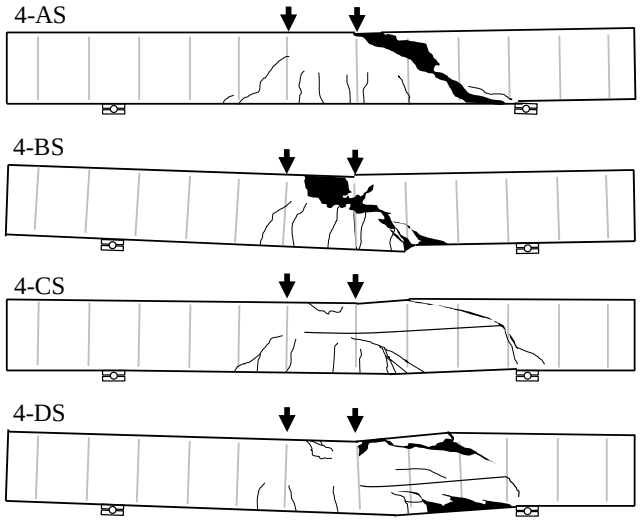

Fig 4.15 Crack pattern of specimen 4-AS ~ 4-DS at the end of test (a/d=3.0, f_{pj}=0.70f_{pu}, s=300 mm)

Table 4.7 Test result of specimen 4-AS ~ 4-DS (a/d=3.0, f_{pj}=0.70f_{pu}, s=300 mm)

Specimens	f_{ck} (MPa)		V_{test} (kN)	$V_{predicted}$ (kN)		$\frac{V_{test}}{V_{general}}$	$\frac{V_{test}}{V_{detailed}}$
	24 MPa	60 MPa		$V_{general}$	$V_{detailed}$		
4-AS	22		138	112	116	1.22	1.19
4-BS		53	341	307	321	1.11	1.06
4-CS	22	53	231	217	267	1.06	0.86
4-DS	22	53	211	157	201	1.34	1.05

4.2.5 Specimens 5-BS ~ 5-DS (a/d=3.0, f_{pj}=0.70f_{pu}, s=450 mm)

Specimens 5-BS ~ 5-DS are a/d=3.0, 0.70f_{pu}, and s=450 mm which is able to resist only horizontal shear. Test results are shown in **Fig 4.16**, **Fig 4.17**, and **Table 4.8**. Shear strengths of specimens increased as prestressed area increased: 5-BS (560 kN) > 5-CS (468 kN) > 5-DS (416 kN) > 2-AS (264 kN). Test result of 2-AS which is same variables with these specimens and nonprestressed member was used to compare with that of 5-BS ~ 5-DS. Early flexural cracks occurred at 350 kN (5-BS), 450 kN (5-CS), and 305 kN (5-DS) and these strengths were 2.67~4.67 times higher than that of 2-AS. Maximum strain is ε_{ps}=9,286 $\mu\varepsilon$ in 4-BS which is less than ε_{pu}=12,803 $\mu\varepsilon$ thus flexural failure did not occur before shear failure. As shown in **Fig 4.16**, slopes of 5-BS, 5-CS, and 5-DS were similar to each other at early stage and then these slopes decreased with flexural cracking.

In regard with crack patterns, compressive shear failure occurred in all specimens at the end of test. As shown in **Fig 4.17**, early flexural cracks developed inclined shear cracks and propagated toward loading point. Then, crack width increased as load increased and finally concrete crushing called compressive shear failure occurred.

In comparison with specimens 3-BS ~ 3-DS and 4-BS ~ 4-DS, center displacement at maximum load increased as shear reinforcement ratio increased whereas shear strength did not increase prominently. In case of the test, horizontal shear cracks did not occur whereas other specimens (3-CS, 3-DS, 4-CS, 4-DS) experienced horizontal shear cracks.

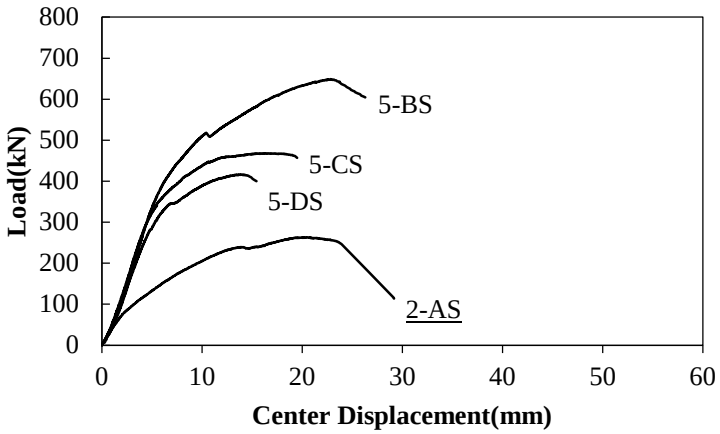

Fig 4.16 Load-center displacement relationship 5-BS ~ 5-DS (a/d=3.0, f_{pj}=0.70f_{pu}, s=450 mm)

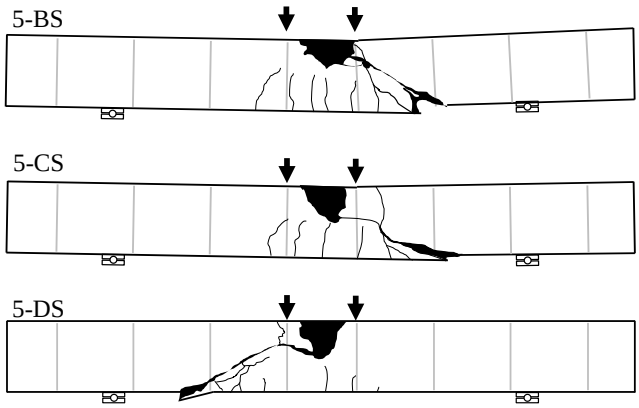

Fig 4.17 Crack pattern of specimen 5-BS ~ 5-DS at the end of test (a/d=3.0, f_{pj}=0.70f_{pu}, s=450 mm)

Table 4.8 Test result of specimen 5-BS ~ 5-DS (a/d=3.0, f_{pj}=0.70f_{pu}, s=450 mm)

Specimens	f_{ck} (MPa)		V_{test} (kN)	$V_{predicted}$ (kN)		$\frac{V_{test}}{V_{general}}$	$\frac{V_{test}}{V_{detailed}}$
	24 MPa	60 MPa		$V_{general}$	$V_{detailed}$		
2-AS	26		132	103	106	1.29	1.24
5-BS		55	325	292	307	1.11	1.05
5-CS	26	55	234	205	256	1.14	0.91
5-DS	26	55	208	146	190	1.42	1.09

4.2.6 Specimens 6-AS ~ 6-DS (a/d=4.0, f_{pj}=0.70f_{pu}, s=450 mm)

Specimens 6-AS ~ 6-DS are a/d=4.0, 0.70f_{pu}, and s=450 mm which is minimum shear reinforcements for horizontal shear strength. Test result are shown in **Fig 4.18**, **Fig 4.19**, and **Table 3.7**. In **Fig 3.15**, the location of shear reinforcement is indicated with gray line. Shear strength of specimens was presented: 6-BS (514 kN) > 6-CS (382 kN) > 6-DS (366 kN) > 6-AS (200 kN). These values also present that shear strength of specimen increases as the prestressed area increases. In case of 4.0 shear span to depth ratio, shear strength is 23~12 percent less than that of 3.0 shear span to depth ratio. Early flexural crack occurred at 75 kN (6-AS), 240 kN (6-BS), 230 kN (6-CS), and 250 kN (6-DS). And early flexural strengths of were 3.07~3.33 times higher than that of 6-AS. And maximum strain of strands was ε_{ps}=9,286 με which was less than ε_{pu}=12,803 με thus also flexural failure did not occur.

According to load-center displacement relationship, flexural stiffness of 6-BS, 6-CS, and 6-DS are similar to each other and were higher than that of 6-AS. After flexural cracking, flexural stiffness of these specimens decreased and then load decreased when inclined crack occurred.

And shear compression failure with diagonal tensile cracks occurred in all the prestressed specimens. Also, early flexural cracks occurred and developed to inclined cracks. These cracks propagated toward loading point. Finally shear compression failure occurred near the loading points.

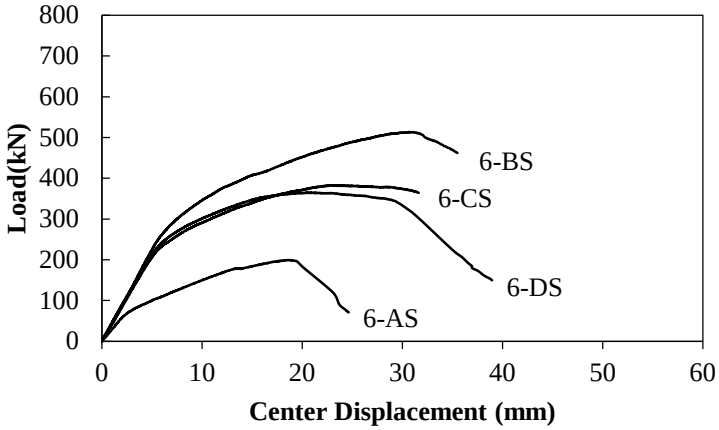

Fig 4.18 Load-center displacement relationship 6-AS ~ 6-DS (*a/d*=4.0, f_{pj}=0.70f_{pu}, *s*=450 mm)

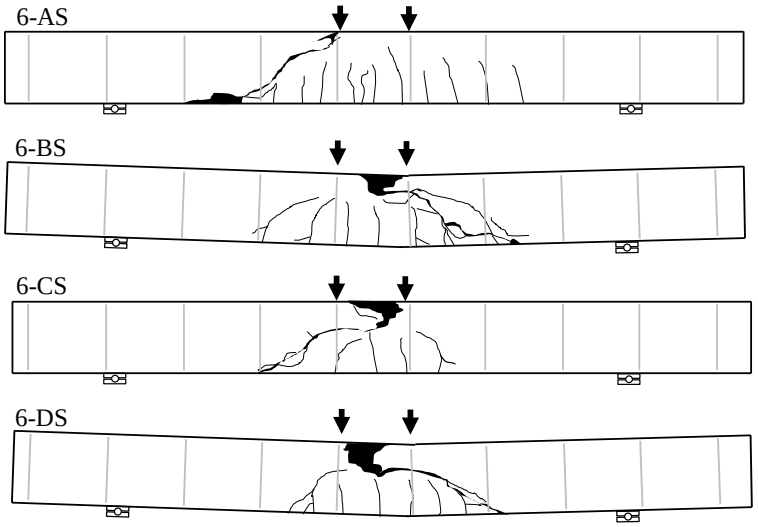

Fig 4.19 Crack pattern of specimen 6-AS ~ 6-DS at the end of test (*a/d*=4.0, f_{pj}=0.70f_{pu}, *s*=450 mm)

Table 4.9 Test result of specimen 6-AS ~ 6-DS (*a/d*=4.0, f_{pj}=0.70f_{pu}, *s*=450 mm)

Specimens	f_{ck} (MPa)		V_{test} (kN)	$V_{predicted}$ (kN)		$\frac{V_{test}}{V_{general}}$	$\frac{V_{test}}{V_{detailed}}$
	24 MPa	60 MPa		$V_{general}$	$V_{detailed}$		
6-AS	22		100	97	99	1.03	1.01
6-BS		53	257	234	245	1.09	1.05
6-CS	22	53	191	171	230	1.11	0.83
6-DS	22	53	183	129	170	1.42	1.08

4.3 Analysis

4.3.1 Effect of Test Parameters

Fig 4.20 shows effect of test parameter to shear strength of prestressed PC-CIP composite beams and parametric studies about prestress force, shear span-to-depth ratio, and shear reinforcement ratio were conducted. Because section A is nonprestressed specimen, it has different flexural stiffness and strength from other prestressed specimens. Thus, section A is excluded from comparison with prestressed specimens.

Fig 4.20(a) shows transition of shear strength from f_{pj}=0.55f_{pu} to f_{pj}=0.70f_{pu}. Specimens having a/d=3.0 are classified by section types. In s=200 mm, shear strength of section B and C did not increase as prestress force increased from 0.55f_{pu} to 0.70f_{pu}. This is influenced by nonprestressed compressive zone. In case of section D, shear strength decreased because of web-shear crack which dominantly occurs in I-shape beams. Thus it is difficult to compare with other specimens.

With regard with cause of web-shear crack in section D, specimens with section D could behave as I-shape beam. Web width of CIP concrete could be decreased assuming that composite section is gross section of 60 MPa because stiffness of low-strength concrete (24 MPa) of CIP concrete is lower than that of PC concrete (60 MPa). There are general cases for occurring web-shear crack in thin web of I-shape beam. Thus depth of low-strength concrete affects crack pattern causing web-shear crack.

In specimens having *a/d*=3.0, s=450 mm, shear strength increased as prestress force increased. Also initial flexural crack and flexural-shear crack occurred near the loading points as prestress force increased.

Fig 4.20(b) shows transition of shear strength from *a/d*=3.0 to *a/d*=4.0. As shown in **Fig 4.20(b)**, section B having *a/d*=4.0 decreased to 80 percent of shear

strength and section C and section D decreased to 0.82 and 0.88 percent respectively. Thus shear strength decreased as shear span-to-depth ratio increased.

Fig 4.20(c) shows effect of shear reinforcement ratio. 0.12 percent ratio indicates 450 mm spacing of shear reinforcement and 0.18 percent and 0.27 percent ratio indicate 300 mm and 200 mm spacing of that. In $0.55f_{pu}$, transition of shear strength from 0.12 percent to 0.27 percent increased. Shear strength of section B with 0.27 percent increased 41 percent rather than that of section B with 0.12 percent. And shear strength of composite section C and D increased 20 percent and 9 percent respectively. In the other hand, shear strength did not increase remarkably in $0.70f_{pu}$. Shear strength of section B and C increased only 5 percent as shear reinforcement ratio increased. Details of contribution of shear reinforcement on shear strength are given in 4.3.2.

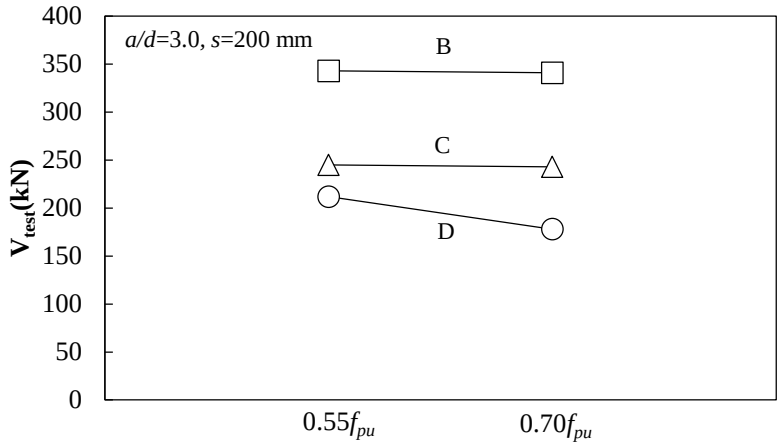

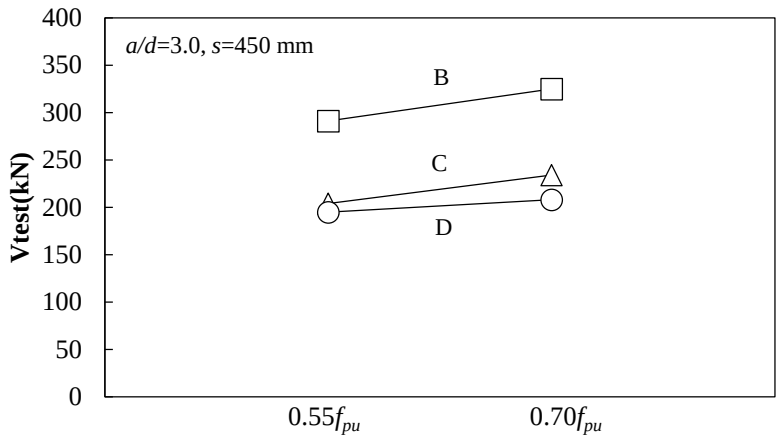

(a) Prestressing force

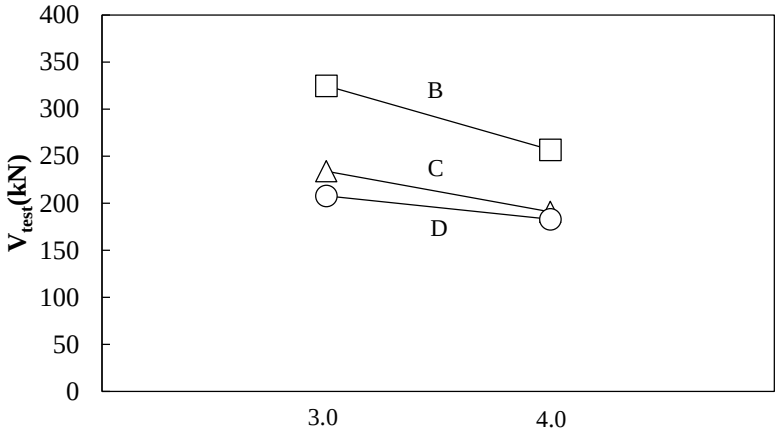

(b) Shear span-to-depth ratio (*a/d*)

Fig 4.20 Effect of test parameters (Continued)

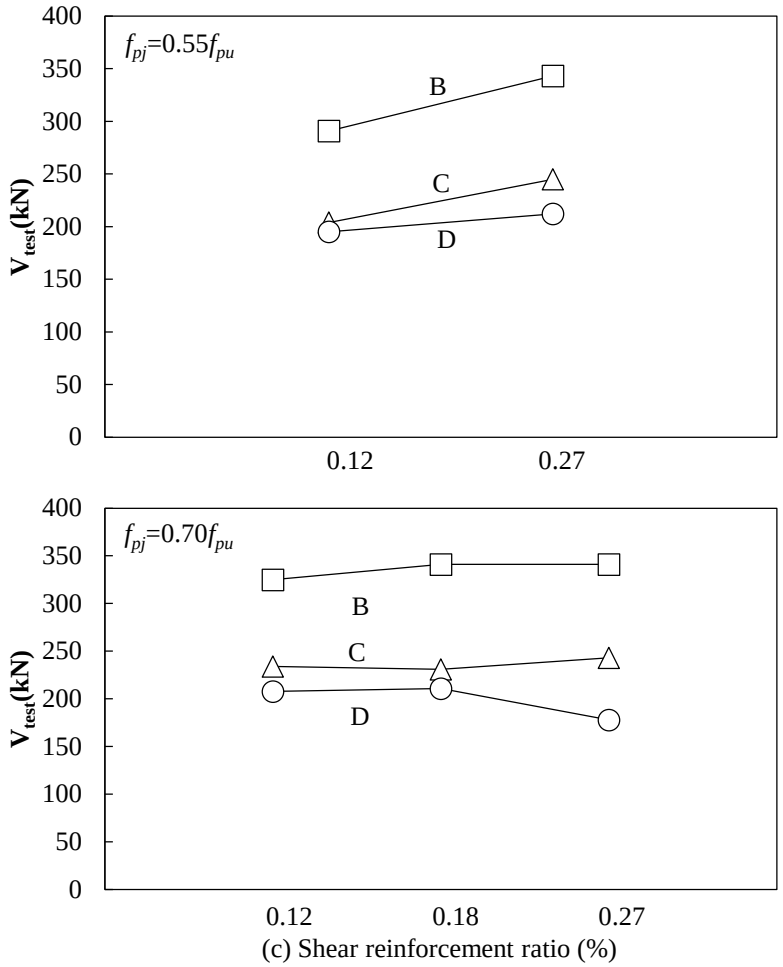

Fig 4.20 Effect of test parameters

4.3.2 Contribution of Shear Reinforcement

Fig 4.21 shows the effect of shear reinforcement on shear strength according to section type. Section A is nonprestressed section and section B, C, and D are prestressed section. Dotted line presents result values without shear reinforcement and solid line presents results values with shear reinforcement.

According to Fig **4.21(a)**, shear strength of section A which is nonprestressed section increased as shear reinforcement ratio increased from 0.12 percent to 0.27 percent. In specimens having a/d=3.0, 0.55f_{pu}, shear strength with 0.12 percent shear reinforcement ratio increased 32 percent rather than shear strength without shear reinforcement. With 0.18 percent and 0.27 percent, shear strength increased 39 percent and 86 percent respectively. In the case of a/d=4.0, 0.70f_{pu}, shear strength increased 42 percent rather than shear strength without shear reinforcement.

For prestressed specimens which are a/d=3.0, 0.55f_{pu}, shear strength increased as shear reinforcement ratio from 0.12 percent to 0.27 percent. Shear strength of section B and section C increased 28 percent and 20 percent and that of section D increased 9 percent rather than shear strength without shear reinforcement. For section C, tensile strain of shear reinforcement (1,963 με) is higher than yield strain (1,847 με) at the point of occurring horizontal shear cracking thus shear reinforcement resisted not only vertical shear force but also horizontal shear force. For section D, tensile strain of shear reinforcement (1,567 με) did not approach yield strain but resisted vertical and horizontal shear forces.

Whereas prestressed specimens which are a/d=3.0, 0.70f_{pu}, shear strength of section B and section C increased only 5 percent rather than shear strength without shear reinforcement. Because section D occurred web-shear cracking, increasing tendency of shear strength was not similar to section B and C. In case of 0.27 percent of shear reinforcement ratio, tensile strains of section B, C

and D when inclined crack penetrated shear reinforcement are 1,445 με, 1,120 με, 1,208 με respectively. Thus all specimens did not approach yield strain (1,847 με) and shear reinforcement resisted vertical shear force and horizontal shear force.

Remarkable thing is that specimens having a/d=3.0, $0.70f_{pu}$ did not show increasing tendency of shear strength. In other words, shear reinforcement did not contribute to increase shear strength. To investigate cause of ineffectiveness of the shear reinforcement on shear strength, theoretical approaches were verified.

According to Vecchio and Collins [16], shear strength is affected by yield of longitudinal reinforcement in case of low shear reinforcement ratio and is affected by concrete strength in high shear reinforcement ratio. Even very small amounts of shear reinforcement are beneficial in increasing shear strength. Yielding of the longitudinal reinforcement at the cracks limits and hence controls the strength for small amounts of shear reinforcement, while concrete shear failures control the strength for larger amount of shear reinforcement. Because yield strength of strands (8,829 με) is extremely high in this study, shear failure caused by concrete strength is expected before yielding of strands.

And prestressed specimens having a/d=3.0, $0.70f_{pu}$ are assumed that specimens can behave like deep beam according to prestress force. According to S.T.Mau et al. [17], therefore, principle compression stress decreases as shear reinforcement ratio increases to be equilibrated state relatively. As a result, this is in turn leads to more concrete softening effect because compressive strain is relatively small.

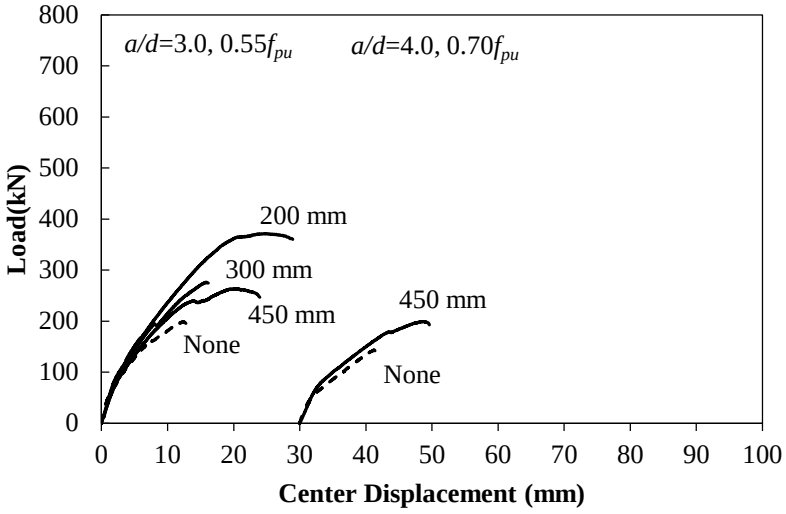

(a) Section A

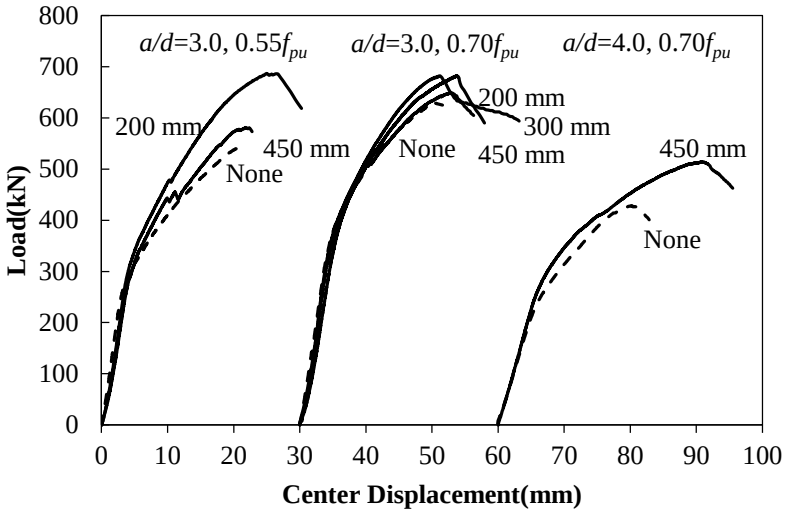

(b) Section B

Fig 4.21 Effect of shear reinforcement (Continued)

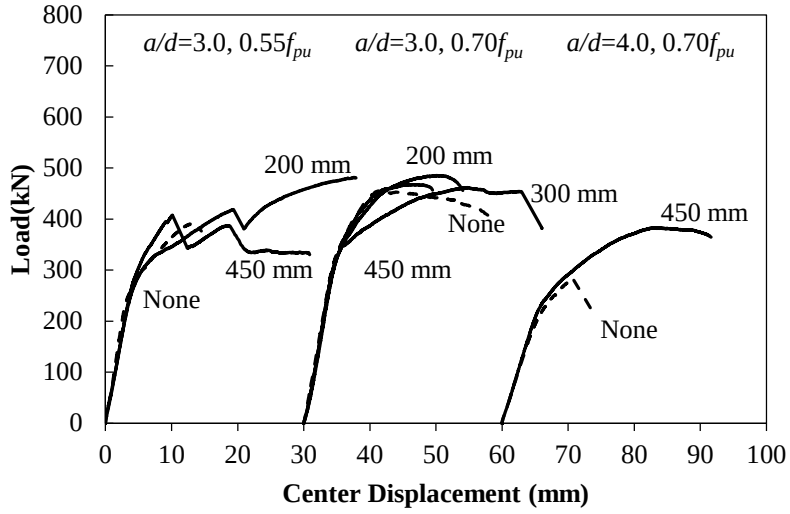

(c) Section C

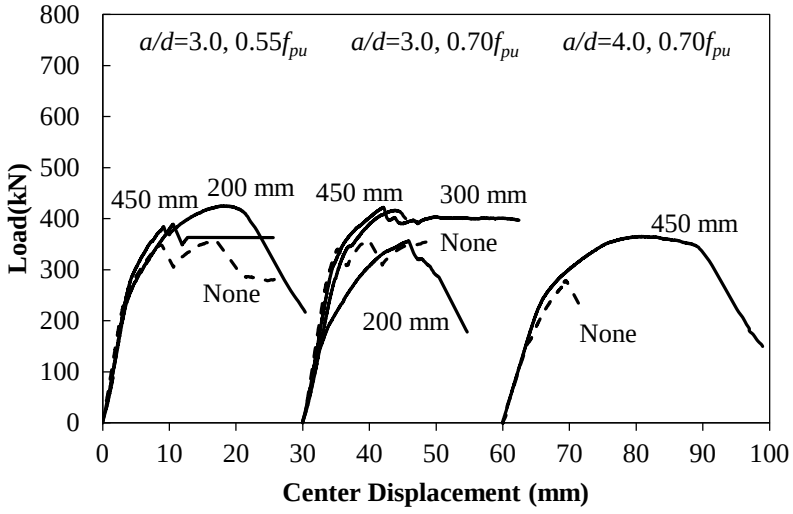

(d) Section D

Fig 4.21 Effect of shear reinforcement

4.3.3 Relationship between tensile strain of shear reinforcement and shear crack occurrence

To investigate relationship shear reinforcement and crack occurrence, strain of shear reinforcement between loading point and hinge support was identified. As shown in **Fig 4.5**, in specimens having a/d=3.0, 0.27 percent of ρ_v (s=200 mm), four strain gauges (L1, L2, L3, L4, R1, R2, R3, R4) were attached to shear reinforcement between loading point and hinge support at each ends. In specimens having a/d=3.0 and 0.12 percent of ρ_v (s=450 mm), only one strain gauges (L1, R1) attached to shear reinforcement at each ends. In case of a/d=4.0, 0.12 percent of shear reinforcement, two strain gauges (L1, L2, R1, R2) were attached to shear reinforcement.

Fig 4.22 shows strain of shear reinforcement of 1-BS, 3-BS and 3-CS. Arrow indicates load at initial tensile strain of shear reinforcement. In case of 1-BS having a/d=3.0, 0.55f_{pu}, 0.27 percent of ρ_v. As shown in **Fig 4.22(a)**, two strain gauges presented tensile strain at 479 kN. Strain gauge L4 presented 2288 με of maximum tensile strain which was higher than yield strain of shear reinforcement (1,847 με) and strain gauge L3 presented 443 με. Whereas 3-BS and 3-CS having 0.70f_{pu} show that only one strain gauge (L4) among four strain gauges presented tensile strain (1,445 με and 1,120 με) which were less than yield strain of shear reinforcement as shown in **Fig 4.22(b) and (c)**. Loads at initial tensile strain are 507 kN and 432 kN respectively. Thus, because inclined shear crack after initial flexural cracks concentrated near the loading points as prestress force increased from 0.55f_{pu} to 0.70f_{pu}, the number of shear reinforcement reacted increased near the loading points.

Fig 4.23 shows crack width of inclined shear crack measured by PI-type gauges. Also, arrow indicates load at initial tensile strain of shear reinforcement and measured specimens are same as above. Loads at occurrence of inclined shear crack are 357 kN, 351 kN and 390 kN which are less than loads at initial

tensile strain of shear reinforcement. Thus shear reinforcement did not appear tensile strain before shear cracking and after cracking it reacted to tensile stress from inclined shear crack.

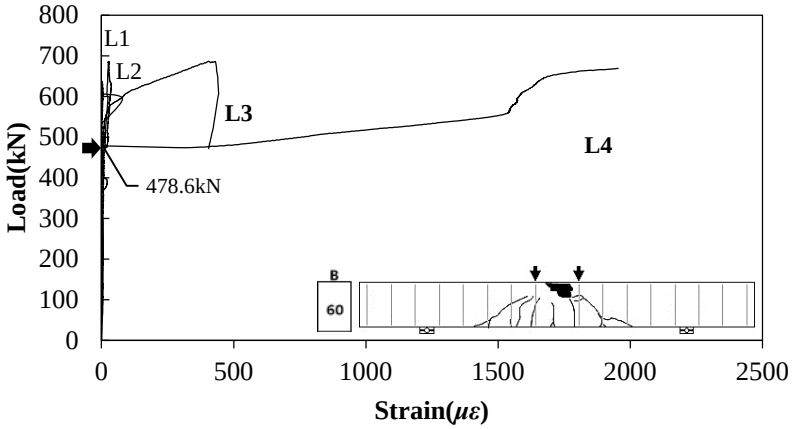

(a) 1-B (a/d=3.0 , 0.55f_{pu}, s=200 mm)

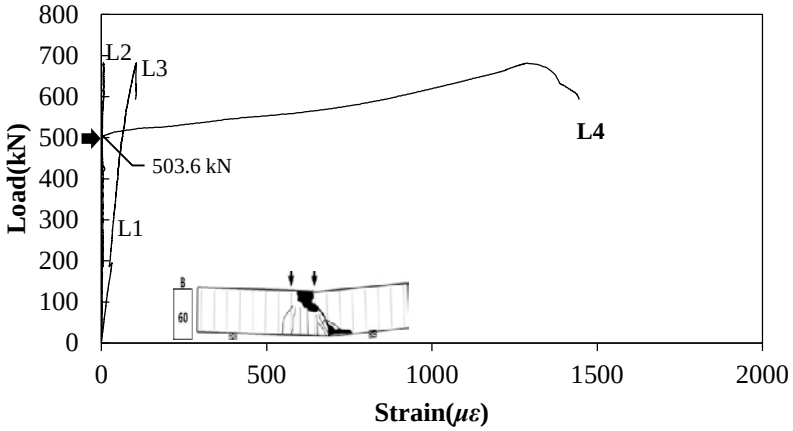

(b) 3-B (a/d=3.0 , 0.70f_{pu}, s=200 mm)

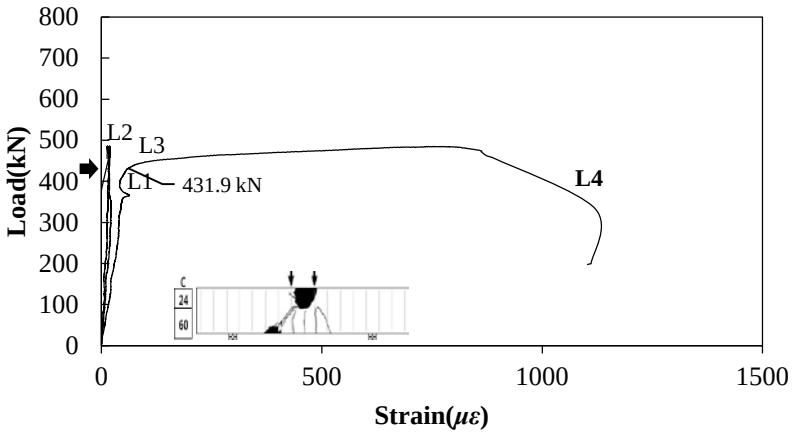

(c) 3-C (a/d=3.0 , 0.70f_{pu}, s=200 mm)

Fig 4.22 Strain of shear reinforcement

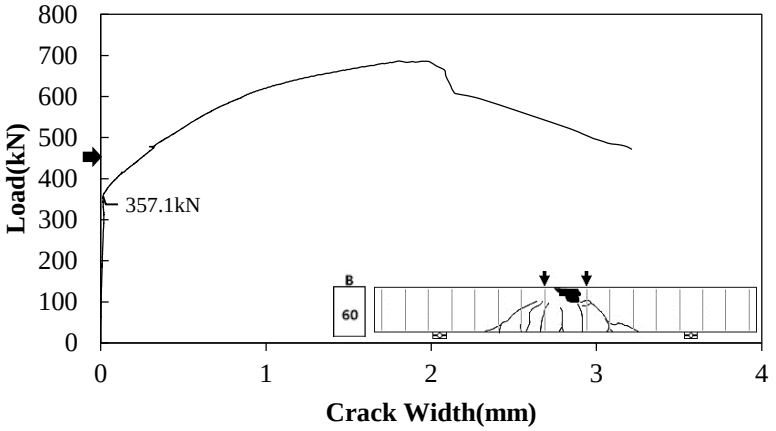

(a) 1-B (a/d=3.0, 0.55f_{pu}, s=200 mm)

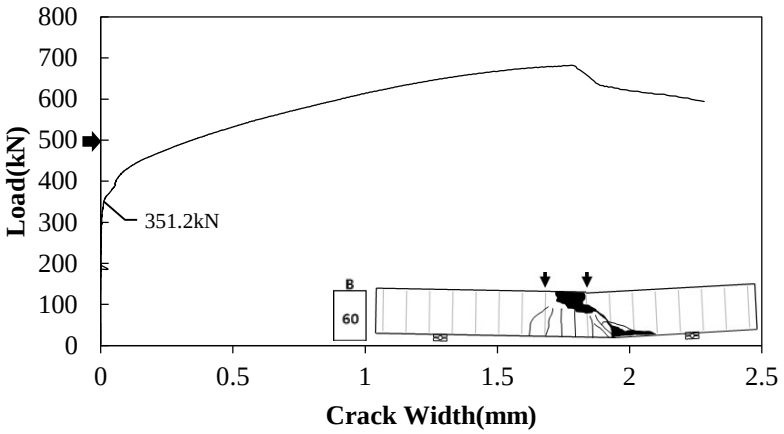

(b) 3-B (a/d=3.0, 0.70f_{pu}, s=200 mm)

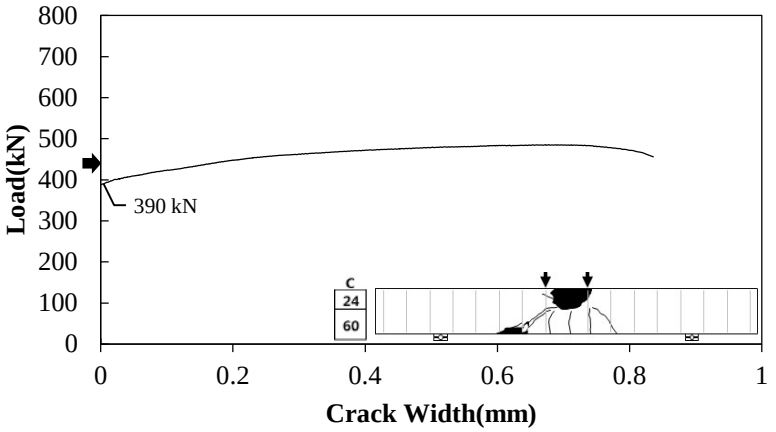

(c) 3-C (a/d=3.0, 0.70f_{pu}, s=200 mm)

Fig 4.23 Crack width of inclined crack

4.3.4 Comparison with Criteria of Vertical Shear Strength

Fig 4.24 compares test results and predicted values with current code to estimate vertical shear strength of prestressed PC-CIP composite beams. Circle shows values used general equations and square shows values detailed equations. Because composite beams consist of two different elements, shear strength of prestressed PC member is calculated by general equation Eq. (2-3) and detailed equation Eq. (2-4), and Eq. (2-6) and that of CIP members is calculated by general equation Eq. (2-1) and detailed equation Eq. (2-2) individually.

Shear strength of prestressed PC members increases due to pre-compression. However shear strength of CIP members does not increase because of nonprestress. Thus, combined method to predict shear strength of composite members which shear strength of prestressed PC member and CIP member are calculated respectively and combined each other were used. In case of values used general equations, shear strength is calculated by combining Eq. (2-1) and Eq. (2-3). And in case of values used detailed equations, shear strength calculated by combining Eq. (2-2) and minimum value between Eq. (2-4) and Eq. (2-6).

When using combined method with general equation, all the specimens are predicted in safety side. Test value versa predicted value of specimens having 0.12 percent ρ_v (s=450 mm) ranges from 1.10 to 1.87 and this range shows rather conservative.

Whereas using combined methods with detailed equation, shear strength of composite section (1-CS, 1-DS, 2-CS, 2-DS, 3-CS, 3-DS, 4-CS, 6-CS) are in non-safety side which ranges from 0.76 to 0.98 and rest of specimens are in safety side. Thus, if shear strength of composite beams are predicted with detailed equation, safety probability shall be considerate. And more theoretical approaches about detailed equations are needed.

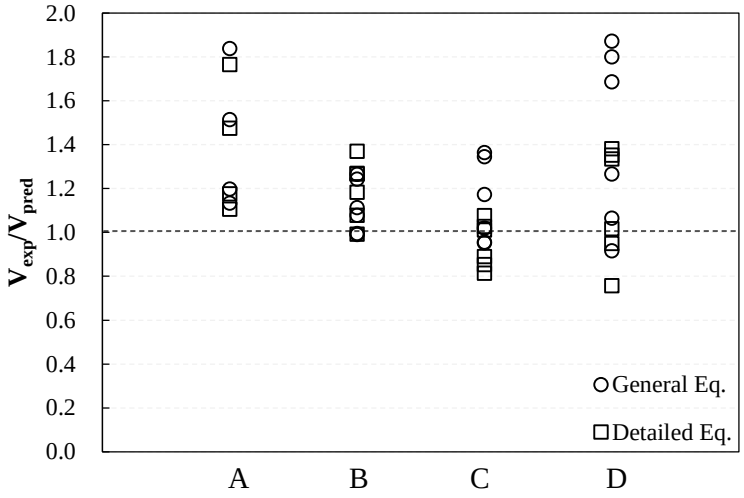

Fig 4.24 Shear strength prediction of specimens

4.3.5 Comparison with Criteria of Horizontal Shear Strength

As shown in **Table 4.10**, in composite specimens 1-CS, 2-CS, DS, 4-CS, DS, horizontal shear cracks occurred in interface between PC and CIP members. At occurring horizontal shear crack, horizontal shear stresses (v_{hv}) are 3.22 MPa, 2.68 MPa, 2.56 MPa, 3.04 MPa, 2.77 MPa which are 1.16~1.38 times higher than nominal horizontal shear stress calculated by Eq. (2-9). Also, horizontal shear strength of specimens which did not occur horizontal shear failure are in safety side. When calculating horizontal shear strength, shear strength at horizontal shear cracking was used for specimens failed in horizontal shear failure and maximum shear strength at vertical shear cracking was used for specimens failed in shear compressive or inclined shear failure. As shown in **Fig 4.25**, ACI 318-11 [2] estimates horizontal shear strength of specimens without shear reinforcement rather conservative whereas horizontal shear strength of specimens with shear reinforcement were in safety side appropriately. Thus with regard with horizontal shear crack in specimens with shear reinforcement, current code (ACI 318-11) is relatively predictable approach.

In spite of arranging shear reinforcement, horizontal shear cracks occurred in composite beams and these phenomena are able to raise a problem of structural safety. Thus additional researches are needed. Halicka [18] et al presented that inclined shear crack and horizontal shear crack occurred in composite beams having roughened interface in spite of arrangement shear reinforcement. Also according to AASHTO LRFD [19], horizontal shear stress is calculated combined with bond stress of 6 mm roughened interface which is assumed 1.7 MPa and friction coefficient. Then, shear reinforcement and state of interface affect horizontal shear.

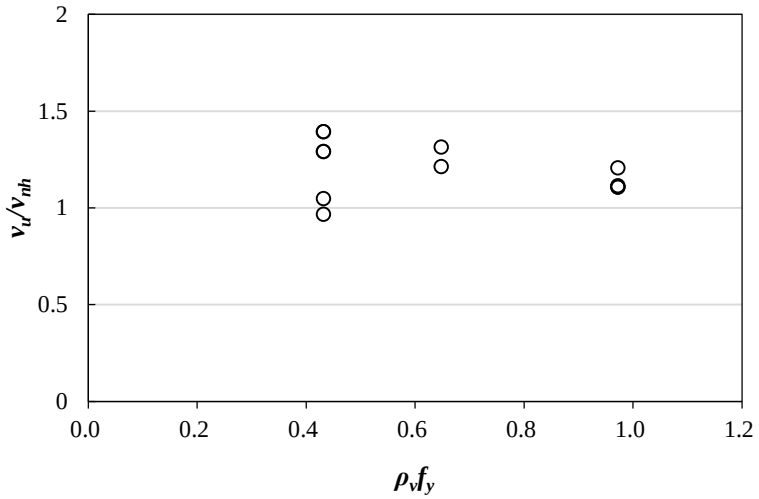

Fig 4.25 Horizontal shear strength ratio with shear transfer mechanism

Table 4.10 Observed horizontal shear strength of specimens with shear reinforcement

Specimens	Section type	Calculated strength		P_{max} (kN)	M_{max} (kN·m)	Horizontal shear at the interface (MPa)		$\frac{v_u}{v_{nh}}$
		V_n (kN)	M_n/a (kN)			v_u	Shear transfer v_{nh}	
1-CS	C	257	276	245	239	3.22	2.38	1.35
1-DS	D	199	371	212	207	2.79	2.38	1.17
2-CS	C	174	274	204	199	2.68	2.06	1.30
2-DS	D	16	371	195	190	2.56	2.06	1.25
3-CS	C	254	231	243	237	3.20	2.38	1.34
3-DS	D	194	356	178	174	2.34	2.38	0.98
4-CS	C	227	231	231	225	3.04	2.19	1.39
4-DS	D	167	356	211	206	2.77	2.19	1.27
5-CS	C	174	267	234	228	3.08	2.06	1.49
5-DS	D	116	371	208	203	2.74	2.06	1.33
6-CS	C	140	173	191	248	2.51	2.06	1.22
6-DS	D	98	267	183	238	2.41	2.06	1.17

Table 4.11 presents design code of horizontal shear strength according to ACI 318-11 [2], Eurocode2 [10], AASHTO LRFD [19] (2012), and CSA [20] (2004). And **Fig 4.26** shows experimental values in this study and other researches based on horizontal shear strength from these design codes. Also, **Fig 4.27** shows experimental values in this study and other researches based on empirical methods (Walraven [21], Mattock [22], Loov and Patnaik [9], Patnaik [23], and Kahn and Mitchell [24]). In case of ACI 318-11, shear transfer mechanism is used when horizontal shear stress is lower than 3.5 MPa and shear friction method is used when horizontal shear stress higher than 3.5 MPa. In the case of Eurcode2, AASHTO LRFD, and CSA, however, shear friction mechanism is used regardless of magnitude of horizontal shear stress and they use cohesion of interface and friction coefficient. As shown in **Fig 4.26**, AASHTO LRFD estimated horizontal shear stress rather unconservative to experimental values whereas these values were in safety side according to ACI 318-11, Eurocode2, and CSA in condition of same state of contact surface and shear reinforcement. Where shear reinforcement are provided in and contact surfaces are clean and free of laitance, and intentionally roughened, ACI 318-11, Eurocode2, AASHTO LRFD, and CSA suggests 1.8 MPa, 0.45 MPa, 1.7 MPa, and 0.5 MPa respectively thus these codes suggest different cohesion factors. As shown in **Fig 4.27**, also, empirical curve of Walraven, Mattock, Loov and Patnaik, and Patnaik shows similar tendency whereas that of Kahn and Mitchell suggested upper bound of $0.2f_{ck}$ thus predict horizontal shear strength conservatively. Experimental values in this study were in safety side accordin to empirical curve of Mattock, and Kahn and Mitchell.

In this study, horizontal shear crack preceded after early flexural crack. In spite of bearing stress of shear reinforcement, horizontal shear crack occurred because aggregate exposure of interface was less than 6 mm and concrete strength of CIP in compression zone was less than that of PC concrete relatively. Thus horizontal shear crack preceded then inclined shear crack occurred.

Table 4.11 Design codes of horizontal shear strength

Researcher	Shear strength model (SI Units)
ACI 318-11 [2]	Case 1. Horizontal shear transfer, 1) and 2) should be satisfied. 1) Where contact surfaces are clean, free of laitance, and intentionally roughened. 2) Where minimum ties are provided and contact surfaces are clean and free of laitance, but not intentionally roughened. $v_u \le \phi 0.56$ Case 2. Horizontal shear transfer, 1) and 2) should be satisfied. 1) Where ties are provided and contact surfaces are clean, free of laitance, and intentionally roughened to a full amplitude of approximately 6 mm 2) $v_u \le \phi 3.5$ $v_{nh} \le (1.8 + 0.6\rho_v f_y)\lambda \le 3.5$ Case 3. Shear friction, 1) should be satisfied. 1) $v_u \le \phi 3.5$ $v_n = \mu\rho_{vf} f_y \le (0.2 f_{ck}, 6.9)$
Eurocode 2 [10]	$V_{Rdi} = cf_{ctd} + \mu\sigma_n + \rho f_{yd}(\mu \sin\alpha + \cos\alpha) \le 0.5\nu f_{cd}$ where: c and μ are factors which depend on the roughness of the interface f_{ctd} is the value of the design tensile strength σ_n is stress per unit area cuased by the minimum external normal force across the interface α should be limited by $45° \le \alpha \le 90°$ ν is a strength reduction factor
AASHTO LRFD [19] (2012)	The nominal shear resistance of the interface plane shall be taken as: $V_n = cA_{cv} + \mu(A_{vf} f_y + P_c)$ The nominal shear resistance, V_{ni}, used in the design shall not be greater than the lesser of: $V_{ni} \le K_1 f'_c A_{cv}$ or $V_{ni} \le K_2 A_{cv}$ where: A_{cv} is area of concrete considered to be engaged in interface shear transfer A_{vf} is area of interface shear reinforcement, crossing the shear plane within the area A_{cv} c is cohesion factor specified in Article 5.8.4.3 of AASHTO LRFD μ is friction factor specified in Article 5.8.4.3 K_1 is fraction of concrete strength available to resist interface shear, as specified in Article 5.8.4.3 K_2 is limiting interface shear resistance specified in Article 5.8.4.3

CSA [20] (2004)	The factored shear stress resistance of the plan shall be computed from $V_r = \lambda\phi_c(c + \mu\sigma) + \phi_s\rho_v f_y \cos\alpha_f$ where the expression $\lambda\phi_c(c+\mu\sigma)$ shall not exceed $0.25\phi_c f'_c$ and α_f is the angle between the shear friction reinforcement and the shear plane.

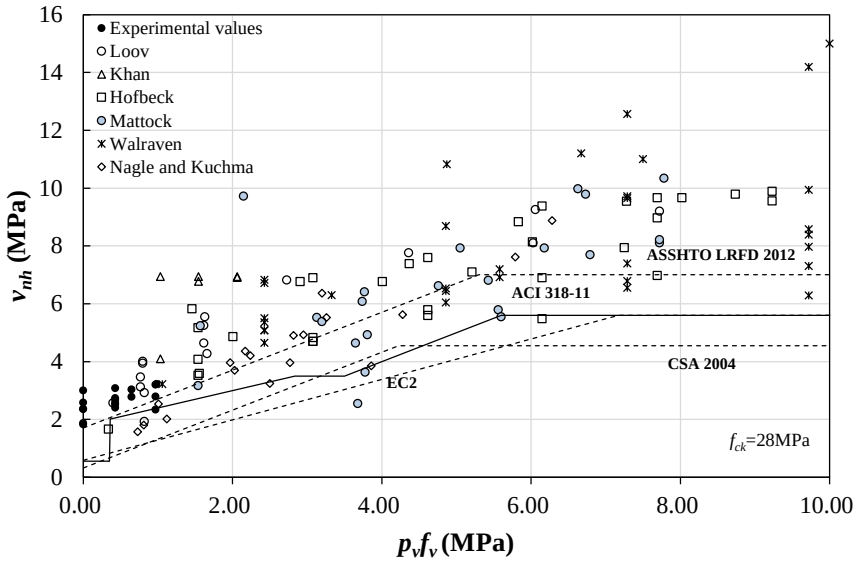

Fig 4.26 Horizontal shear strength for specimens with design codes

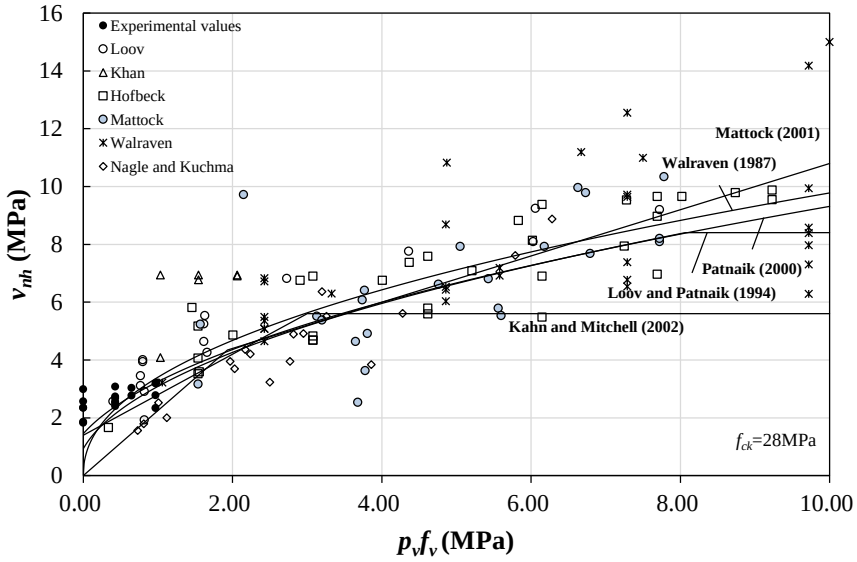

Fig 4.27 Horizontal shear strength for specimens with empirical equation

4.4 Discussion

22 specimens were tested to investigate shear strength of prestressed PC-CIP composite beams with shear reinforcement. Test variables were area ratio of prestressed PC and CIP, prestress force, shear span-to-depth ratio, and shear reinforcement ratio. On basis of the test results, shear behaviors of composite beams were analyzed and conclusion of this study is as follows:

1) Prestressed section B and composite section C and D presented similar shear behavior and early flexural strength and stiffness were higher than that of section A which was nonprestressed section. Test result is that shear strength increased as prestressed area and prestress force increased and shear span-to-depth ratio decreased. In the case of a/d=3.0, $0.70f_{pu}$, shear strength increased less than 5 percent in spite of increasing shear reinforcement ratio because of concrete softening effect.

2) Failure mechanism of prestressed composite beams with shear reinforcement is as follows. Early flexural crack developed inclined cracks and flexural shear cracks occurred. Conclusively, compressive shear failure with inclined cracks or diagonal tensile failure with horizontal shear crack occurred. In spite of horizontal shear crack, brittle failure did not occur because of bearing stress of shear reinforcement. Occurrence location of inclined cracks were concentrated near loading points as prestress force increased. Thereby the number of shear reinforcement which presented tensile strain also decreased.

3) Cause of web-shear crack within composite section was judged by difference of stiffness according to concrete strength of PC and CIP concrete. Low-strength concrete (24 MPa) of CIP concrete could be substituted to high-strength concrete (60 MPa) which equal to that of

PC concrete. This substitution leads to decrease web width which is able to behave like I-shape beam.

4) In regard with horizontal shear of interface between prestressed PC and CIP composite beams, comparison with test results and predicted values with current design code was conducted. Horizontal shear strength of composite beams without shear reinforcement shows 1.03~1.36 times higher than current design code and thus current code has predicted horizontal shear strength as reasonable assessment. Despite shear reinforcements were arranged, horizontal shear crack occurred in composite beams. Thus except shear reinforcement ratio which is able to resist horizontal shear roughness of contact surface is important factor to resist horizontal crack.

Chapter 5. Shear Database for Prestressed Concrete Members

5.1 Introduction

To investigate feasibility of current estimation method, experimental values of this study are compared with predicted values with current design code, empirical or theoretical method by other researchers. Thus design models of ACI 318-11 [2], Eurocode 2 [10], Sozen et al. [11], and Bažant et al. [12] are used to predict shear strength. Also shear strength ratio is investigated which is experimental value over predicted value.

And to compared between experimental values of this study and other experimental values, 'The University of Texas Prestressed Concrete Shear Database (UTPCSDB) [13]' is used which was was developed and expanded to include 1696 tests reported in North America, Japan, and Europe from 1954 to 2010 as shown in **Table 5.3**. The UTPCSDB was subsequently used to examine the accuracy and conservativeness of shear design procedures based on different rationales. In this study, we input data getting within prestressed I-shape beams and rectangular beams. If properties of data is not clear, they exclude from comparison. For more detailed information about UTPCSDB, please see Appendix.

5.2 Prediction of Experimental Values

Table 5.1 shows experimental values and predicted values of current codes and by other researchers. Also **Table 5.2** shows shear strength ratio compared between experimental values and predicted values.

In the case of simplified method in ACI 318-11 [2], mean value of shear strength ratio presented 0.15 and coefficient of variation (COV) presented 0.16 which are the smallest values. This shows that current design code is able to estimate shear strength of prestressed composite beams accurately. In the case of detailed method in ACI 318-11, mean values is 1.33 and COV is 0.24 which are rather higher than that of simplified method.

With regard to Eurocode2 [10], mean values and COV of shear strength ratio are also 23 percent and 15 percent higher than that of ACI 318-11 respectively as design code. In other words, Eurocode2 estimate shear strength of prestressed composite beams conservatively.

And mean value and COV of empirical equation of Sozen et al. [11] estimate are 1.07 and 0.15 respectively which are the lowest values. Whereas theoretical method of Bažant et al. [12] shows the highest mean value and COV which are 2.08 and 0.49.

Table 5.1 Prediction of shear strength

Specimens	v_{exp}	v_{exp}/v_{pred}				
		ACI 318-11 Simplified Method	ACI 318-11 Detailed Method	Eurocode2	Sozen, Zwoyer, and Siess	Bažant and Cao
1-B	3.22	3.09	2.50	1.49	2.67	1.10
1-C	2.32	2.03	2.73	1.30	2.25	0.80
1-D	2.12	1.33	1.82	0.76	1.77	0.88
2-B	3.74	3.10	3.07	1.75	3.15	1.26
2-C	2.70	2.04	1.68	1.56	2.66	0.88
2-D	2.12	1.33	0.92	0.99	2.03	0.93
3-B	2.53	2.42	2.41	1.75	2.36	0.95
3-C	1.68	1.67	1.36	1.54	1.97	0.75
3-D	1.64	1.17	0.84	0.99	1.52	0.85
1-BS	4.06	4.07	3.44	2.35	3.62	2.07
1-CS	2.90	3.00	2.36	2.16	3.20	1.77
1-DS	2.51	2.30	1.82	1.62	1.75	1.85
2-BS	3.44	3.52	2.96	1.89	3.12	1.54
2-CS	2.41	2.49	1.88	1.73	2.74	1.26
2-DS	2.31	1.80	1.32	1.16	1.83	1.35
3-BS	4.04	4.01	4.05	2.63	4.11	2.22
3-CS	2.88	2.97	2.65	2.45	3.62	1.84
3-DS	2.11	2.27	1.89	1.93	2.06	1.90
4-BS	4.04	3.68	3.73	2.34	3.79	1.90
4-CS	2.73	2.64	2.33	2.15	3.30	1.52
4-DS	2.50	1.95	1.56	1.63	2.06	1.58
5-BS	3.85	3.52	3.48	2.13	3.55	1.68
5-CS	2.77	2.49	2.12	1.97	3.10	1.33
5-DS	2.46	1.80	1.39	1.40	2.10	1.41
6-BS	3.04	2.84	2.85	2.14	2.79	1.37
6-CS	2.26	2.09	1.81	1.96	2.42	1.17
6-DS	2.17	1.59	1.27	1.44	1.55	1.28

Table 5.2 Shear strength ratio

Specimens	v_{exp}	v_{exp}/v_{pred}				
		ACI 318-11 Simplified Method	ACI 318-11 Detailed Method	Eurocode2	Sozen, Zwoyer, and Siess	Bažant and Cao
1-B	3.22	1.04	1.29	2.17	1.21	2.92
1-C	2.32	1.14	0.85	1.78	1.03	2.90
1-D	2.12	1.60	1.17	2.78	1.20	2.41
2-B	3.74	1.21	1.22	2.13	1.19	2.96
2-C	2.70	1.32	1.61	1.73	1.01	3.07
2-D	2.12	1.59	2.31	2.13	1.04	2.27
3-B	2.53	1.05	1.05	1.44	1.07	2.68
3-C	1.68	1.01	1.23	1.09	0.86	2.25
3-D	1.64	1.40	1.95	1.65	1.08	1.93
1-BS	4.06	1.00	1.18	1.73	1.12	1.96
1-CS	2.90	0.96	1.23	1.34	0.91	1.64
1-DS	2.51	1.09	1.38	1.55	1.44	1.36
2-BS	3.44	0.98	1.16	1.82	1.10	2.23
2-CS	2.41	0.97	1.29	1.40	0.88	1.92
2-DS	2.31	1.28	1.74	1.98	1.26	1.70
3-BS	4.04	1.01	1.00	1.53	0.98	1.82
3-CS	2.88	0.97	1.09	1.18	0.79	1.56
3-DS	2.11	0.93	1.12	1.09	1.02	1.11
4-BS	4.04	1.10	1.08	1.73	1.07	2.13
4-CS	2.73	1.03	1.18	1.27	0.83	1.80
4-DS	2.50	1.28	1.60	1.53	1.21	1.58
5-BS	3.85	1.09	1.11	1.81	1.08	2.29
5-CS	2.77	1.11	1.30	1.41	0.89	2.08
5-DS	2.46	1.37	1.77	1.75	1.17	1.75
6-BS	3.04	1.07	1.07	1.42	1.09	2.22
6-CS	2.26	1.08	1.25	1.15	0.93	1.93
6-DS	2.17	1.36	1.70	1.50	1.40	1.69
Mean		1.15	1.33	1.63	1.07	2.08
COV		0.16	0.24	0.38	0.15	0.49

Fig 5.1 shows experimental values of this study according to shear span-to-depth ratio (a/d), shear reinforce index ($\rho_v f_v$), effective prestress force (f_{se}/f_{pu}), and concrete strength (f'_c) according to shear failure modes which are shear compression failure, horizontal shear failure and web shear failure. And **Fig 5.2**, **Fig 5.3**, **Fig 5.4**, **Fig 5.5**, and **Fig 5.6** shows shear strength ratio between experimental values and predicted values of ACI 318-11, Eurocode2, Sozen et al, Bažant et al. In these figures, white circle shows specimens failed in shear compression failure and black circle shows specimens failed in horizontal shear failure and triangle shows specimen failed in web shear failure. And white rectangular and black rectangular show specimens having total cross section with or without shear reinforcement respectively in effect of concrete strength.

As shown in **Fig 5.1**, specimens failed shear compression failure show higher shear strength than that of specimens failed horizontal shear failure and web shear failure in each shear span-to-depth ratio 3.0 and 4.0. One specimen which occurred web shear failure shows the lowest value in 3.0 a/d. And shear strength increased as shear reinforcement ratio increased in case of specimens failed horizontal shear failure. But in specimens failed shear compression failure, shear strength did not increase as shear reinforcement increased. Specimens occurred web shear failure shows the lowest shear strength in spite of high shear reinforcement ratio. Section B which is total cross section of 60 MPa did not show definite difference of shear strength as concrete compressive strength increased from 53 Mpa to 57 MPa.

Fig 5.2 shows shear strength ratio based on predicted values in simplified method of ACI 318-11. All specimens are in safety side ranging from 0.93 to 1.60 except specimen occurred web shear failure (0.93). And variation of shear strength ratio decreases as $\rho_v f_v$ increases ranging from 0.93 to 1.00.

Fig 5.3 is shear strength ratio in detailed method of ACI 318-11. This shows conservative tendency rather than that of simplified method. In case of specimens failed shear compression failure, shear strength ratio ranges from

0.85 to 1.77 and specimens failed horizontal shear failure shows shear strength ratio ranging 1.17 to 2.31. Also, variation of shear strength ratio decreases as $\rho_v f_v$ increases from 1.0 to 1.23

As shown in **Fig 5.4**, Eurocode 2 predicts that shear strength of all specimens are in safety side ranging from 1.09 to 2.78. But COV is 15 percent higher than that of detailed method of ACI 318-11. Especially specimens of section B shows shear strength ratio from 1.42 to 2.78.

Fig 5.5 represents shear strength ratio based on empirical equation of Sozen et al. In the estimation method, results of specimens occurred shear compression failure is conservative rather than that of specimens occurred horizontal shear failure but this difference is not critical. In the case of specimens which failed horizontal shear and web shear failure, minimum value of shear strength ratio is 0.80. Thus this empirical method is able to predict shear strength accurately. Whereas theoretical method of Bažant et al shows the most conservative results ranging from 1.11 to 3.07 as shown in **Fig 5.6**. Particularly, it is conservative excessively in the case of specimens without shear reinforcement.

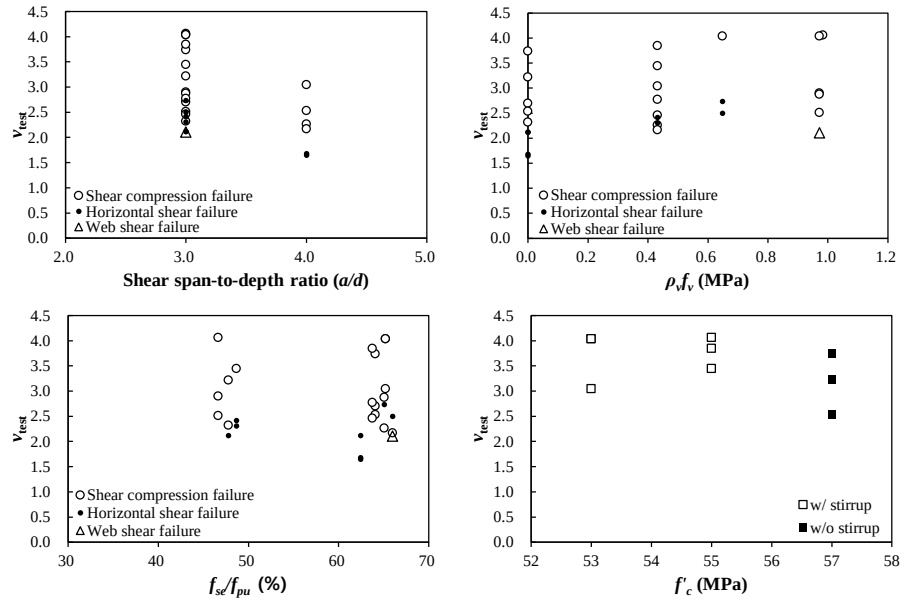

Fig 5.1 Experimental values according to experimental variables

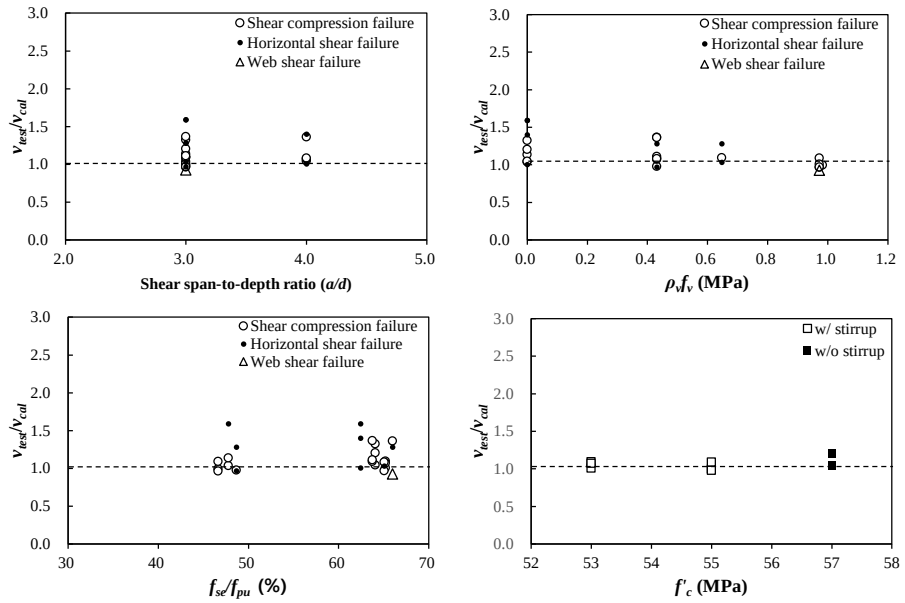

Fig 5.2 ACI 318-11 simplified method

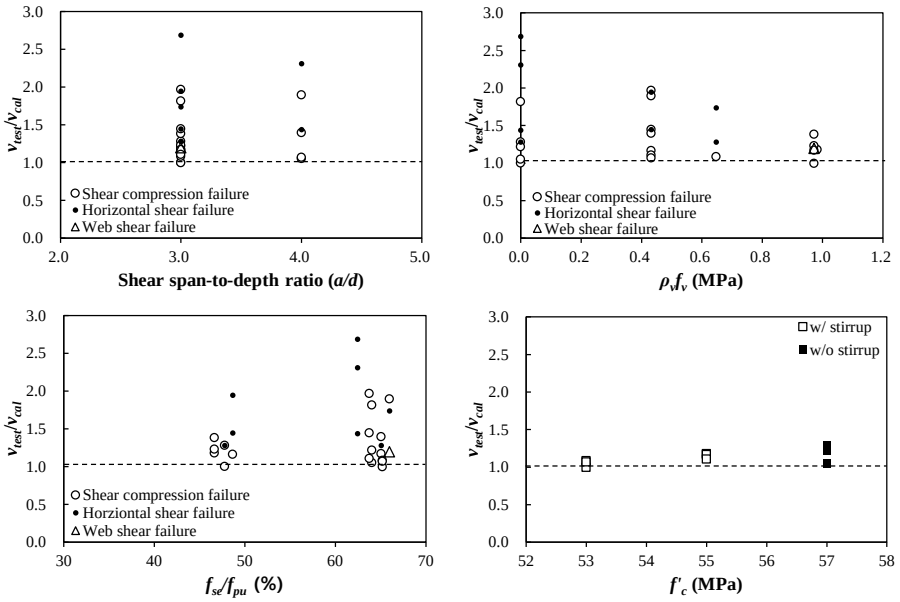

Fig 5.3 ACI 318-11 detailed method

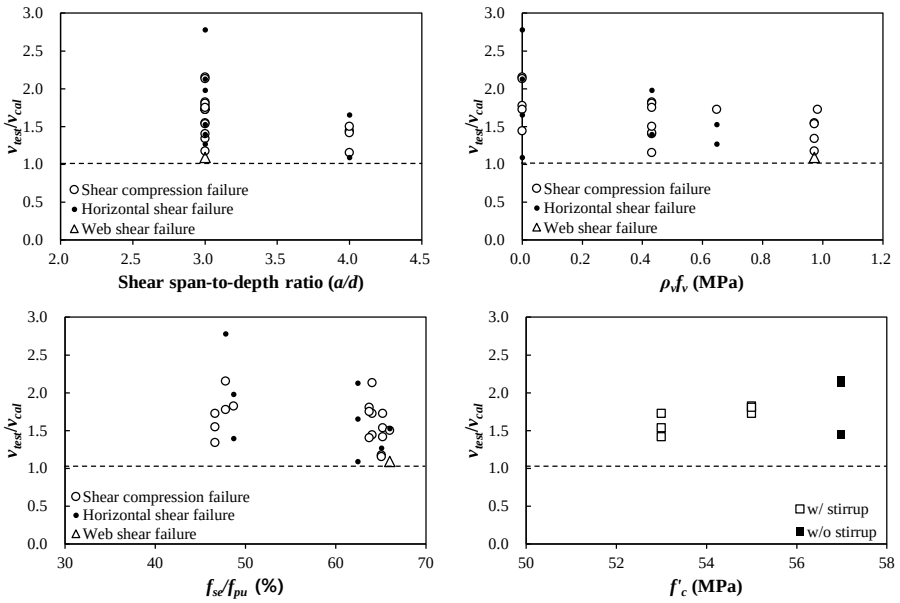

Fig 5.4 Eurocode2

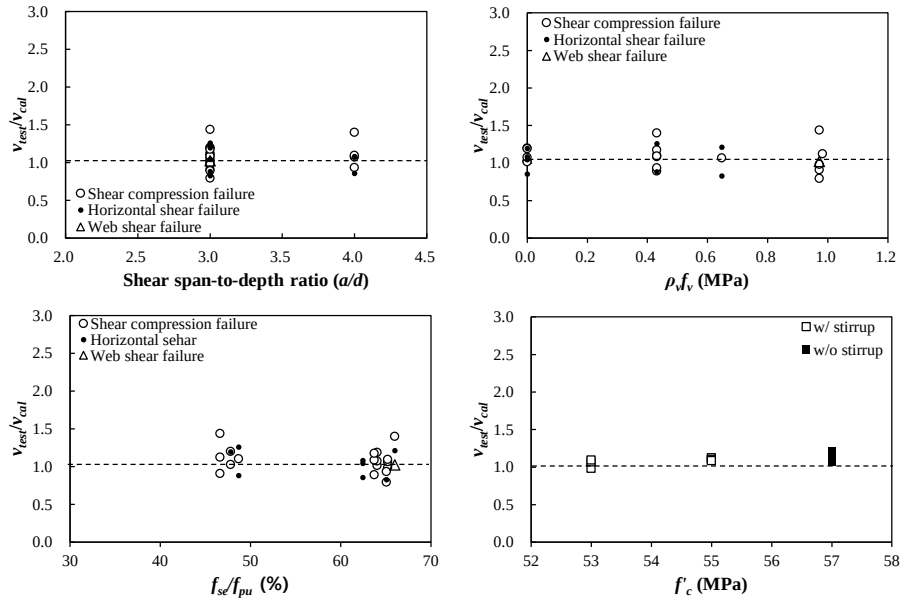

Fig 5.5 Sozen, Zwoyer, and Siess

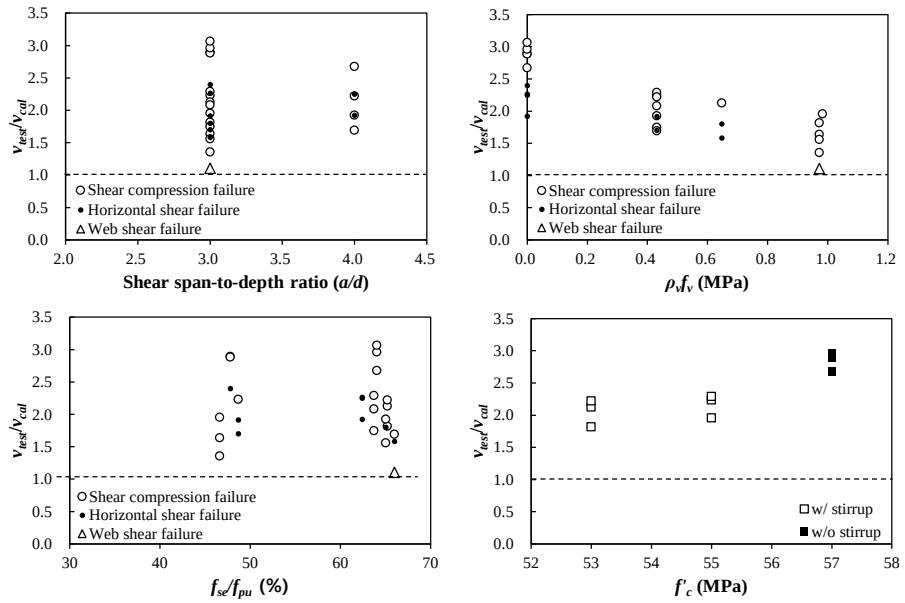

Fig 5.6 Bažant and Cao

5.3 Shear Database Analysis

Table 5.3 shows evaluation of 131 specimens reported by 13 reference. Based on **Table 5.3**, as shown in **Fig 5.7**, histogram shows shear strength ratio between experimental values and predicted values of UTPCSDB [13] and this test.

Mean value and COV of Sozen et al [11] show the lowest values and unconservative ratio is 4.4 percent rather lower than simplified method of ACI 318-11 [2]. In the case of ACI 318-11, mean values of simplified method and detailed method are 1.35 and 1.33 but coefficients of variation are 0.32 and 0.24 respectively which are rather higher than other methods. Unconservative of simplified method is 2.3 percent for members with effective prestress force not less than 40 percent of the tensile strength of flexural reinforcement. Whereas unconservative of detailed method is zero percent. In the case of Eurocode2 [10] and Bažant et al [12], mean values are higher than other estimation method but unconservative ratio is 1.9 percent and 3.1 percent which is rather low. Thus these methods predict experimental values conservatively.

Fig 5.8 presents shear strength of experimental values UTPCSDB and this study according to experimental variables. Also, **Fig 5.9**, **Fig 5.10**, **Fig 5.11**, **Fig 5.12**, and **Fig 5.13** shows shear strength ratio between experimental values and predicted values of ACI318-11, Eurocode2, Sozen et al, Bažant et al. In these graph, cross point indicates experimental values of UTPCSDB and white circle indicates experimental values of specimens with shear reinforcement in this study and black circle indicates that of specimens without shear reinforcement.

As shown in **Fig 5.8**, shear strength included experimental values of this study increases as shear span-to-depth ratio decreases. And it also increases as shear reinforcement index ($\rho_v f_y$) and effective prestressing force (f_{se}/f_{pu}) increases. But in the range of 62 percent to 65 percent, experimental values of

this study does not present tendency like UTPCSDB.

Table 5.3 Evaluation database

Researcher	No.	Cross section	f'_c (MPa)	h (mm)	b_w (mm)	a/d	$p_v f_v$ (MPa)	f_{se}/f_{pu} (%)	v_{test} (MPa)	Shear failure mode
Alshegeir & Ramirez (1992)	3	I	61~62	711~914	152	2.16~2.35	0.97~1.31	65~66	5.10~7.17	SC,SD
Avendaño & Bayrak (2008)	4	I,deck	78~95	914	177	2.92~3.75	2.00~2.41	55.10	13~14	HS,SC,AD
Choulli, Marí & Cladera (2008)	4	I	81~90	749	99	3.13	2.62	30.00	9.44~11.17	S
Elzanaty, Nilson & Slate (1986)	7	I	40~73	457	50	3.8	2.41~3.45	41.50~58.80	7.30~9.72	S
Hanson & Hulsbos (1964)	12	I	44~51	457	76.2	2.53~3.8	0.83~1.31	45.90~50.30	4.68~6.96	SC,ST
Heckmann (2008)	6	I	83~88	1016	178	22	0.97	59.30~62.10	10.2~11.2	ST
Kaufman & Ramirez (1988)	4	I	58~63	711~914	152	2.2~2.4	0.83~0.97	64.40~68.00	4.48~6.55	SC,ST
MacGregor, Sozen & Siess (1960)	38	R,I	14~43	305	72~152	3.56~5.34	0~0.95	22.66~49.53	1.55~3.88	S
Ramirez & Aguilar (2005)	2	I	92~111	711.2	152.4	3.62~3.66	2.14	63.80	8.14~9.72	SC
Rangan (1991)	12	I	29~45	615	61~76	2.48~2.62	7.58~15.72	62.30	9.17~12.76	SC
Runzell, Shield & French (2007)	1	I	70	1372	203	3.57	1.10	46.40	5.65	SC
Teoh, Mansur & Wee (2002)	1	I	106	701	150	2.71	0.90	60	4.34	S
Sozen, Zwoyer & Siess (1959)	37	R	17~55	305	152	2.81~6.73	0	0~48.99	0.54~2.46	S
Total	131									

※ S: shear failure, SC: shear compression failure, ST: shear tension failure, HS: shear failure with signs of horizontal damage, AD: shear failure with sign of anchorage zone distress

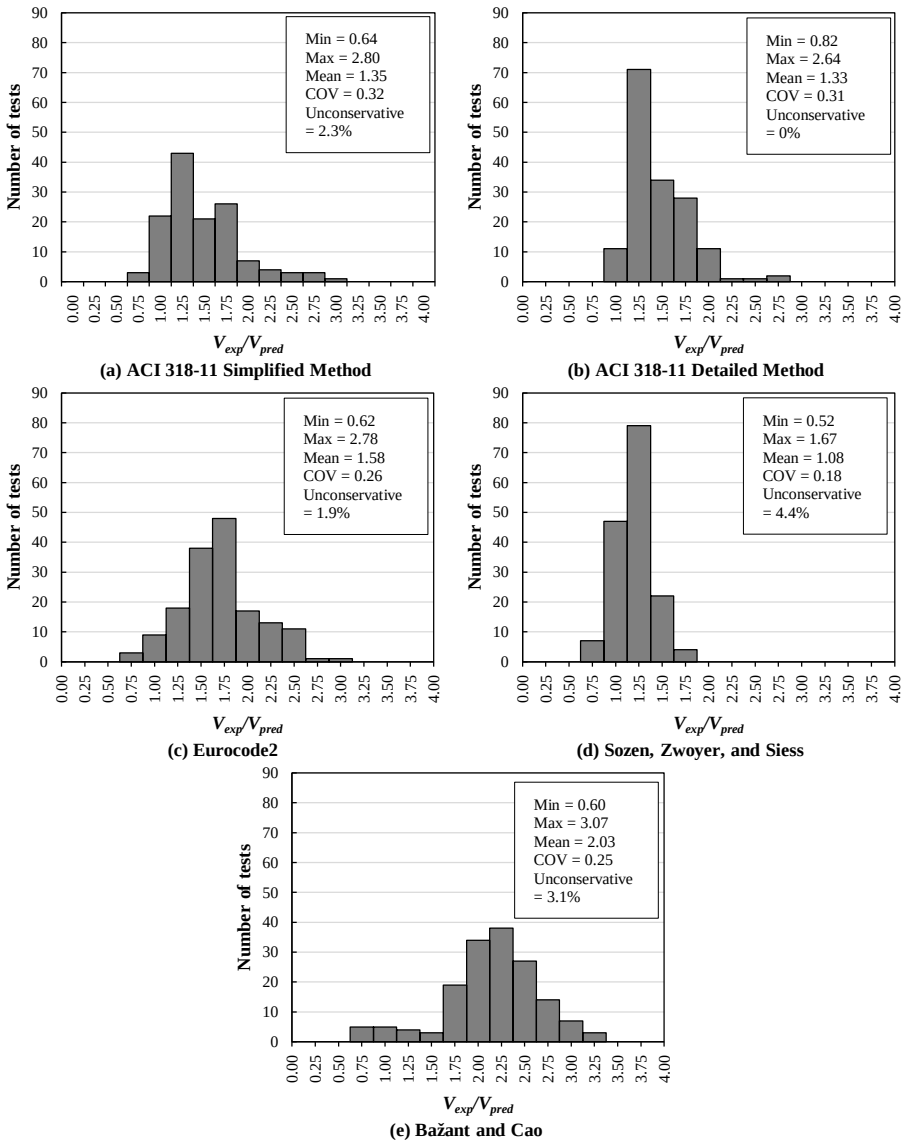

Fig 5.7 Distribution of shear strength ratio

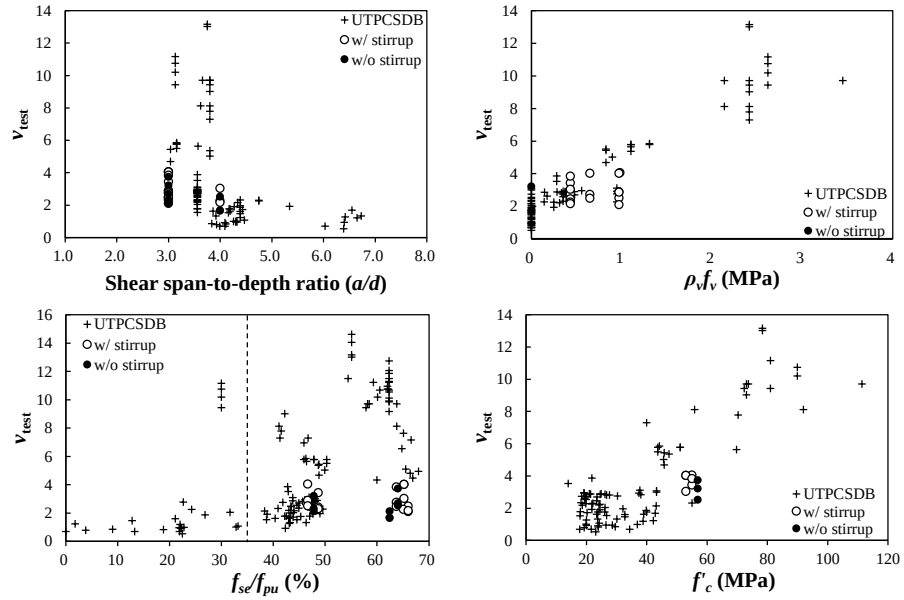

Fig 5.8 Experimental values according to experimental variables

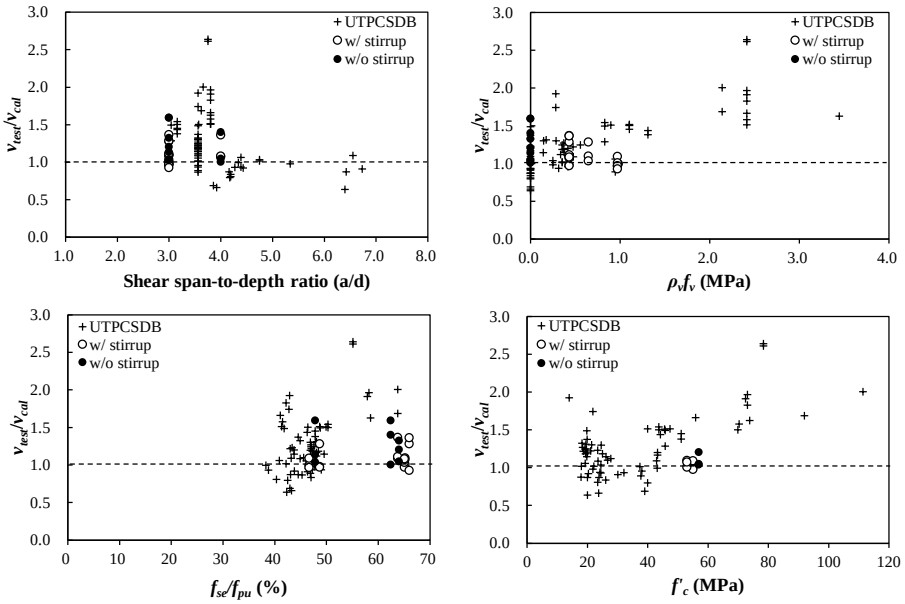

Fig 5.9 ACI 318-11 simplified method

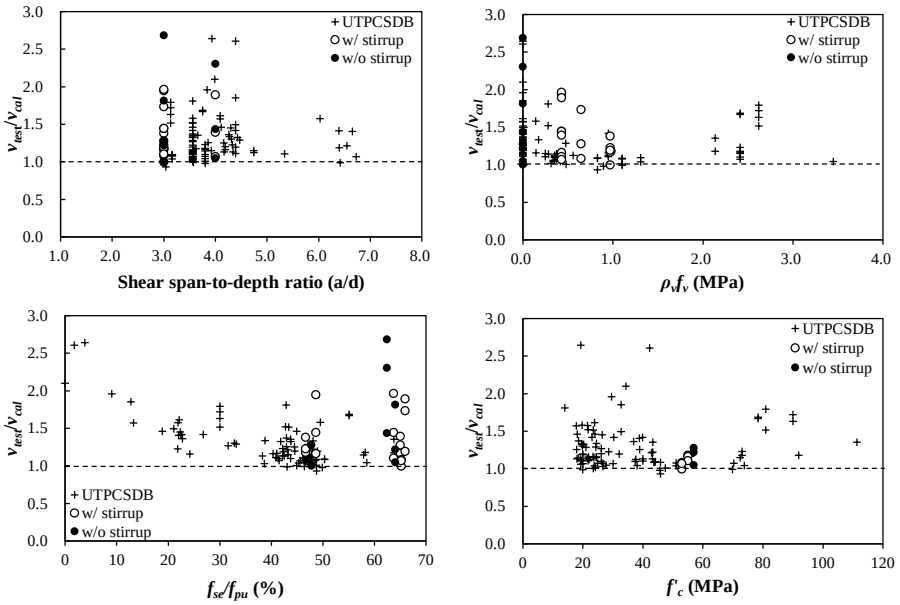

Fig 5.10 ACI 318-11 detailed method

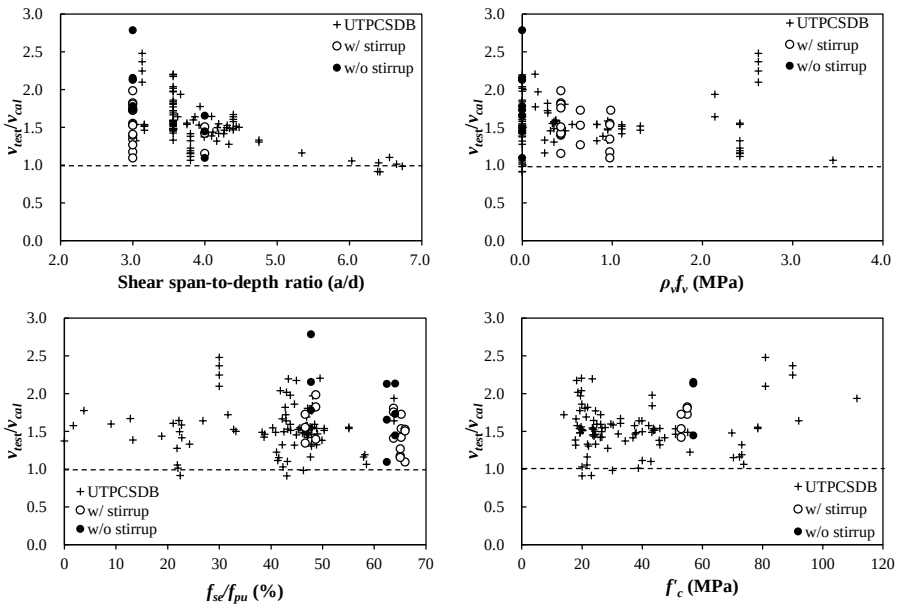

Fig 5.11 Eurocode 2

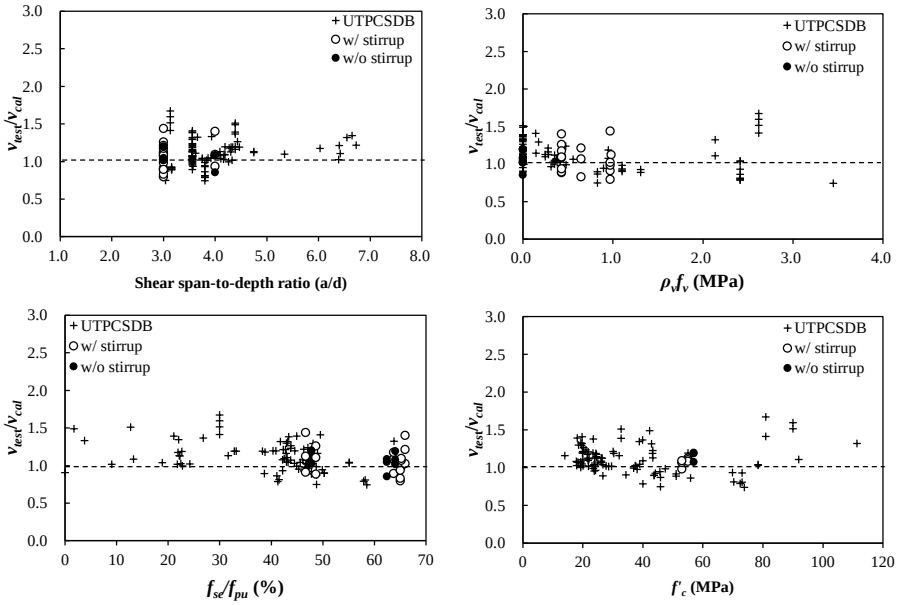

Fig 5.12 Sozen, Zwoyer, and Siess

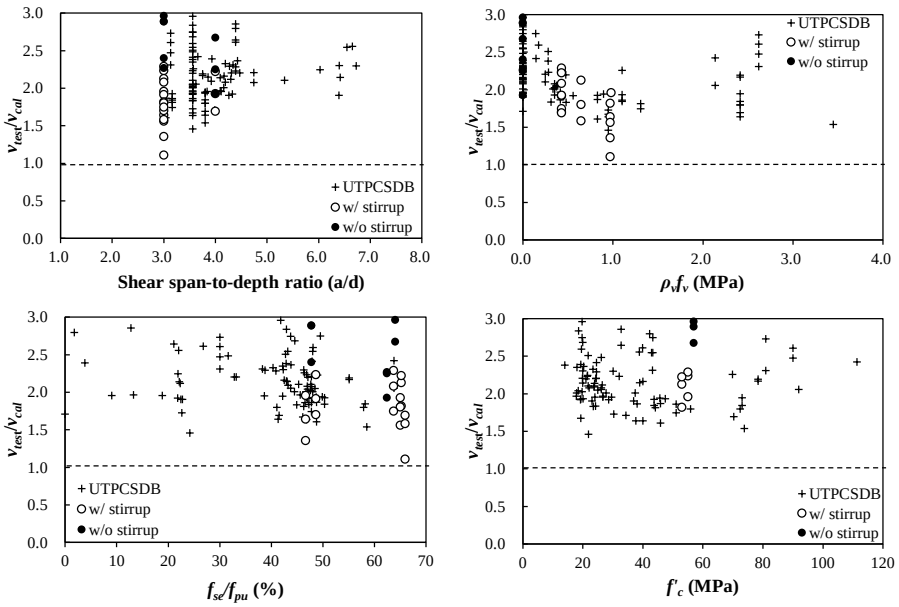

Fig 5.13 Bažant and Cao

Chapter 6. Conclusion

In this study, to investigate feasibility of applying current code (KCI 2012 [1], ACI 318-11 [2]) to estimate shear strength of prestressed PC-CIP composite beams, test was performed. And based on results, experimental values compared with shear database (UTPCSDB [13]) of prestressed concrete beams with other design codes.

1) In the case of specimens without shear reinforcement, early flexural cracks developed inclined shear cracks and these cracks propagated to compression zone near loading points. Finally brittle failure occurred. In the case of specimens with shear reinforcement, whereas, shear strength and center displacement increased before failure. Crack patterns at these failure modes are shear compression failure, horizontal shear failure, and web shear failure. In the case of horizontal shear failure, horizontal shear cracks occurred in spite of arrangement of shear reinforcement which was able to resist horizontal shear force. It means that state of contact surface, that is aggregate exposure, is also important factor beside shear reinforcement

2) In condition of 3.0 shear span-to-depth ratio(a/d) and more than 60 percent effective prestressing force (f_{se}/f_{pu}), shear strength did not increase in spite of increasing shear reinforcement ratio. Because of prestressing force, early flexural cracks and inclined shear cracks were concentrated to near loading points in other words location of critical section decreased and finally specimens failed shear compression failure. Thus shear span to-depth ratio is able to be assumed less than 3.0 like deep beam behavior.

3) Based on UPTCSDB, experimental values were compared with

predicted values according to shear span-to-depth ratio (a/d), shear reinforcement index ($\rho_v f_y$), effective prestressing force (f_{se}/f_{pu}), and concrete compressive strength (f'_c). In the results, shear strength of specimens which shear compression failure occurred was higher than that of specimens which horizontal shear failure and web shear failure occurred in this study. And mean value of shear strength ratio (V_{exp}/V_{pred}) with simplified method of ACI 318-11 was similar with detailed method but coefficient of variation (COV) was 0.32 which is higher than 0.24 of detailed method. And unconservative ratio using simplified method of ACI 318-11 was 2.3 percent whereas all specimens were in safety side in case of detailed method.

References

[1] Korean Concrete Institute, *Korean Structural Design Code (KCI 2012)*. Seoul: Korean Concrete Institute, 2012.

[2] ACI Committee 318, *Building Code Requirements for Structural Concrete (ACI 318-11)*. MI: American Concrete Institute, 2011.

[3] C. G. Kim., H. G. Park., G. H. Hong., and S. M. Kang., "Shear Strength of PC-CIP Composite Beams with Shear Reinforcement," *Journal of Architectural Institute of Korea*, vol. 26, pp. 189-199, 2014.

[4] C. G. Kim., H. G. Park., G. H. Hong., and S. M. Kang., "Shear Strength of Hybrid Beams Combining Precast Concrete and Cast-In-Place Concrete," *Journal of Architectural Institute of Korea*, vol. 25, pp. 175-185, 2013.

[5] C. G. Kim., H. G. Park., G. H. Hong., S. M. Kang., and J. I. Suh., "Shear Strength of Prestressed PC-CIP Composite Beams without Vertical Shear Reinforcements," *Journal of Architectural Institute of Korea*, vol. 26, pp. 533-543, 2014.

[6] S. Revesz, "Behavior of Compressive T-Bemas with Prestressed and Unprestressed Reinforcement," *ACI Journal Proceedings*, vol. 49, pp. 585-592, 1953.

[7] J. Saemann and G. W. Washa, "Horizontal Shear Connections Between Precast Beams and Cast-in-Place," *ACI Journal Proceedings*, vol. 61, pp. 1383-1410, 1964.

[8] J. O. Bryson, L. F. Skoda, and D. Watstein, "Flexural Behavior of Prestressed Split-Beam Composite Concrete Sections," *PCI Journal Proceeding*, vol. 10, pp. 77-91, 1965.

[9] D. Phil and A. Patnaik, "Horizontal Shear Strength of Composite Concrete Beams with a Rough Interface," *PCI Journal*, vol. 39, pp. 48-68, 1994.

[10] Eurocode 2, *Design of Concrete Structures - Part1-1: General Rules and Rules for Buildings*. Brussels, Belgium, 2004.

[11] M. A. Sozen, E. M. Zwoyer, and C. P. Siess, "Investigation of Prestressed Concrete for Highway Bridges: Part I Strength in Shear of Beams without Web Reinforcement," University of Illinois. Engineering Experiment Station. Bulletin ; no. 452, Urbana1959.

[12] Z. P. Bazant and Z. Cao, "Size effect of shear failure in prestressed concrete beams," *ACI Journal Proceedings*, vol. 83, pp. 260-268, 1986.

[13] Eisuke Nakamura, A. R. Avendaño, and B. Oguzhan, "Shear Database for Prestressed Concrete Members," *ACI Structural Journal*, vol. 110, pp. 909-918, 2013.
[14] Concrete Technology Assosiates, "Composite Systems without Ties," Technical Bulletin 76-B41976.
[15] J. D. Kovach and C. Naito, "Horizontal Shear Capacity of Composite Concrete Beams without Interface Ties," *Theses and Dissertations*, 2008.
[16] F. J. Vecchio and M. P. Collins, "The modified compression-field theory for reinforced concrete elements subjected to shear," *ACI Journal Proceedings*, vol. 83, pp. 219-231, 1986.
[17] S. Mau and T. T. Hsu, "Shear strength prediction for deep beams with web reinforcement," *ACI Structural Journal*, vol. 84, pp. 513-523, 1987.
[18] A. Halicka, "Influence new-to-old concrete interface qualities on the behaviour of support zones of composite concrete beams," *Construction and Building Materials*, vol. 25, pp. 4072-4078, 10// 2011.
[19] AASHTO LRFD, "LRFD bridge design specifications," *Washington, DC: American Association of State Highway and Transportation Officials*, 1998.
[20] Canadian Standards Association, *Design of Concrete Structures [electronic Resource]*: Mississauga, Ont.: Canadian Standard Association, 2004.
[21] J. Walraven, J. Frenay, and A. Pruijssers, "Influence of concrete strength and load history on the shear friction capacity of concrete members," *PCI journal*, vol. 32, pp. 66-84, 1987.
[22] A. H. Mattock, "Shear friction and high-strength concrete," *ACI Structural Journal*, vol. 98, pp. 50-59, 2001.
[23] A. K. Patnaik, "Behavior of composite concrete beams with smooth interface," *Journal of Structural Engineering*, vol. 127, pp. 359-366, 2001.
[24] L. F. Kahn and A. D. Mitchell, "Shear friction tests with high-strength concrete," *ACI Structural Journal*, vol. 99, pp. 98-103, 2002.

Appendix A: List of Collected References

[1] Alshegier, A., and Ramirez, J.A., "Strut-Tie Aproach in Prestressed Deep beams," ACI Structural Journal, Vol.89, No.3, May-June, 1992, pp. 296-304

[2] Avendano, A., and Bayrak, O., "Shear Strength and Behavior of Prestressed Concrete Beams," Technical Report: IAC-88-5DD1A003-3, Center for Transportation Research, The University of Texas at Austin, Austin, TX, 2008, 170pp.

[3] Choulli, Y., Mari, A. R., and Cladera, A., "shear Behavior of Full-Scale Prestressed I-beams Made with Self Compacting Concrete," Materials and Structures, Vol.41, No.1, 2008, pp.131-141.

[4] Elzanaty, A. H., Nilson, A. H., and Slate, F. O., "Shear Capacity of Prestressed Concrete Beams Using High-Strength Concrete," ACI Structural Journal, Vol.83, No.2, March-April, 1987, pp.359-368.

[5] Hanson, J. M., and Hulsbos, C. L., "Ultimate Shear Tests of Prestressed Concrete I-Beams under Concentrated and Uniformed Loadings," PCI Journal, Vol.9, No.3, June, 1964, pp.15-28.

[6] Hanson, J. M., and Hulsbos, C. L., "Ultimate Shear Tests of Large Prestressed Bridge Beams," American Concrete Institute SP-26 Concrete Bridge Design, American Concrete Institute, Farmington Hills, MI, 1969, pp.523-549.

[7] Heckmann, C. P., "Effects of Increasing the Allowable Compressive Stress at Release on the Shear Strength of Prestressed Concrete Girders," Master Thesis, The university of Texas at Austin, Austin, TX, 2008, 175pp.

[8] Kaufman, M. K., and Ramirez, J. A., "Re-evaluation of the Ultimate Shear Behavior of High-Strnegth Concrete Prestressed I-Beams," ACI Structural Journal, Vol.85, No.3, May-June, 1987, pp.295-303.

[9] MacGregor, J. G., Sozen, M. A., and Siess, C. P., "Effect of Draped Reinforcement on Behavior of Prestressed Concrete Beams," Journal of the American Concrete Institute, Vol.57, No. 12, December, 1960, pp.649-677.

[10] MacGregor, J. G., Sozen, M. A., and Siess, C. P., "Strength and Behavior of Prestressed Concrete Beams with Web Reinforcement,"

Civil Engineering Studies, Structural Research Series No.201, University of Illinois, Urbana, IL, 1960, 314pp.

[11] Ramirez, J. A., and Aguilar, G., “Shear Reinforcement Requirements for High-Strength Concrete Bridege Girders,” Final Report, FHWA/IN/JTRP-2005/19, Purdue University, West Lafayette, IN, 2005, 127pp.

[12] Rangan, B. V., “Web Crushing Strength of Reinforced and Prestressed Concrete Beams,” ACI Structural Journal, Vol.88, No.1, January-February, 1991, pp.12-16.

[13] Runzell, B., Shield, C., and French, C., “Shear Capacity of Prestressed Concrete Beams,” Final Reports, MN/RC 2007-47, University of Minnesota, Minneapolis, MN, 2007, 237pp.

[14] Teoh, B. K., Mansur, M. A., and Wee, T. H., “behavior of High-Strength Concrete I-Bemas with Low Shear Reinforcement,” ACI Structural Journal, Vol.99, No.3, May-Jun, 2002, pp.299-307.

[15] Sozen, M. A., Zwoyer, E. M., and Siess, C. P., “Investigation of Prestressed Concrete for Highway Bridge, Part1-Strength in Shear of Beams without Web Reinforcement,” Engineering Experiemnt Station Bulletin No.452, University of Illinois, Urana, April, 1959, 68pp.

Appendix B: Evaluation Database

Specimens I.D	specimen's identification reported in the original references
Cross section	I: I-shaped beam, R: rectangular beam, deck: beam has a deck on top
f'_c	concrete compressive strength, MPa
h	overall member depth, mm
b_w	web width, mm
a/d	shear span-to-depth ratio
$\rho_v f_y$	shear reinforcement index, MPa
f_{se}/f_{pu}	percentage of effective prestress in prestressing steel, f_{se}, to tensile strength of prestressing steel, f_{pu}, %
v_{test}	shear stress at failure, MPa
Loading condition	C: concentrated loads, U: uniform loads
Prestressing type	Pre: pretensioned, Post: post-tensioned
Failure mode	S: shear failure, SC: shear compression failure, ST: shear tension failure, HS: shear failure with signs of horizontal shear damage AD: shear failure with signs of anchorage zone distress

Table A. Evaluation database of UTPCSDB

Specimen I.D	Cross section	f'_c (MPa)	h (mm)	b_w (mm)	a/d	$p_v f_v$ (MPa)	f_{se}/f_{pu} (%)	v_{test} (MPa)	Loading condition	Prestressing type	Shear failure mode
Alshegeir & Ramirez (1992)											
Type I-4A	I	61	711.2	152.4	2.31	1.31	66.60	7.17	C	Pre	SC
Type II-1A	I	62	914.4	152.4	2.16	1.17	65.10	7.65	C	Pre	SC
Type I-3A	I	61	711.2	152.4	2.35	0.97	65.50	5.10	C	Pre	SC,AD
Avendaño & Bayrak (2008)											
TX28-I-L	I,deck	95	914.4	177.8	2.92	2.00	55.10	14.07	C	Pre	HS,SC,AD
TX28-I-D	I,deck	95	914.4	177.8	2.92	2.00	55.10	14.62	C	Pre	HS,SC,AD
TX28-II-L	I,deck	78	914.4	177.8	3.75	2.41	55.10	13.03	C	Pre	HS,SC,AD
TX28-II-D	I,deck	78	914.4	177.8	3.75	2.41	55.10	13.17	C	Pre	HS,SC,AD
Choulli, Marí & Cladera (2008)											
C2TE	I	90	749.3	99.06	3.13	2.62	30.00	10.76	C	Pre	S
C2TW	I	90	749.3	99.06	3.13	2.62	30.00	10.20	C	Pre	S
C1TE	I	81	749.3	99.06	3.13	2.62	30.00	9.45	C	Pre	S
C1TW	I	81	749.3	99.06	3.13	2.62	30.00	11.17	C	Pre	S
Elzanaty, Nilson & Slate (1986)											
CW10	I	73	457.2	50.8	3.8	2.41	42.20	9.03	C	Pre	S
CW11	I	56	457.2	50.8	3.8	2.41	41.10	8.14	C	Pre	S
CW12	I	40	457.2	50.8	3.8	2.41	41.30	7.31	C	Pre	S
CW13	I	72	457.2	50.8	3.8	2.41	57.90	9.45	C	Pre	S
CW14	I	74	457.2	50.8	3.8	3.45	58.50	9.72	C	Pre	S
CW15	I	70	457.2	50.8	3.8	2.41	41.50	7.79	C	Pre	S
CW16	I	73	457.2	50.8	3.8	2.41	58.20	9.72	C	Pre	S
Hanson & Hulsbos (1964)											
F-X1-1st	I	46	457.2	76.2	3.04	0.83	48.80	4.69	C	Pre	SC
F-2-1st	I	45	457.2	76.2	2.53	0.83	45.90	5.79	C	Pre	SC

Specimen I.D	Cross section	f'_c (MPa)	h (mm)	b_w (mm)	a/d	$p_v f_v$ (MPa)	f_{se}/f_{pu} (%)	v_{test} (MPa)	Loading condition	Prestressing type	Shear failure mode
F-4-1st	I	44	457.2	76.2	3.16	0.83	50.30	5.52	C	Pre	ST
F-19-1st	I	51	457.2	76.2	3.16	1.10	47.80	5.79	C	Pre	ST
F-X1-2nd	I	46	457.2	76.2	3.04	0.83	48.80	5.45	C	Pre	SC
F-2-2nd	I	45	457.2	76.2	2.53	1.31	45.90	6.96	C	Pre	ST
F-3-2nd	I	47	457.2	76.2	2.53	2.00	46.70	7.31	C	Pre	SC
F-4-2nd	I	44	457.2	76.2	3.16	1.10	50.30	5.79	C	Pre	SC
F-5-2nd	I	44	457.2	76.2	3.16	1.31	46.30	5.86	C	Pre	SC
F-7-2nd	I	46	457.2	76.2	3.8	0.90	49.90	5.03	C	Pre	SC
F-8-2nd	I	47	457.2	76.2	3.8	1.10	48.70	5.38	C	Pre	SC
F-19-2nd	I	51	457.2	76.2	3.16	1.31	47.80	5.79	C	Pre	SC
Heckmann (2008)											
CB-70-1	I	83	1016	177.8	2.2	0.97	62.00	10.76	C	Pre	ST
CB-70-4	I	86	1016	177.8	2.2	0.97	60.50	10.69	C	Pre	ST
CB-70-5	I	86	1016	177.8	2.2	0.97	60.10	10.20	C	Pre	ST
CB-70-6	I	88	1016	177.8	2.2	0.97	59.30	11.24	C	Pre	ST
CB-60-1	I	85	1016	177.8	2.2	0.97	62.00	10.96	C	Pre	ST
CB-60-2	I	88	1016	177.8	2.2	0.97	62.10	10.76	C	Pre	ST
Kaufman & Ramirez (1988)											
I-2	I	58	711.2	152.4	2.2	0.83	64.80	6.55	C	Pre	SC
I-3	I	58	711.2	152.4	2.2	0.97	66.90	4.48	C	Pre	ST
I-4	I	58	711.2	152.4	2.2	0.83	68.00	4.96	C	Pre	ST
II-1	I	63	914.4	152.4	2.4	1.10	66.40	4.83	C	Pre	ST
MacGregor, Sozen & Siess (1960)											
AW.14.39	R	38	304.8	152.4	3.56	0.95	46.88	3.12	C	Pre	S
AW.14.79	R	19	304.8	152.4	3.56	0.95	46.09	2.94	C	Pre	S
AW.24.48	R	30	304.8	152.4	3.56	0.95	22.66	2.78	C	Pre	S
AW.24.68	R	22	304.8	152.4	3.56	0.95	24.22	2.28	C	Pre	S
B.14.34	I	18	304.8	78.74	3.56	0.00	44.92	2.35	C	Pre	S

Specimen I.D	Cross section	f'_c (MPa)	h (mm)	b_w (mm)	a/d	$p_v f_v$ (MPa)	f_{se}/f_{pu} (%)	v_{test} (MPa)	Loading condition	Prestressing type	Shear failure mode
B.14.41	I	20	304.8	76.2	3.56	0.00	44.53	2.55	C	Pre	S
BD.14.18	I	43	304.8	72.644	3.56	0.00	48.05	3.01	C	Pre	S
BD.14.19	I	43	304.8	73.66	3.56	0.00	43.75	3.09	C	Pre	S
BD.14.23	I	27	304.8	76.2	3.56	0.00	38.67	1.55	C	Pre	S
BD.14.26	I	24	304.8	76.2	3.56	0.00	45.31	1.77	C	Pre	S
BD.14.27	I	23	304.8	76.2	3.56	0.00	43.36	2.48	C	Pre	S
BD.14.34	I	19	304.8	76.2	3.56	0.00	42.97	2.19	C	Pre	S
BD.14.35	I	18	304.8	74.93	3.56	0.00	42.19	1.80	C	Pre	S
BD.14.42	I	20	304.8	73.66	3.56	0.00	41.80	2.76	C	Pre	S
BD.24.32	I	26	304.8	76.2	3.56	0.00	31.64	2.06	C	Pre	S
BV.14.30	I	28	304.8	74.93	3.56	0.33	48.05	2.83	C	Pre	S
BV.14.32	I	26	304.8	72.39	3.56	0.38	43.75	2.87	C	Pre	S
BV.14.34	I	25	304.8	76.2	3.56	0.37	48.44	2.90	C	Pre	S
BV.14.35	I	24	304.8	74.168	3.56	0.48	44.92	2.72	C	Pre	S
BV.14.42	I	20	304.8	73.152	3.56	0.42	46.88	2.73	C	Pre	S
BW.14.20	I	20	304.8	74.93	3.56	0.14	49.53	2.29	C	Pre	S
BW.14.22	I	37	304.8	76.2	3.56	0.35	46.76	2.94	C	Pre	S
BW.14.23	I	38	304.8	76.708	3.56	0.42	46.52	2.84	C	Pre	S
BW.14.26	I	24	304.8	72.644	3.56	0.31	47.27	2.21	C	Pre	S
BW.14.31	I	27	304.8	76.2	3.56	0.42	45.63	2.83	C	Pre	S
BW.14.32	I	20	304.8	72.644	3.56	0.18	48.09	2.64	C	Pre	S
BW.14.34	I	25	304.8	73.66	3.56	0.15	47.89	2.87	C	Pre	S
BW.14.38	I	21	304.8	74.93	3.56	0.28	46.88	2.88	C	Pre	S
BW.14.39	I	21	304.8	99.06	3.56	0.48	47.11	2.91	C	Pre	S
BW.14.41	I	20	304.8	74.93	3.56	0.35	47.58	2.74	C	Pre	S
BW.14.42	I	19	304.8	75.184	3.56	0.35	47.27	2.59	C	Pre	S
BW.14.43	I	19	304.8	74.93	3.56	0.56	46.99	2.97	C	Pre	S
BW.14.45	I	18	304.8	76.2	3.56	0.37	47.03	2.74	C	Pre	S

Specimen I.D	Cross section	f'_c (MPa)	h (mm)	b_w (mm)	a/d	$p_v f_v$ (MPa)	f_{se}/f_{pu} (%)	v_{test} (MPa)	Loading condition	Prestressing type	Shear failure mode
BW.14.58	I	22	304.8	73.914	3.56	0.28	42.73	3.88	C	Pre	S
BW.14.60	I	14	304.8	73.406	3.56	0.28	42.89	3.54	C	Pre	S
BW.15.34	I	24	304.8	76.2	4.75	0.25	47.81	2.26	C	Pre	S
BW.15.37	I	22	304.8	76.2	4.75	0.35	47.85	2.31	C	Pre	S
BW.16.38	I	22	304.8	76.2	5.34	0.25	47.66	1.94	C	Pre	S
Ramirez & Aguilar (2005)											
13.3-5.1-326P	I	92	711.2	152.4	3.62	2.14	63.80	8.13	C	Pre	SC
16.2-5.1-326P	I	111	711.2	152.4	3.66	2.14	63.80	9.72	C	Pre	SC
Rangan (1991)											
II-1	I	45	614.68	63.5	2.48	9.17	62.30	12.76	C	Pre	SC
II-2	I	32	614.68	63.5	2.48	15.44	62.30	10.69	C	Pre	SC
II-3	I	45	614.68	73.66	2.48	8.00	62.30	11.86	C	Pre	SC
II-4	I	43	614.68	73.66	2.48	13.17	62.30	11.51	C	Pre	SC
III-1	I	40	614.68	66.04	2.5	8.89	62.30	9.93	C	Pre	SC
III-2	I	37	614.68	66.04	2.5	14.76	62.30	10.55	C	Pre	SC
III-3	I	39	614.68	76.2	2.5	7.58	62.30	9.17	C	Pre	SC
III-4	I	37	614.68	71.12	2.5	13.51	62.30	11.24	C	Pre	SC
IV-1	I	37	614.68	60.96	2.62	15.72	62.30	11.31	C	Pre	SC
IV-2	I	33	614.68	63.5	2.62	9.17	62.30	9.86	C	Pre	SC
IV-3	I	36	614.68	71.12	2.62	13.51	62.30	12.07	C	Pre	SC
IV-4	I	29	614.68	71.12	2.62	8.14	62.30	10.14	C	Pre	SC
Runzell, Shield & French (2007)											
II	I	70	1371.6	203.2	3.57	1.10	46.40	5.65	C	Pre	SC
Teoh, Mansur & Wee (2002)											
B6-12	I	106	701.04	149.86	2.71	0.90	60.00	4.34	C	Pre	S
Sozen, Zwoyer & Siess (1959)											
A.11.43	R	43	305	152	6.55	0.00	43.17	1.69	C	Pre	S
A.11.51	R	20	305	152	6.4	0.00	42.33	0.94	C	Pre	S

Specimen I.D	Cross section	f'_c (MPa)	h (mm)	b_w (mm)	a/d	$p_v f_v$ (MPa)	f_{se}/f_{pu} (%)	v_{test} (MPa)	Loading condition	Prestressing type	Shear failure mode
A.11.53	R	30	305	152	6.73	0.00	46.31	1.33	C	Pre	S
A.11.96	R	20	305	152	6.42	0.00	43.06	1.28	C	Pre	S
A.12.23	R	39	305	152	3.86	0.00	42.93	1.64	C	Pre	S
A.12.31	R	40	305	152	4.17	0.00	42.53	1.78	C	Pre	S
A.12.34	R	55	305	152	4.39	0.00	40.90	2.33	C	Pre	S
A.12.36	R	24	305	152	3.92	0.00	43.27	1.34	C	Pre	S
A.12.42	R	43	305	152	4.34	0.00	38.31	2.16	C	Pre	S
A.12.46	R	32	305	152	4.39	0.00	48.99	1.97	C	Pre	S
A.12.53	R	23	305	152	4.19	0.00	40.36	1.63	C	Pre	S
A.12.56	R	26	305	152	4.19	0.00	46.99	1.78	C	Pre	S
A.12.69	R	20	305	152	4.43	0.00	43.80	1.73	C	Pre	S
A.12.73	R	25	305	152	4.27	0.00	38.80	1.92	C	Pre	S
A.12.81	R	18	305	152	4.16	0.00	44.52	1.54	C	Pre	S
A.14.39	R	23	305	152	2.87	0.00	43.34	2.01	C	Pre	S
A.14.44	R	23	305	152	2.82	0.00	43.96	2.18	C	Pre	S
A.14.55	R	23	305	152	2.81	0.00	43.43	2.46	C	Pre	S
A.14.68	R	17	305	152	2.85	0.00	43.86	2.05	C	Pre	S
A.21.29	R	23	305	152	6.39	0.00	22.43	0.54	C	Pre	S
A.21.39	R	22	305	152	6.03	0.00	21.88	0.7	C	Pre	S
A.21.51	R	39	305	152	6.65	0.00	22.02	1.21	C	Pre	S
A.22.20	R	37	305	152	4.26	0.00	22.76	1	C	Pre	S
A.22.24	R	24	305	152	4.09	0.00	22.15	0.93	C	Pre	S
A.22.27	R	27	305	152	4.3	0.00	22.30	0.97	C	Pre	S
A.22.28	R	24	305	152	4.11	0.00	18.83	0.85	C	Pre	S
A.22.31	R	24	305	152	4.47	0.00	33.18	1.08	C	Pre	S
A.22.34	R	29	305	152	4.33	0.00	21.80	0.97	C	Pre	S
A.22.36	R	20	305	152	4.31	0.00	32.80	1.03	C	Pre	S
A.22.39	R	18	305	152	4.09	0.00	13.28	0.71	C	Pre	S

Specimen I.D	Cross section	f'_c (MPa)	h (mm)	b_w (mm)	a/d	$p_v f_v$ (MPa)	f_{se}/f_{pu} (%)	v_{test} (MPa)	Loading condition	Prestressing type	Shear failure mode
A.22.40	R	40	305	152	4.39	0.00	26.80	1.87	C	Pre	S
A.22.49	R	33	305	152	4.39	0.00	21.09	1.62	C	Pre	S
A.32.19	R	34	305	152	3.99	0.00	0.00	0.71	C	Pre	S
A.32.22	R	30	305	152	3.84	0.00	9.02	0.87	C	Pre	S
A.32.27	R	19	305	152	3.93	0.00	3.80	0.8	C	Pre	S
A.32.37	R	42	305	152	4.39	0.00	1.76	1.24	C	Pre	S
A.32.49	R	33	305	152	4.39	0.00	12.74	1.48	C	Pre	S

초 록

프리스트레스트 PC-CIP 복합보의 전단강도에 대한 실험적 연구

서 정 일

서울대학교 건축학과 대학원

최근 들어, 모듈화된 건축물에 프리스트레스된 프리캐스트 콘크리트와 현장콘크리트를 합성한 복합화 공법사용이 증가하고 있다. 이러한 공법의 증가에도 불구하고 합성 부재의 전단 강도를 산정하는 구조 기준이 마련되어 않아 실무자들의 어려움을 초래하고 있는 실정이다. 현행구조 기준(KCI 2012, ACI 318-11)에서는 단일 단면에 대한 전단 강도식만 제시하고 있으며, 합성 단면에 대해서는 단면 중 불리한 값 또는 각각의 특성을 반영한 값으로 수직 전단 강도를 산정하도록 명시되어있다. 따라서 본 연구에서는 현행 구조 기준을 바탕으로 프리스트레스트된 프리캐스트 콘크리트와 현장타설 콘크리트 합성보의 전단 강도 실험을 수행하고 합성보 설계시 고려해야할 사항에 대하여 알아보았다. 변수로는 콘크리트의 면적비, 긴장재의 긴장력, 전단경간비, 그리고 전단철근비를 고려하였다.

총 34개의 실험체에 대하여 전단 실험을 수행한 결과, 최종 파괴 양상은 전단 압축 파괴, 수평 전단 파괴 그리고 복부 전단 파괴가 발생하였으며 전단 압축파괴가 발생한 실험체의 전단강도가 수평

전단파괴, 복부 전단 파괴가 발생한 실험체의 전단강도보다 최대 2.4배 컸다. 또한 긴장력이 가해진 단면적의 면적비, 유효 프리스트레스 힘에 비례하여 증가하였고 전단 경간비가 증가할수록 감소하였다. 특히 전단경간비가 3.0으로 비교적 짧고, 62%~65%의 높은 유효프리스트레스 힘이 가해질 경우, 전단 철근비가 증가하여도 전단 강도는 증가하지 않았다.

본 연구의 실험값을 현행구조기준(KCI 2012, ACI 318-11) 외에 Eurocod 2와 Sozen et al.의 경험식, Bažant et al.의 이론식으로 산정한 예측값으로 비교해 본 결과, 현행 구조 기준(KCI 2012, ACI 318-11)의 약산식과 정밀식 모두 안전측으로 예측하였고 특히 정밀식이 약산식보다 다소 보수적으로 평가하고 있음을 확인하였다. 따라서 합성단면에 대하여 현행 구조 기준으로 각각의 부재 특성을 반영한 전단강도를 산정하는 것은 타당하다고 판단된다. 더불어 shear database (UTPCSDB)와 본 연구의 실험값을 현행구조기준으로 예측하여 실험 변수 별로 분석해본 결과, 약산식의 경우 40% 이상 유효프리스트레스 힘이 작용하는 실험체에 대하여 2.3% 비안전측으로 예측하였으나 정밀식은 모두 안전측으로 예측하였다. 또한 전단 강도 예측 방법 중에서 Sozen et al.의 경험식으로 예측할 경우, 전단강도비(V_{exp}/V_{pred})의 평균값이 1.08, 변동계수 역시 0.18로 가장 작은 것으로 나타났다.

핵심용어: 전단강도, 프리스트레스, 프리캐스트, 합성보

학번: 2013-20561